NOTE TO USERS

This reproduction is the best copy available.

The Early Host Responses upon HBV Replication

MA, Yan

A Thesis Submitted in Partial Fulfillment
of the Requirements for the Degree of
Doctor of Philosophy
in
Public Health

The Chinese University of Hong Kong
February 2010

ProQuest LLC
789 East Eisenhower Parkway
P.O. Box 1346
Ann Arbor, MI 48106-1346

Thesis/Assessment Committee

Professor YU Tak Sun Ignatius (Chair)
Professor HE Mingliang (Thesis Supervisor)
Professor CHENG Hon Ki (Thesis Supervisor)
Professor KUNG Hsiang Fu (Committee Member)
Professor YU Jun (Committee Member)
Professor LIN Marier (External Examiner)

Abstract of thesis entitled:

"The Early Host Responses upon HBV Replication"

Submitted by MA, Yan

for the degree of Doctor of Philosophy

at The Chinese University of Hong Kong in November 2009

Hepatitis B virus (HBV) infection is a global public health problem, which plays a crucial role in the pathogenesis of chronic hepatitis, cirrhosis and hepatocellular carcinoma. Although considerable progress has been made over the past decade, the pathogenesis of HBV infection and the mechanisms of host-virus interactions are still elusive.

In this study, we applied a two-dimensional gel electrophoresis and mass spectrometry-based comparative proteomic approach to globally analyze the host early response to HBV by using an inducible HBV-producing cell line HepAD38. Twenty-three proteins were identified as differentially expressed, with glucose-regulated protein 78 (GRP78) as one of the most significantly up-regulated proteins induced by HBV replication. This induction was further confirmed in both HepAD38 and HepG2 cells transfected with HBV-producing plasmids by real-time reverse transcription-polymerase chain reaction (RT-PCR) and Western blotting, as well as in HBV-infected human liver biopsies by immunohistochemistry.

Further functional investigation revealed that knockdown of GRP78 expression by RNA interference resulted in a significant increase of both intracellular and extracellular HBV virions in the transient HBV-producing HepG2 cells, concomitant with enhanced levels of hepatitis B surface antigen and e antigen in the culture medium. Conversely, overexpression of GRP78 in HepG2 cells led to HBV suppression concomitant with induction of the positive regulatory circuit of GRP78 and interferon-beta 1 (IFN-β1). In this connection, IFN-β1-mediated 2', 5'-oligoadenylate synthetase (OAS) and ribonuclease L (RNase L) signaling pathway was noted to be activated in GRP78-overexpressing HepG2 cells. Moreover, GRP78 was significantly down-regulated in the livers of chronic hepatitis B patients after effective anti-HBV treatment ($p = 0.019$) as compared with their counterpart pre-treatment liver biopsies.

In conclusion, the present study demonstrates for the first time that GRP78 functions as an endogenous anti-HBV factor *via* IFN-β1-OAS-RNase L pathway in hepatocytes. Induction of hepatic GRP78 may provide a novel therapeutic approach in treating HBV infection.

摘 要

乙肝病毒(HBV)感染是全球性的公共衛生問題，它在慢性肝炎， 肝硬化和肝癌的發生發展中扮演著重要角色。但是，至今，乙肝病毒感染的發病機理和宿主與病毒之間的相互作用機理還研究得不透徹。

在本研究中，我們運用比較蛋白質組學的方法, 通過雙向凝膠電泳分離技術和質譜分析技術，在 HBV 誘導產毒細胞株 HepAD38 中，全面分析了宿主細胞對 HBV 複製的早期反應。研究發現 23 個宿主蛋白的表達水平在 HBV 被誘導複製時發生顯著改變，葡萄糖調節蛋白 GRP78 是其中一個受 HBV 複製影響而顯著上升的蛋白。爲了進一步確證蛋白質組學的研究發現，利用即時螢光定量 RT-PCR 和 Western 雜交免疫印跡法，在 HBV 誘導產生的 HepAD38 和 HBV 表達質粒轉染的 HepG2 細胞中，我們再次證實了 GRP78 表達水平的上調，這一結果在受 HBV 感染的臨床病人肝臟活組織檢查樣本中也得到了進一步的證實。

進一步功能分析顯示，在 HBV 質粒瞬時轉染的 HepG2 細胞中，以 RNA 干擾技術下調 GRP78 的表達水平會導致細胞內和細胞外的 HBV 病毒顆粒顯著上升，同時伴隨著胞外 HBV 表面抗原和 e 抗原的上升。相反地，GRP78 的超量表達抑制了 HBV 的複製，並引起干擾素 IFN-β1 的上調。研究還發現，GRP78 和 IFN-β1 之間互相形成正向調節作用, 以及在 GRP78 超量表達的 HepG2 細胞中，由 IFN-β1 介導的抗病毒效應因子 OAS 和 Rnase L 信號通路被啓動。此外，我們的研究還發現，在抗 HBV 治療有效的慢性乙肝患者的肝臟中，GRP78 的蛋白表達水平，與治療前相比，在接受治療後顯著下降。

綜上所述，我們的研究首次證明了 GRP78 是一個內源性的抗 HBV 蛋白，它在肝細胞中通過啓動 IFN-β1-OAS-Rnase L 信號通路來抑制 HBV 複製。 誘導肝細胞內 GRP78 的表達可能爲抗乙肝病毒感染提供一種全新的治療方法。

Acknowledgements

Firstly, I would like to sincerely thank my supervisor Prof. Ming-liang He and co-supervisor Prof. Christopher Hon-ki Cheng, for their guidance, encouragement and advice throughout this thesis. I am fortunate enough to benefit from their hard work and talent. Without their help, support and trust, neither I nor the project could carry on.

I am also grateful to the many people who have helped me during my doctoral study, particularly, Prof. Hsiang-fu Kung, Prof. Jun Yu, Prof. Joseph Jao-yiu Sung, Prof. Henry Lik-yuen Chan, Prof. Sai-ming Ngai, Prof. Ka-fai To and Prof. Yang-chao Chen, for providing valuable advice, support and inspiration.

Thanks also to all my labmates, especially to Ying Chen, Hua Wang, Qing-ming Dong, Qi Dong, Lai He, Jin Zhao, Jing Lu, Li-na Yi, Juan Lu, Ishtar Wu, Guo Li, Chun-ling Meng, Xin Wang and Shu Diao, for their unselfish assistance and constant encouragement.

Big thanks to Ms. Minnie Y. Y. Go for assistance in the immunochemical staining, to Ms. Sau-na Tsai for helps in mass spectrometry analysis and to Ms. Chu-yan Chan for reviewing my papers.

I could not have got through the three-year Ph.D. study without my dear friends Jie Yang, Li-juan Wang, Yan-er Zhu, and Shu-yan Chen, and I thank them wholeheartedly for their love, understanding and unconditional friendship.

Finally, I would like to thank my parents and grandparents, for their continuous love and support throughout my education. What they mean to me goes too deep for words.

Contents

List of Tables

List of Figures

Abbreviations

APOBEC	apolipoprotein B mRNA-editing enzyme catalytic-polypeptide
APP	amyloid precursor protein
ATF6	activating transcription factor 6
Bip	immunoglobulin heavy-chain binding protein
cccDNA	covalently closed circular DNA
CHB	chronic hepatitis B
CHOP	C/EBP-homologous protein
CID	collision-induced dissociation
eIF2α	the α subunit of eukaryotic translation initiation factor 2
ER	endoplasmic reticulum
ERAD	ER-associated protein degradation
ERSE	ER stress response element
GADD34	growth arrest and DNA damage-inducible protein 34
GAF	IFN-γ activation factor
GAPDH	glyceraldehyde-3-phosphate dehydrogenase
GAS	γ-IFN-activated sequence
GRP78	glucose-regulated protein 78 kDa
HBsAg	hepatitis B surface antigen
HBV	hepatitis B virus
HCC	hepatocellular carcinoma
HCV	hepatitis C virus
HDV	hepatitis D virus
HepB	hepatitis B
HIV	human immunodeficiency virus
HNRPK	heterogeneous nuclear ribonucleoprotein K

IEF	isoelectric focusing
IFNAR	IFN-α receptor
IFNGR	IFN-γ receptors
IFNLR1	IFN-λ receptor 1
IFN-α	interferon-alpha
IFN-β1	interferon-beta 1
IL-10R2	interleukin-10 receptor 2
IRE1	inositol-requiring enzyme 1
IRF9	IFN-regulatory factor 9
ISG15	IFN-stimulated protein of 15 kDa
ISGF3	IFN-stimulated gene factor 3
ISGs	IFN-stimulated genes
ISREs	IFN-stimulated regulatory elements
JAK	Janus tyrosine kinase
L	large
M	middle
MALDI-TOF	matrix-assisted laser desorption/ionization time of flying
MS	mass spectrometry
Mx1	myxovirus resistance 1
NF-Y	nuclear transcription factor Y
OAS	2', 5'-oligoadenylate synthetase
OASL	OAS-like
PDI	protein disulfide isomerase
PERK	protein kinase-like ER resident kinase
pg	pregenomic
PKR	protein kinase R
PPIase B	peptidyl-prolyl isomerase B

PVDF	polyvinylidene difluoride
RNase L	ribonuclease L
RT	reverse transcriptase
RT-PCR	reverse transcription-polymerase chain reaction
S	small
S1P	Site 1 Protease
S2P	Site 2 Protease
SARS-CoV	severe acute respiratory syndrome coronavirus
SD	standard deviation
sg	subgenomic
siRNA	small interfering RNA
STAT	signal transducer and activator of transcription
TYK2	tyrosine kinases 2
UPR	unfolded protein response
UPRE	unfolded protein response element
XBP-1	X-box-binding protein-1

Chapter 1

Introduction

1.1 Hepatitis B virus

The human hepatitis B virus, which predominantly infects the liver, is a prototype virus of the *Hepadnaviridae* family. Other hepatitis viruses belonging to this family are also found in woodchucks (Summers *et al.*, 1978), ground squirrels (Marion *et al.*, 1980), tree squirrels (Feitelson *et al.*, 1986), Peking ducks (Mason *et al.*, 1980) and herons (Sprengel *et al.*, 1988).

Despite recent medical advances and the remarkable progress has been made in the understanding of the molecular virology of HBV, HBV infection continues to be a major international health problem. An estimated 2 billion (one third of the world's population) people are infected with HBV globally, and more than 400 million are chronic hepatitis B (CHB) carriers (Lai *et al.*, 2003). Accumulating evidence has shown that HBV infection can lead to a wide spectrum of liver diseases, which progress from acute to chronic hepatitis, cirrhosis and ultimately hepatocellular carcinoma (HCC) with severe morbidity and mortality (Nassal, 1999; Seeger and Mason, 2000; Arbuthnot and Kew, 2001).

1.1.1 Epidemiology

The prevalence of HBV infection varies geographically, from high (>8%), intermediate (2-7%) to low (<2%) prevalence based on the hepatitis B surface antigen (HBsAg) carrier rate. As shown in Fig. 1-1, the developing regions such as China, Southeast Asia and Africa are areas of high endemicity of HBV infection. In these areas, most infections are acquired during infancy or childhood. Outside of the highly endemic areas, regions with moderate rates of chronic HBV infection include Eastern, Southern and Central Europe, the Middle East, Japan, India and part of South America, where HBV infection occurs in infants, adolescents or adults. In contrast, most developed countries and regions, such as Australia, Western and Northern Europe and North America, are low prevalence areas with HBsAg carrier rates less than 2%. And in these areas, HBV infection is typically acquired during adulthood *via* horizontal transmission, such as percutaneous or sexual transmission.

Epidemiological studies have shown that HBV infection is one of the most important causes of chronic liver diseases. About 15-40% of infected patients will develop cirrhosis, liver failure or HCC (Lok, 2002). Every year, over one million people die of HBV-related liver diseases, 30%-50% of which are attributed to HCC (Parkin *et al.*, 2001). It's estimated that chronic HBV carriers bear a potential 100-fold increased risk for HCC development compared with non-carriers (Beasley *et al.*, 1981). Since 1997, HBV infection has become the 10^{th} leading cause of death in the world (Lavanchy, 2004), and HCC has been ranked as the 5^{th} most frequent cancer (Parkin, 2001). The worldwide annual incidence of primary HCC is shown in Fig. 1-2.

In China, more than 130 million (10% of the national population and one-third of the world's infected population) people are suffering from CHB (Custer *et al.*, 2004) and HCC has been ranked as the second major cause of cancer-related death since 1990 (Pisani *et al.*, 1999).

1.1.2 The virology of HBV

1.1.2.1 HBV structure and genome organization

HBV is an enveloped, partially double stranded DNA virus with a 3200 base pair genome. The unique structure of the genome is that the two DNA strands are not symmetrical. The minus strand DNA is almost a complete circle and the viral polymerase is covalently bound to its 5' end, whereas the plus strand DNA is shorter and variable in length.

The compact genome of HBV contains four overlapping open reading frames, which encode the envelope proteins [large (L), middle (M), small (S) surface proteins], the core/pre-core protein, the polymerase and a transactivating X protein. The HBV gene expression is controlled by four promoters, which include preS1, preS2, C and X promoters. And these promoters are under the regulation of two enhancers, enhancer I and II, which locates upstream to the X promoter and core promoter respectively (Huan and Siddiqui, 1993). At present, five major unspliced HBV transcripts have been demonstrated, which include 3.9 kb long X mRNA, 3.5 kb precore mRNA, 2.4 kb pre

S1 mRNA, 2.1 kb pre S2/S mRNA and 0.7 kb X mRNA (Guo *et al.*, 1991; Kim *et al.*, 1992; Doitsh and Shaul, 2003). The genomic organization and transcription map of HBV is shown in Fig. 1-3.

1.1.2.2 The life cycle of HBV

HBV has a very narrow host range and exhibits a specific tropism for hepatocytes. One of the possible reasons is that some cellular surface receptors or host factors encoded by the liver-specific genes are required for binding, uncoating and transport of viral particles. Several researchers also proposed that the low rate of cell division of primary hepatocytes favored the retrovirus infection (Miller *et al.*, 1990; Roe *et al.*, 1993; Sung and Lai, 2002). However, so far, the critical cellular factors, in particular the viral receptors have not yet been identified, which is in part due to the lack of either plaque assays or the efficient *in vitro* HBV infection systems.

In spite of the lack of HBV susceptible cell lines and limited animal models for HBV infection study, the life cycle of HBV has been gradually characterized since 1970s. The HBV virion, with its relaxed circular DNA genome, first attaches the cellular membrane and enters into the hepatocytes *via* an unknown mechanism. After the lipoprotein envelope is removed and the nucleocapsid is uncoated, the viral genome is transported into host nucleus, where the viral partially double-stranded DNA is repaired to form a covalently closed circular DNA (cccDNA). cccDNA functions as the template for RNA synthesis. With the help of the host RNA polymerase II, cccDNA is transcribed into

pregenomic (pg) and subgenomic (sg) RNA. Then the viral RNAs are transported into cytoplasm, where pg RNA is translated into core protein and reverse transcriptase (RT) while sg RNA is translated into envelope proteins (L, M and S proteins) and X protein. After that, the pg RNA is encapdidated within the core particles with RT *via* interacting with host-derived heat-shock proteins (Hu and Seeger, 1996). Within the nucleocapsid, the pg RNA is then reverse transcribed into the minus strand of HBV DNA by RT, and is concomitantly degraded by the RNase H activity of RT. Based on the sequence of the minus strand DNA, the complementary plus strand DNA is then synthesized. After that, parts of the newly uncoated nucleocapsids recycle viral DNA back to the host nucleus to generate more cccDNA, which is referred to as the intracellular conversion pathway. The remaining nucleocapsids bind to viral envelope proteins, bud into the endoplasmic reticulum (ER) and ultimately exit the cell. The life cycle of HBV is illustrated in Fig. 1-4.

1.1.2.3 HBV serotypes and genotypes

The genetic variability of HBV is very high. Based on the antigenic determinants of the HBsAg, HBV is classified into four major serotypes, *i.e.* adr, adw, ayr and ayw (Le Bouvier, 1971; Bancroft *et al.*, 1972). Meanwhile, HBV can also be divided into eight genotypes based on the divergence of the nucleotide sequences ≥8% in the whole genome or ≥4% in the S gene, which are designated A to H (Okamoto *et al.*, 1986; Okamoto *et al.*, 1988; Orito *et al.*, 1989; Norder *et al.*, 1992; Kidd-Ljunggren *et al.*, 2002; Norder *et al.*, 2004). And some HBV genotypes can be further divided into

subgenotypes based on the variance of the overall genome greater than 4% but less than 8%. Each HBV genotype/subgenotype exhibits distinct virological and epidemiological properties. They show geographic preferences and influence the severity and course of liver diseases and treatment outcomes (Magnius and Norder, 1995; Kidd-Ljunggren *et al.*, 2002; Miyakawa and Mizokami, 2003; Sugauchi *et al.*, 2003; Kramvis and Kew, 2005).

As shown in Fig. 1-5, genotype A is predominant in Northern and Western Europe as well as Southern Africa; genotype B and C are prevalent in Asia and the Southern Pacific region; genotype D prevails in the Mediterranean area, Eastern Europe, the Middle East and Northern Africa; genotype E is confined in the western sub-Saharan areas; genotype F is present in South America, and genotype G and H are mainly found in Mexico and Central America respectively within the populations originating from American continent. In China, genotype B and C are prevalent with uneven distribution. Genotype C is predominant (85.1%) in northern China while genotype B prevails (55.0%) in southern China (Hou *et al.*, 2005; Wang *et al.*, 2007).

1.1.3 Vaccination

To decrease the risk of chronic HBV infection and subsequent complications, vaccination is a very important and effective strategy. The first generation of plasma-derived hepatitis B (HepB) vaccine was licensed in United States in 1982. Consequently, in 1986, the second generation of HepB vaccine produced by

recombinant DNA technology was available. In 1991, the World Health Organization firstly recommended HepB vaccine to be universally administered to neonates and adolescents in countries with moderate to high prevalence of HBV infection. So far, the efficacy of routine infant HepB immunization in reducing chronic HBV infection and preventing liver cancer has been widely demonstrated in different countries and settings.

1.1.4 Treatment of HBV infection

Currently, two major therapies are widely applied for treatment of chronic hepatitis B infection: immunotherapy and chemotherapy. Unfortunately, neither of the two therapies is highly efficient and safe enough to fully eradicate HBV.

1.1.4.1 Immunotherapy

Interferon-alpha (IFN-α) is the first licensed treatment for HBV infection four decades ago. It's also the only drug for hepatitis B that possesses both immunomodulatory and anti-viral activities. The immunomodulatory properties of IFN-α include the activation of cellular and humoral immune responses that target and eliminate the infected hepatocytes. Antiviral activity of IFN-α includes the induction of intracellular anti-viral genes and signaling pathways. However, accumulated clinical data have shown that IFN-α has a modest efficacy rate, serious side effects, and is inconvenient for administration for its short half-life. To partially overcome these disadvantages, pegylated IFN-α was developed. Both PEG-IFNα-2a and PEG-IFNα-2b have been proven to have superior efficacy to standard unmodified IFN-α in clinics.

1.1.4.2 Chemotherapy

Having greater efficacy and fewer side effects, oral nucleotide and nucleoside analogues are frequently used to replace IFN-α. Lamivudine was the first licensed oral drug for CHB treatment. Other nucleotide analogues used in clinics include adefovir, tenofovir, entecavir, telbivudine, tenofovir, emtricitabine and clevudine. The nucleotide/nucleoside analogues suppress HBV replication mainly through inhibition of HBV DNA polymerase and/or chain termination. Their unique advantages over IFN-based therapy include efficacy in prior IFN nonresponders and patients with high-level HBV DNA, and efficacy in preventing and reversing fibrosis, cirrhosis and hepatic decompensation. However, prolonged usage of nucleotide/nucleoside analogues leads to a high rate of viral resistance.

More and more clinical trials have demonstrated that combination therapy appears to be more effective than either IFN or nucleotide/nucleoside analogue alone in treatment of CHB, which serves as the first-line regimen.

1.1.5 HBV and hepatocellular carcinoma

Epidemiological and experimental studies have demonstrated that HBV infection is one of the major risk factors for hepatocarcinogenesis and HBV is one of the few human oncogenic viruses. Globally, about 300,000-500,000 people die of HBV-induced HCC per year (Parkin *et al.*, 2001). And HCC has been ranked as the 3rd leading cause of

cancer death worldwide, after lung cancer and stomach cancer (Parkin *et al.*, 2001).

At present, it's commonly believed that the carcinogenic effects of HBV in HCC development are attributed to the following aspects. First, HBV DNA integrates into host genome. The random integration of HBV DNA into cellular DNA and the rearrangement of integrated HBV DNA have been found in most chronic hepatitis and HCC tissues (Brechot *et al.*, 1981a; Brechot *et al.*, 1981b; Shafritz *et al.*, 1981; Yaginuma *et al.*, 1987; Takada *et al.*, 1990), which lead to chromosome instability and tumor progression. Second, the integrated HBV DNA can trans-activate certain cellular genes, such as retinoic acid β -receptor (Dejean *et al.*, 1986), cyclin A (Wang *et al.*, 1990), mevalonate kinase (Graef *et al.*, 1994), c-myc/N-myc (Bruni *et al.*, 2004; Jacob *et al.*, 2004), sarco/endoplasmic reticulum calcium ATPase 1 (Brechot *et al.*, 2000) and human telomerase reverse transcriptase (Horikawa and Barrett, 2001; Hytiroglou and Theise, 2006). Therefore, the viral integration in the vicinity of genes controlling cell growth, division and differentiation, as well as the insertional activation of these genes, alter the genes' functions and probably induce cellular malignant transformation. Third, HBx, the 154 amino acid gene product of the HBV X gene, functions as a transcriptional transactivator that activates a wide range of viral and cellular genes and oncogenic signaling pathways (Kim *et al.*, 1991; Yen, 1996; Elmore *et al.*, 1997; Gottlob *et al.*, 1998; Zhang *et al.*, 2006). Thus, the proapoptotic activity of HBx may contribute to the viral carcinogenesis. Fourth, other HBV gene products [*i.e.* Pre S1, Pre S2, S, hepatitis e antigen (HBeAg)] and specific HBV mutants (*e.g.* the

A1762T/G1764A mutation in the basal core promoter) are also shown to promote tumorigenesis (Ono *et al.*, 1998; Yang *et al.*, 2002; Kuang *et al.*, 2005; Wang *et al.*, 2006; Liang *et al.*, 2008).

1.2 The heat shock protein glucose-regulated protein 78

Glucose-regulated protein 78 kDa, also known as immunoglobulin heavy-chain binding protein (Bip), is a member of heat shock protein 70 family which is primarily located in the ER. It was first discovered in the late 1970s as cell protein induced by glucose deprivation in culture medium (Lee, 2001). Subsequent studies reveal GRP78 can also be stimulated by a variety of environmental and physiological stress conditions, such as hypoxia, low pH, intracellular Ca^{2+} efflux and viral/bacteria infection.

1.2.1 Biochemical properties of GRP78

In the ER, GRP78 is a molecular chaperone that binds transiently to a variety of the unfolded/misfolded proteins and regulates protein folding in cooperation with the proteins of protein disulfide isomerase (PDI) family.

Biochemical studies have revealed there are two major functional domains in GRP78: an N-terminal ATPase domain and a C-terminal polypeptide-binding domain. These two domains cooperate and communicate to regulate the repetitive cycles of ATP hydrolysis, ADP exchange, as well as binding and release of the unfolded protein.

When unfolded/misfolded proteins accumulate in the ER, GRP78 recognizes and binds to the exposed hydrophobic residues of them. Subsequent ATP hydrolysis strengthens the interaction between GRP78 and the unfolded/misfolded protein substrates, which are then submitted to PDI for disulfide oxidation and rearrangement. When the correct protein conformation is formed, ADP-ATP exchange occurs in the ATPase domain of GRP78, and the prefolded protein is released. Hydrolysis of ATP returns GRP78 to the ADP-bound form with high affinity for the unfolded protein substrates in the next cycle. Therefore, on one hand, the ATP/ADP binding in the ATPase domain determines the affinity and duration of GRP78-substrate complex; on the other hand, the interaction between GRP78 and substrates defines the rate of ATP/ADP exchange.

1.2.2 Functions of GRP78

As a highly conserved protein from yeast to man, GRP78 is indispensable for a variety of fundamental biological functions, including facilitating protein folding and assembly, preventing intermediates aggregation, targeting misfolded protein for degradation, maintaining Ca^{2+} homeostasis, protein transportation and signaling the unfolded protein response (Kaufman, 1999; Lee, 2001). These functions of GRP78 are mainly linked with its ER location. Interestingly, continuous work have demonstrated that GRP78 is also found in a variety of subcellular compartments when cells are experiencing ER-stress, including nuclear envelope (Bole *et al.*, 1989), mitochondria (Sun *et al.*, 2006), cytosol (Duriez *et al.*, 2008) and plasma membrane (Triantafilou *et al.*, 2001; Arap *et al.*, 2004; Davidson *et al.*, 2005). Thus, the non-ER locations of GRP78 extend

its basic function in ER quality control to intracellular communication (Sun *et al.*, 2006), protein secretion (Duriez *et al.*, 2008), signal transduction (Misra *et al.*, 2005, 2006), viral entry (Triantafilou *et al.*, 2002; Jindadamrongwech *et al.*, 2004) and antigen presentation (Hegde *et al.*, 2006).

1.2.3 Regulation of GRP78 transcription

The transcriptional activation of GRP78 is widely used as a marker for ER stress and the unfolded protein response (UPR) activation. It has been demonstrated that ER stress response element (ERSE) was the most critical element in GRP78 promoter that mediated stress induction of GRP78 (Mao *et al.*, 2006). Specific transcription factors that bind to the ERSE sequence include NF-Y, YY1, TFII-I, Sp1 and the nuclear fraction of ATF6 (Li *et al.*, 2000; Yoshida *et al.*, 2000; Parker *et al.*, 2001; Abdelrahim *et al.*, 2005; Baumeister *et al.*, 2005; Hong *et al.*, 2005). Among them, the nuclear fraction of ATF6 is the most potent activator for GRP78 induction. It is released by proteolysis from the inactive form of ATF6 in cytoplasm, then the cleaved ATF6 is transported into nucleus and enhances the transcription of GRP78 in combination with YY1, ATFII-I and NF-Y during the UPR activation (Yoshida *et al.*, 2001b). Additional chromatin changes of the histone H4 protein, including acetylation and arginine 3 methylation, are also observed in the enhanced transcription of GRP78 induced by ER stress (Baumeister *et al.*, 2005).

1.2.4 The roles of GRP78 in mammalian development and human diseases

Luo *et al.* reported that the complete deletion of GRP78 in 3.5-day-old mouse embryos was lethal using traditional knockout approach, while 50% level of wild-type GRP78 was sufficient to maintain ER homeostasis and embryonic cell growth (Luo *et al.*, 2006). Using transgenic mouse, Mao *et al.* further demonstrated the transcriptional activation of GRP78 during embryonic development was ERSE sequence dependent (Mao *et al.*, 2006). In addition, accumulating evidence has revealed that GRP78 is up-regulated during embryonic cardiac development, which suggests physiological ER stress and high demand for glucose as major energy source exist during cardiogenesis due to the increased protein synthesis and secretion (Mesaeli *et al.*, 2001; Mao *et al.*, 2004; Mao *et al.*, 2006).

In addition to its important roles in the early embryonic development, GRP78 is also positively correlated with tumor progression, metastasis and chemotherapeutic resistance, as evidenced by the overexpression of GRP78 in malignant and metastatic cancer cells and tissues (Fu and Lee, 2006; Li and Lee, 2006; Lee, 2007). So far, the elevated GRP78 level has been detected in acute myeloid leukemia, breast cancer, lung cancer, gastric cancer, hepatocellular cancer and prostate cancer (Thomas *et al.*, 2005; Li and Lee, 2006). Suppression of GRP78 by antisense sensitizes cancer cells to chemotherapy or reverses the chemotherapy resistance (Dong *et al.*, 2005; Li and Lee, 2006).

Emerging evidence has shown that GRP78 binds to amyloid precursor protein (APP)

and its overexpression inhibits APP maturation and reduces the production and accumulation of β -amyloid peptides, which suggests GRP78 can ameliorate the accumulation of misfolded proteins and protect neuronal cells from neurotoxicity during neurodegeneration (Hoshino *et al.*, 2007).

As a versatile molecule, GRP78 also plays a role in diabetes, which is well-characterized by perturbed glucose metabolism (Scheuner *et al.*, 2005). The disregulation of GRP78 is also implicated in atherosclerosis (Werstuck *et al.*, 2001; Watson *et al.*, 2003), thrombosis (Kumar *et al.*, 2003; Paschen and Mengesdorf, 2005), and rheumatoid arthritis (Nagaraju *et al.*, 2005; Panayi and Corrigall, 2006).

1.2.5 GRP78 and the unfolded protein response

ER is an important organelle that serves essential functions in protein synthesis, folding, assembly, posttranslational modifications and secretion (Kaufman, 2002; Rutkowski and Kaufman, 2004). It's also the major site for calcium storage and cholesterol and lipid biosynthesis. Once the ER homeostasis is broken under the pathophysiological conditions, such as ischemia, hypoxia, intracellular Ca^{2+} disturbance, glucose deprivation and viral/ bacteria infection, the normal protein folding and maturation are perturbed and the accumulation of unfolded or misfolded proteins in ER is resulted, which leads to ER stress (Kaufman, 1999; Lee, 2001). As a cellular adaptive and cytoprotective response to ER stress, the unfolded protein response (UPR) is then activated.

Tremendous studies have demonstrated UPR is highly conserved during evolution (Kozutsumi *et al.*, 1988; Foti *et al.*, 1999). In mammalian cells, the UPR is mediated by three ER transmembrane proteins: 1) the protein kinase-like ER resident kinase (PERK), 2) the inositol-requiring enzyme 1 (IRE1) and 3) the activating transcription factor 6 (ATF6). Among UPR, GRP78, one of the best-characterized molecules, plays a central role in sensing ER stress and triggering UPR signaling. In the absence of ER stress, GRP78 is mainly associated with PERK, IRE1 and ATF6, which keeps them in an inactive state. However, upon ER stress, GRP78 is released from the three ER membrane-anchored proteins and binds to unfolded/misfolded proteins in ER lumen, which leads to the activation of PERK, IRE1 ATF6 and the UPR signaling from ER to nucleus (Bertolotti *et al.*, 2000). Multiple studies have shown that the UPR signaling transducers PERK, IRE1 and ATF6 regulate their distinct down-stream targets and ultimately cope with ER stress through up-regulation of ER chaperones and folding enzymes, transient inhibition of protein synthesis, enhanced degradation of unfolded/misfolded proteins and cell cycle arrest (Lee *et al.*, 1986; Brostrom *et al.*, 1996; Brodsky *et al.*, 1999; Kostova and Wolf, 2003). The first three strategies contribute to increasing the ER folding and secretory capacities, as well as preventing the aggregation of unfolded/misfolded proteins in ER, whereas the cell cycle arrest, which inhibits the proliferation of stress-experiencing cells, is considered to be a protection against both cell and organism damages. If extreme or prolonged ER stress occurs and can't be alleviated, apoptosis is initiated by another ER stress sensor caspase 12 to destroy the

cell (Nakagawa *et al.*, 2000). At present, the molecular events of how GRP78 sense ER stress and how the UPR signal transduction network is regulated to meet cellular demand according to the variable extent of ER stress in different cell types are not well understood. The UPR pathways in mammalian cells are illustrated in Fig. 1-6.

1.2.5.1 The IRE1 branch

The first identified and characterized UPR component is Ire1p in yeast (Cox *et al.*, 1993; Mori *et al.*, 1993). Sharing the same features as yeast Ire1p, two IreI homologues-IRE1 α and IRE1 β, exist in mammalian cells (Tirasophon *et al.*, 1998; Wang *et al.*, 1998). In both human and mouse, IRE1 α is ubiquitously expressed, while IRE1 β is restricted to intestinal epithelial cells (Bertolotti *et al.*, 2001). IRE1 is a serine/threonine protein kinase that possesses endoribonuclease activity (Niwa *et al.*, 1999; Tirasophon *et al.*, 2000; Iwawaki *et al.*, 2001). Activated IRE1 initiates the unconventional splicing of the X-box-binding protein-1 (XBP-1) mRNA, which leads to a translational frame shift in XBP1 coding sequence, producing a spliced XBP1 protein (Yoshida *et al.*, 2001a; Calfon *et al.*, 2002; Lee *et al.*, 2002). This spliced form of XBP1 contains both a DNA binding domain and a transactivation domain, through which it binds directly to the unfolded protein response element (UPRE) of target genes and activates their transcription. Accumulating data have demonstrated that genes involved in the ER-associated protein degradation (ERAD) pathway (Yoshida *et al.*, 2003), co-factors of the ER chaperone GRP78 (Lee *et al.*, 2003), the inhibitor of PERK p58IPK (Yan *et*

al., 2002) and components of lipid synthesis (Sriburi *et al.*, 2004) are all regulated by the spliced XBP1 during UPR.

1.2.5.2 The PERK branch

Among the three UPR branches, PERK-mediated signaling pathway serves the most important functions in governing cell survival and death. Similar to IRE1, PERK is also a serine/threonine kinase that phosphorylateds the α subunit of eukaryotic translation initiation factor 2 (eIF2 α), leading to the overall translation repression to alleviate the protein folding burden on the ER (Shi *et al.*, 1998; Harding *et al.*, 1999). PERK-mediated eIF2 α phosphorylation also inhibits cyclin D1 translation, causing a G1 phase cell-cycle arrest (Brewer and Diehl, 2000). In contrast to translational inhibition, PERK-eIF2 α pathway specifically activate the transcription of ATF4 (Harding *et al.*, 2000; Scheuner *et al.*, 2001), which transactivates the downstream gene encoding C/EBP-homologous protein (CHOP) and then induces apoptotic cell death (Zinszner *et al.*, 1998; McCullough *et al.*, 2001). Additional data also show ATF4 can up-regulate the growth arrest and DNA damage-inducible protein 34 (GADD34), the regulatory subunit of the PP1 phosphatase that dephosphorylates eIF2 α , causing the reversion of translation arrest and leading to apoptosis (Novoa *et al.*, 2001; Ma and Hendershot, 2003). Thus, PERK plays a role in activating apoptotic genes.

On the contrary, PERK-mediated eIF2 α phosphorylation is also required for NF- κ B activation (Jiang *et al.*, 2003), which positively regulates anti-apoptotic proteins like

BCL2 during ER stress. Thus, PERK regulates both cell survival and cell death pathways.

1.2.5.3 The ATF6 branch

ATF6 is a type-II ER-transmembrane transcription factor, with a stress sensing domain located in the C-terminal luminal portion and a transcription activation domain present in the N-terminal cytosolic portion (Haze *et al.*, 1999). Under non-stressed conditions, ATF6 is sequestered from activation by binding to GRP78. Once ER-stress is induced, with the dissociation from GRP78, ATF6 is released from ER membrane and moves to Golgi (Shen *et al.*, 2002), where it is sequentially cleaved by the Golgi-resident proteases Site 1 Protease (S1P) and Site 2 Protease (S2P) and the cytosolic fragment is then released (Haze *et al.*, 1999; Ye *et al.*, 2000; Haze *et al.*, 2001). After that, the cytosolic fragment of ATF6 is transported into the nucleus and functions as a potent transcription factor, which binds directly to the ERSE of UPR-target genes in collaboration with nuclear transcription factor Y (NF-Y) (Wang *et al.*, 2000; Yoshida *et al.*, 2000; Kokame *et al.*, 2001; Yoshida *et al.*, 2001b) and up-regulates the transcription of XBP1 (Yoshida *et al.*, 2001a; Lee *et al.*, 2002) and ER chaperons such as GRP78, GRP94 and calreticulin, as well as folding enzymes like peptidyl-prolyl isomerase B (PPIase B) and PDI (Yoshida *et al.*, 1998).

1.3 Objectives of the study

HBV infection is a severe health problem, which has attracted world-wide attention. Although great progress has been made in the prevention and treatment of HBV infection, the pathogenesis of the HBV and the mechanisms of HBV-host interactions are still poorly understood. And the lack of efficient HBV infection systems also hinders our understanding of the progression of HBV-associated liver diseases.

In order to reveal the host early response to HBV replication and to delineate a comprehensive picture of the interactions between HBV and hepatocytes, we performed the comparative proteomic analysis to characterize the host responsive factors using an inducible HBV-producing cell line. GRP78, as one of the most significantly up-regulated host proteins induced by HBV replication, was further selected for validation in different HBV-transfected cell lines and clinical HBV-infected liver biopsies.

Considering the important roles played by GRP78 in viral infection and cell survival, we postulated that GRP78 might be a key host responsive factor. To study the functions of GRP78 in HBV replication, we performed both the loss- and gain-of-function studies in HBV-transfected HepG2 cells, and investigated whether GRP78 deficiency or overexpression would alter HBV replication efficiency. Finally, we investigated the mechanisms involved in the anti-HBV activities of GRP78 in hepatocytes.

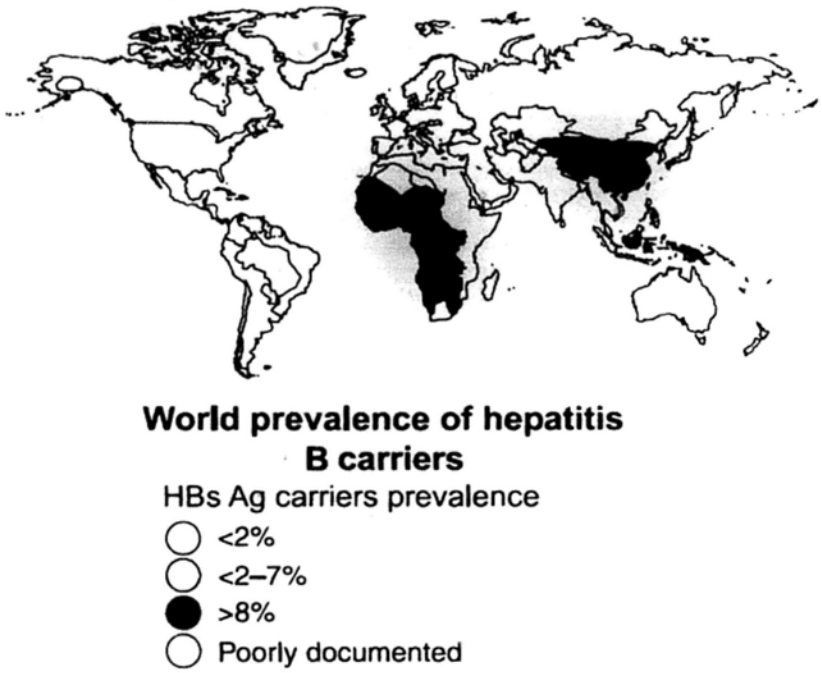

Fig. 1-1. Worldwide distribution of chronic HBV infection. HBsAg, hepatitis B surface antigen. (Lavanchy, 2004)

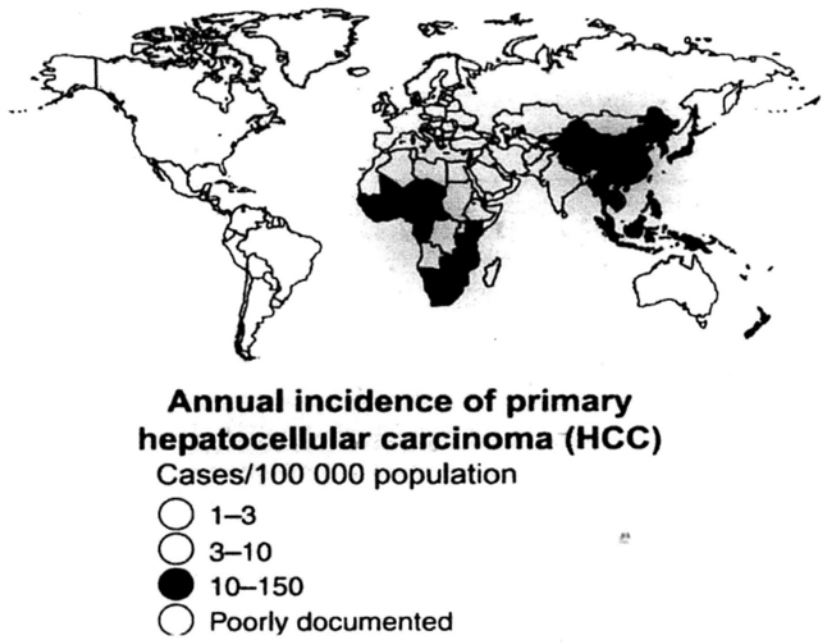

Fig. 1-2. Worldwide annual incidence of primary hepatocellular carcinoma. (Lavanchy, 2004)

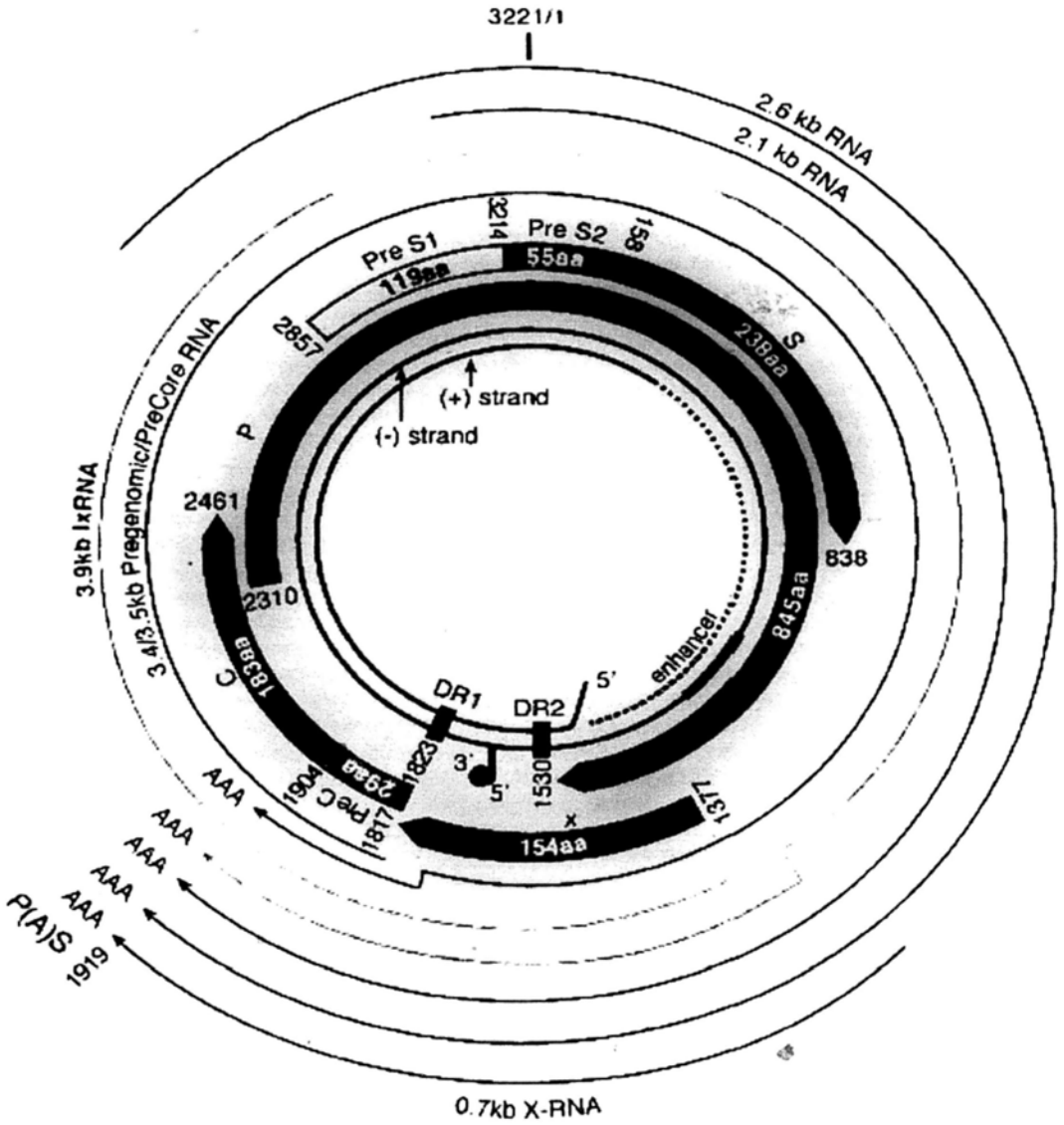

Fig. 1-3. The genomic organization and transcription map of HBV (adw). Inner circles represent the viral partial dsDNA, wide arrows represent the overlapping viral ORFs, and the outer thin arrows represent the five viral transcripts labeled with their respective length in kilobases (kb). P, RT-polymerase; DR, direct repeats. (Doitsh and Shaul, 2003)

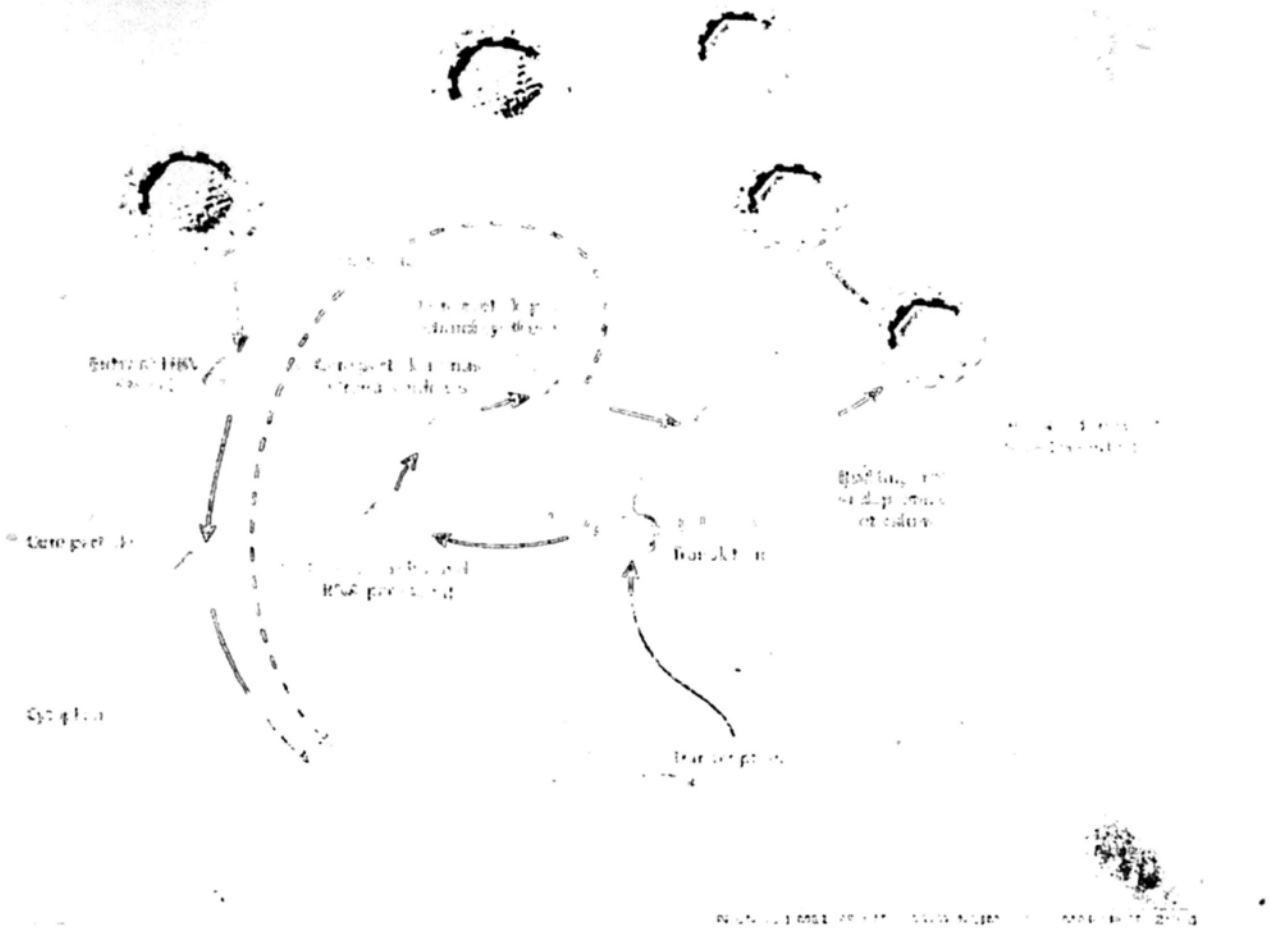

Fig. 1-4. The life cycle of HBV. HBV enters the hepatocyte, and the envelope is subsequently removed. Within the nucleus, the partially double-stranded DNA is repaired to form a cccDNA, which serves as the stable template for the transcription of the viral mRNA necessary for productive viral replication. This cccDNA template remains in the nucleus during chronic viral infection and may persist in the liver for the lifetime of the patient. The HBV mRNA is then packaged into capsid in the cytoplasm and reversely transcripted into DNA. Finally, the nucleocapsids are enveloped in the ER and transported to the cell membrane. (Wands, 2004)

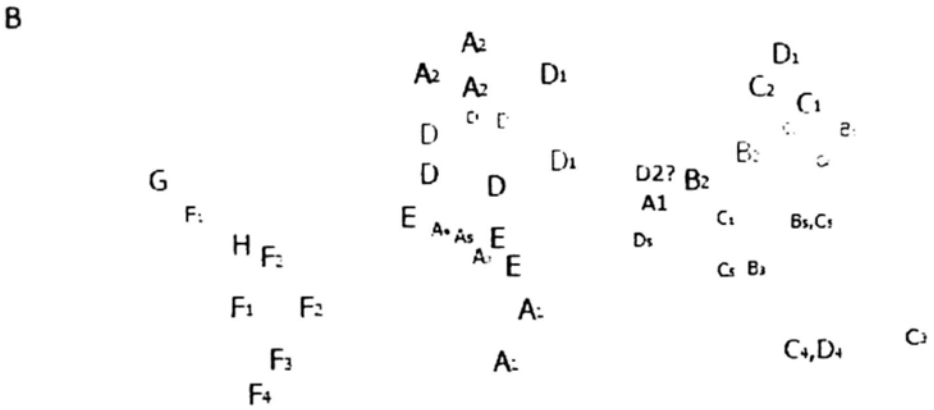

Fig. 1-5. Geographic distribution of HBV genotypes and subgenotypes. (Schaefer, 2007)

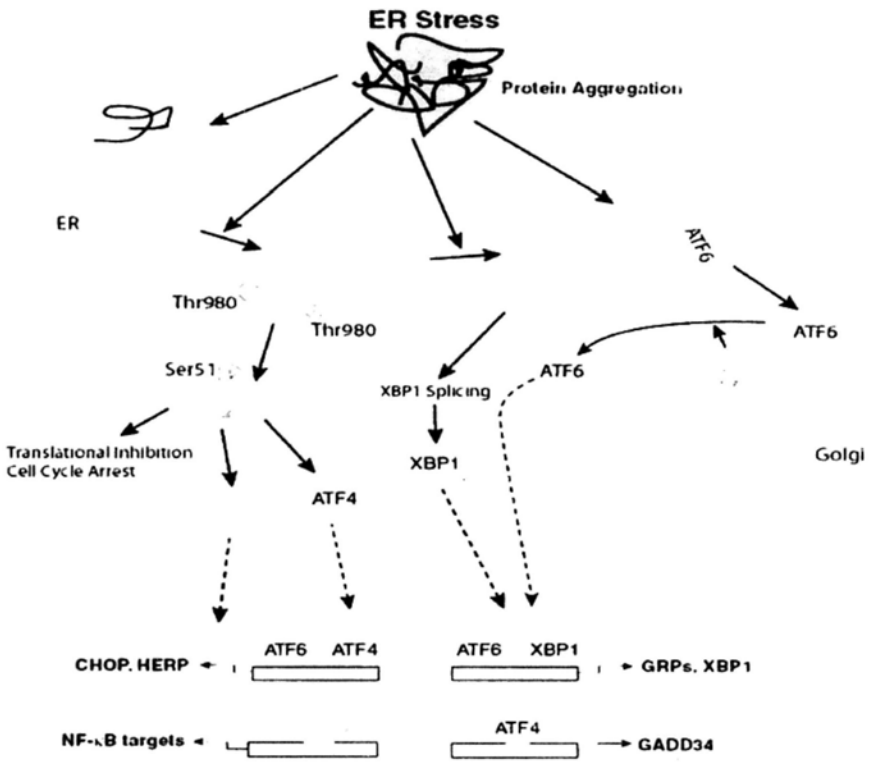

Fig. 1-6. The unfolded protein response pathways in mammalian cells. (http://www.cellsignal.com/)

Chapter 2

Proteomic Analysis of the Host Early Response to HBV

2.1 Introduction

Although the prevention and treatment of chronic HBV infection is improving, the limited efficacy of antiviral therapies, high rates of post-treatment HBV relapse and the emergence of drug-resistant viral mutants have greatly hindered the effective management of CHB infection. Therefore, it is of prime importance to understand the mechanisms of HBV-host interactions during malignant transformation in CHB infection to identify novel therapeutic anti-HBV targets.

Because human HBV is incapable of infecting hepatocytes *in vitro* efficiently and the availability of reliable *in vitro* culture systems that favor HBV replication is limited, the pathogenetic studies of HBV and the development of anti-HBV drugs have long been hampered. HepAD38 and HepG2.2.15, both of which are derived from HepG2 cells and integrated with a more-than-one-unit-length HBV genome, have been widely accepted and are well established cell lines for the study of HBV life cycle and screening potential HBV inhibitors since the late 1990s (Sells *et al.*, 1987; Ladner *et al.*, 1997). Recently, the comparative proteomic analysis of the HBV-expressing HepG2.2.15 cells and the parental HepG2 cells has been performed in two independent laboratories to characterize the altered proteome profile induced by HBV (Tong *et al.*, 2008; Liu *et al.*,

2009). However, the different genetic backgrounds of HepG2.2.15 and HepG2 may lead to an inaccurate evaluation of the impact of HBV replication on host genes. When compared with HepG2.2.15 cells which produce HBV particles in a continuous manner, HepAD38 cells produce higher levels of HBV DNA in a controllable and inducible way (Ladner *et al.*, 1997). HBV production in HepAD38 is under the strict control of a tetracycline-responsive promoter; therefore, a direct comparison of cellular characteristics with or without HBV replication in HepAD38 is easily achieved. To date, changes in proteome profile of HepAD38 induced by HBV replication have not been reported.

In this part of study, we performed comparative proteomics to globally analyze the host early response to HBV by using an inducible HBV-producing cell line HepAD38. The combination of two-dimensional gel electrophoresis (2-DE) and matrix-assisted laser desorption/ionization time of flying mass spectrometry (MALDI-TOF MS) revealed that 23 cellular proteins were differentially expressed when HBV replicated. Among them, GRP78, which was one of the most highly up-regulated proteins, was further selected for validation.

2.2 Materials and methods

2.2.1 Plasmid constructs

The pHBV (1.1-fold HBV genome, genotype C) was used to produce HBV virion as previously described (Chen *et al.*, 2003).

2.2.2 Cell culture

The human hepatoma cell lines HepAD38 and HepG2 were maintained in Gibco Dulbecco's Modified Eagle's Medium supplemented with 10% fetal bovine serum, 1% penicillin/streptomycin and 1% glutamine at a humidified condition of 5% CO_2 at 37°C. For HepAD38 cells, the medium was further supplied with 400 μg/ml G418 and 2 μg/ml tetracycline.

To begin an assay, confluent HepAD38 cells were washed with pre-warmed PBS sufficiently and then fed with medium without tetracycline in which the replication of wide-type HBV was induced. Forty-eight hours later, both tetracycline-treated and non-tetracycline-treated HepAD38 cells were submitted to 2-DE analysis. To rule out the effects of tetracycline instead of HBV replication on host proteome profile, comparative proteomic analysis of tetracycline-treated and non-tetracycline-treated HepG2 cells was performed in parallel.

2.2.3 Cell transfection

To detect the expression level of GRP78, 2 x 10^6 HepG2 cells were transfected with 5 μg of pHBV or empty vector by nucleofection using Cell Line Nucleofector™ kit V and Amaxa Nucleofector II device (program T-28, Amaxa biosystems, Germany). After nucleofection, cells were transferred to 6-well plates and left for incubation for 48 h before real-time RT-PCR and Western blot analysis.

2.2.4 Clinical specimens

Paired pre- and post-lamivudine treatment paraffin-embedded liver biopsies were collected from19 patients [mean age ± standard deviation (S.D.), 35.3 ± 10.3 years; range, 21-57 years; male : female, 14:5] who were diagnosed with chronic hepatitis B at the Hepatitis Clinic of the Prince of Wales Hospital, Hong Kong, between June 2000 and January 2003. All patients had been positive for HBsAg for at least 6 months, were HBeAg-positive, had a serum HBV DNA level of at least 500,000 copies/mL with an alanine aminotransferase level that was 1.3 to 5 times the upper limit of normal, and were treatment-naïve before receiving the 52-week lamivudine monotherapy. Patients who met one of the following criteria were excluded from the study: history of decompensated liver disease or interferon or antiviral agent use; co-infection with hepatitis C virus (HCV), hepatitis D virus (HDV) or human immunodeficiency virus (HIV); history of HCC; other causes of liver disease (Chan *et al.*, 2005); serious medical or psychiatric illness; concurrent use of corticosteroid or immunosuppressive agents; and pregnancy. Liver biopsy was performed within 4 weeks before treatment began and at the end of treatment. Sera were collected immediately before and after lamivudine treatment for HBV DNA quantification. The study was approved by the ethics committee of the Chinese University of Hong Kong and written informed consent was obtained from each patient.

2.2.5 Sample preparation for 2-DE

The HepAD38 cells and the parental HepG2 cells were harvested 48 h post treatment (with and without tetracycline). HepG2 cells were used to exclude the cell responses to tetracycline. Cells were washed with PBS, lysed in lysis buffer (8 M urea, 2 M thiourea, 2% CHAPS, 1% Nonidet P-40, 2 mM tributylphosphine, 1 x Roche protease inhibitor cocktail, 1 x nuclease mix, 1 mM PMSF, and 2% IPG buffer) and then left on ice for 45 min. After centrifugation at 14,000 x g for 15 min at 4°C, the supernatant was collected and stored at -80°C until use. Protein concentrations were determined by the Bradford method (Bio-Rad, USA).

2.2.6 2-DE

Isoelectric focusing (IEF) was performed using 13-cm precast IPG strips (pH 4 to 7, linear, GE Healthcare, USA) in Ettan IPGphor II IEF System (Amersham, USA) according to the manufacturer's instructions. The IPG strips were rehydrated for 10 h at 30 V with 250 µl of rehydration buffer (8 M Urea, 2% CHAPS, 0.4% DTT, 0.5% IPG buffer, 0.002% bromophenol blue) containing 150 µg of protein samples. The rehydrated strips were then focused by using a stepwise voltage increment program: 500 V and 1000 V for one hour each, and 8000 V afterwards until 64 KV/h. After IEF, the isoelectrically focused strips were incubated in an equilibration buffer (6 M urea, 1% DTT, 2% SDS, 30% glycerol, 0.002% bromophenol blue, 50 mM Tris-HCl, pH 6.8) for 15 min with gentle agitation followed by an incubation in the same buffer containing 2.5% iodoacetamide in place of DTT for another 15 min. The equilibrated strips were loaded onto 12.5% SDS-PAGE gels. The gels were run at 15 mA/gel for 30 min and

then 30 mA/gel until the dye fronts reached the bottoms of the gels.

2.2.7 Image analysis

The gels were stained by the modified silver staining method compatible with MS analysis. The staining procedure was carried out as previously described (Chen *et al.*, 2007). Gel images were acquired with a calibrated GS-800 scanner and Quantity One software (Bio-Rad, USA). Further data processing was completed by using PDQuest 2-D analysis software (version 8.0, Bio-Rad, USA) for spot detection, spot matching, volume normalization and quantitative intensity analysis. The parameters for spot detection were set as follows: ruby speckles, 50; smoothing, medium 7×7; background removal, floating ball, 61; removal vertical streaks, 93; removal horizontal streaks, 93; sensitivity, 16.51; size scale, 5; and min peak, 868. After manual editing, spots on different gels were matched, compared and analyzed. All paired samples were run thrice independently to guarantee reproducibility. A 2-fold increase/decrease (non-tetracycline-treated HepAD38 *versus* tetracycline-treated HepAD38) in spot intensities was set as the threshold for indicating significant changes.

2.2.8 In-gel tryptic digestion

Spots showing significant changes in intensities were manually cut from the gels. Gel pieces were destained and washed before in-gel digestion as described previously (Chen *et al.*, 2007). Gels were then dried completely by vacuum and digested with 10 μg/mL of trypsin (Promega, USA) in 25 mM ammonium bicarbonate (pH 8.0) for 16-18 h at

37°C. Thereafter, the supernatants containing tryptic peptides were collected.

2.2.9 MALDI-TOF/TOF MS and MS/MS spectrometry analysis

For acquisition of mass spectra, 0.5 µl of peptide solution was mixed with 0.5 µl of matrix (4 mg/mL α-cyano-4- hydroxylcinnamic acid in 35 % ACN and 1% TFA) before spotting onto the MALDI plate. Mass spectrometric analyses were performed on a MALDI-TOF/TOF tandem mass spectrometer ABI 4700 proteomics analyzer (Applied Biosystems, USA). The instrument was equipped with a 337 nm nitrogen laser and was operated in batched processing and automatic MS to MS/MS switching modes. All mass spectra were accumulated from 2000 laser shots with an accelerating voltage of 20 kV and acquired over a mass range of 800-3500 *m/z* in a positive-ion reflectron mode by using the 4000 Series Explorer™ V3.0 software package. An internal calibration in MS mode was achieved with the ions of porcine trypsin autolysis peptides at *m/z* 842.509, *m/z* 1045.564, *m/z* 1940.935 and *m/z* 2211.104, resulting in mass errors of less than 30 ppm. The MS spectrum exclusion lists are shown in the appendix Fig. A1. The MS peaks (MH^+) were detected on a minimum S/N ratio ≥20 and cluster area S/N threshold ≥25 without smoothing and raw spectrum filtering. Peptide precursor ions corresponding to contaminants, including human keratin and trypsin autolysis peptides, were excluded in a mass tolerance of ± 0.2 Da. The precursor ions with a minimum signal to noise ratio of 50 were selected for MS/MS scanning. Fragmentation of precursor ions was performed in a collision-induced dissociation (CID) cell using argon as collision gas with 1 kV energy in the positive ion mode. MS/MS spectra were

obtained by collecting 3000 laser shots with a default calibration. The MS/MS peaks were detected on a minimum S/N ratio ≥3 and cluster area S/N threshold ≥15 with smoothing.

2.2.10 Database search

Combined MS (peptide mass fingerprint approach) and MS/MS (de novo sequencing approach) analysis was applied for protein identification. The MS and MS/MS spectra were submitted to Mascot search engine (version 1.9.05, Matrix science, UK) and searched against NCBInr database (5,825,255 protein sequences; released on January 10, 2008) using GPS Explorer™ software (version 3.5, Applied Biosystems, USA). The search parameters were defined as follows: taxonomy of Homo sapiens, trypsin digest with a maximum of one missed cleavage, fixed modification of cysteine carbamidomethylation, variable modification of methionine oxidation, monoisotopic peptide mass (MH^+), mass range of 800-3,500 Da, pI of 0-14, precursor tolerance of 50 ppm, and MS/MS fragment tolerance of 0.1 Da. Known contaminant ions corresponding to human keratin and trypsin autolysis peptides were removed from the spectra before database searching. The top five hits for each protein search were reported. Only proteins with Mascot protein scores (based on both MS and MS/MS spectra) over 67 ($p < 0.05$), sequence coverage over 13% as well as a minimum of two matched peptides were considered to be positively identified. If a protein spot matched multiple members of a protein family, the protein candidate with the maximum number of matched peptides and a pI value nearest to the observed value was chosen to report.

Each isoform of a protein family identified in our study was considered to be a distinct protein for analysis.

2.2.11 Quantitation of GRP78 messenger RNA (mRNA) expression level

Total RNA was isolated from HepG2 cells using TRIzol reagent (Invitrogen, USA) according to the manufacturer's instructions. 1 μg of total RNA was subjected to reverse transcription using the ImProm-II™ Reverse Transcription System (Promega, USA). The quantitative real-time PCR was carried out in the ABI 7500 Real-Time PCR system with Power SYBR Green Master Mix (Applied Biosystems, USA), using the following program: 50 °C for 2 min, 95°C for 10 min followed by 40 cycles of 95°C for 15 s and 60°C for 1 min. Fluorescence signals were collected during the extension phase of each PCR cycle. Primers used for GRP78 and glyceraldehyde-3-phosphate dehydrogenase (GAPDH, internal control) are as follows: GRP78, forward, 5'-GACGGGCAAAGATGTCAGGAA-3', reverse, 5'-TCATAGTAGACCGGAACAGATCCA-3'; GAPDH, forward, 5'-GATTCCACCCATGGCAAATTCCA-3', reverse, 5'-TGGTGATGGGATTTCCATTGATGA-3'. Standard curves for quantification were obtained by serial dilutions of the PCR products containing corresponding gene fragments. All samples were run in triplicate and the experiment was repeated thrice. The mRNA level of GRP78 was normalized to the mRNA copies of GAPDH in the same sample and results were expressed as a percentage of the negative control (set as 100%).

2.2.12 Western blotting

Cells were washed with PBS and lysed on ice for 30 min in RIPA buffer (50 mM Tris•HCl, pH 7.5, 150 mM NaCl, 1 mM EDTA, 1% Triton X-100, 0.1% SDS, 1 x Roche protease inhibitor cocktail, 1 x Roche PhosSTOP^{TM} phosphatase inhibitor cocktail) with occasional vortexing. Lysates were then collected by centrifugation at 14,000 rpm for 10 min at 4°C, and protein concentrations were determined by the Bradford method (Bio-Rad, USA). Total proteins (20 μg/sample) were separated by 12% SDS-PAGE and transferred onto polyvinylidene difluoride (PVDF) membranes (Amersham Biosciences, USA). Membranes were blocked by 5% skim milk in TBST (20 mM Tris•HCl, pH 7.4, 150 mM NaCl, 0.1% Tween 20) followed by an incubation with specific antibodies (Santa Cruz Biotechnology, USA) against GRP78 (1:500 dilution) or GAPDH (1:10,000 dilution). Target proteins were finally visualized with horseradish peroxidase-conjugated secondary antibodies (1:3,000 dilution, Santa Cruz Biotechnology, USA) using a chemiluminescence detection system (Amersham Biosciences, USA). Each immunoblot was done thrice to confirm the results.

2.2.13 Immunohistochemistry

Paraffin sections from 19 paired liver biopsy specimens were used in this study. After deparaffinization and rehydration, tissue sections (4 μm thick) were microwaved in citrate buffer (pH 6.0) for 5 min in a pressure cooker for antigen retrieval. Hydrogen peroxide (3%) was then applied to the sections to quench endogenous peroxidase

activity. After blocking nonspecific binding with 10% non-immune goat serum, sections were incubated with primary antibodies against GRP78 (1:200 dilution in 1% BSA; Cell signaling Technology, USA) for 2 h at room temperature. A negative control was done by replacing the primary antibody with 1% BSA in PBS. After extensive rinse, sections were successively treated with biotinylated secondary antibodies and horseradish peroxidase-streptavidin conjugate (Histostain-Plus Kits, ZYMED Laboratories, USA). GRP78 signals were visualized by diaminobenzidine, and the sections were counterstained with hematoxylin. The immunoreactivity of GRP78 was evaluated by two independent investigators who were blinded to all clinical data and was scored by staining intensity and immunoreactive cell percentage (1, weak staining; 2, moderate staining in ≤30% of cells; 3, moderate staining in 30% to 80% of cells; 4, intense staining in ≥80% of cells). In case of disagreement, slides were re-evaluated until consensus was achieved.

2.2.14 Statistical analysis

Data are expressed as mean ± S.D.. All statistical analyses were carried out with SPSS 14.0 software (SPSS Inc., USA). Two-tailed Student's *t* test was applied for two-group comparison. A p value less than 0.05 was considered as statistically significant.

2.3 Results

2.3.1 2-DE profiling of tetracycline-treated and non-tetracycline-treated HepAD38 cells

To study the effects of HBV replication on the proteome profile of the host cell, proteins from tetracycline-treated (HBV suppression, Tet^+) and non-tetracycline-treated (HBV induction, Tet^-) HepAD38 were extracted and resolved by 2-DE 48 h post treatment. Fig. 2-1 shows a representative pair of silver stained 2-DE maps between two samples (Fig. 2-1 A and B). After compared the images from HepG2 and HepAD38 cells treated with or without tetracycline, 40 protein spots were found to be differentially expressed (± over 2-fold, $p < 0.05$) in three pairs of gels. Cropped and enlarged images of five paired spots are presented in Fig. 2-1 C.

2.3.2 Identification and classification of differentially expressed proteins

Among the 40 selected spots, a total of 23 proteins were successfully identified by MALDI-TOF MS and MS/MS analysis. Sixteen proteins (70%) were markedly up-regulated whereas seven (30%) were down-regulated in HBV-replicating (Tet^-) HepAD38 cells. The characteristics of all identified proteins, including protein name, NCBI accession number, theoretical molecular mass/pI, peptide count, protein score (confidence interval in percent), number of unmatched masses, sequence coverage, -fold change and functions, are listed in Table 2-1 and the MS spectrum and peak lists for each protein are listed in the appendix Fig. A2-A24. In general, the 23 proteins can be functionally categorized into 6 categories: antioxidant enzymes (13%), metabolism (26%), cytoskeleton and transport proteins (17%), gene transcription-associated proteins (9%), heat shock proteins and chaperones (26%), cell proliferation, metastasis and signaling-associated proteins (9%).

In the present study, GRP78 (also known as heat shock 70-kDa protein 5) was one of the most striking proteins elevated by HBV replication in HepAD38 cells. It was up-regulated by 5-fold in the non-tetracycline-treated HepAD38 cells when compared with the tetracycline-treated counterparts. Fig. 2-2 illustrates the MS and MS/MS spectrums of GRP78. As shown in Table 2-1, the protein score of 791 in the Mascot search, indicated a highly significant match of GRP78 protein sequences ($p < 0.05$).

2.3.3 Validation of differentially expressed GRP78 by real-time RT-PCR and Western blotting

To confirm the overexpression of GRP78 induced by HBV replication, Western blotting was carried out to detect the expression level of GRP78 in HepAD38 cells at day 1, 2, 3 and 4 post tetracycline treatment. As shown in Fig. 2-3 A, a time-dependent decrease in GRP78 expression was observed when tetracycline, which suppressed HBV replication, was added into the medium. In addition, both quantitative real-time PCR and immunoblot data (Fig. 2-3 B) showed a convincing elevation of GRP78 in HepG2 cells that were transiently transfected with pHBV as compared with the control.

2.3.4 Down-regulation of GRP78 in post-lamivudine treatment liver biopsies

To confirm whether GRP78 overexpression was triggered in HBV-infected liver tissues, GRP78 immunoreactivity was examined in 19 paired pre- and post-lamivudine treatment liver biopsies of CHB patients by immunohistochemical staining. All selected

patients have been demonstrated to have a remarkable reduction of HBV DNA in serum after receiving lamivudine monotherapy in our previous study (Chan *et al.*, 2005). The serum HBV DNA levels ($\log_{10}$ copies/mL) in patients before and after lamivudine treatment are shown in Fig. 2-4 A. As illustrated, a significant drop in serum HBV viral load was observed in the post-treatment group when compared with the pre-treatment group (pre-treatment serum HBV load, 8.12 ± 1.19 $\log_{10}$ copies/mL; post-treatment serum HBV load, 5.23 ± 2.25 $\log_{10}$ copies/mL; $p < 0.001$). The paraffin-embedded liver biopsies of these lamivudine sensitive patients were then processed and immunostained with anti-GRP78 antibodies.

In the present study, all liver sections showed diffuse positive staining for GRP78. In general, 52.6% (10/19) of cases showed decreased staining in post-treatment biopsies, 31.6% (6/19) presented equal staining, and 15.8% (3/19) exhibited increased staining. In addition, the GRP78 staining scores were significantly lower in post-treatment group than those of the pre-treatment group (Fig. 2-4 B, pre-treatment GRP78 scores, 2.68 ± 0.61; post-treatment GRP78 scores, 2.34 ± 0.60; $p = 0.019$). As shown in Fig. 2-4, a uniform moderate-to-intense staining of GRP78 was noted in the pre-lamivudine treatment biopsy (Fig. 2-4 C1) in contrast to the weak staining observed in the post-lamivudine treatment sample (Fig. 2-4 C2). Moreover, the GRP78 staining displayed a general cytoplasmic distribution in hepatocytes with partial enrichment in the perinuclear region. On the contrary, no GRP78 signal was detected in the negative control where primary antibodies were omitted (Fig. 2-4 C3).

2.4 Discussion

HBV infection is an intricate process and chronic hepatitis induced by HBV infection may progress to cirrhosis and HCC. Therefore, understanding the interplay between HBV and host is one of the most challenges in the fight against HBV and is urgently needed.

Proteomics analysis, as a new revolution in the post-genome era, is currently a powerful tool for systematic evaluation of protein expression profile and understanding gene functions. Recent rapid technological advances in proteomics have ignited considerable research efforts to identify potential disease biomarkers, drug targets and functional/signaling pathways. As such, comparative proteomics, as a major proteomic approach, has been successfully and extensively applied in the pathological studies of various viral diseases, including HIV (Ringrose *et al.*, 2008), HCV (Mannova *et al.*, 2006), severe acute respiratory syndrome coronavirus (SARS-CoV) (Jiang *et al.*, 2005), influenza virus (Baas *et al.*, 2006), human papilloma virus (Yim *et al.*, 2004) etc. Promising progress has been made in the comprehensive understanding of molecular mechanisms of viral pathogenesis and in developing effective diagnostics and therapeutics for these viral infections.

Although in the past decades, considerable efforts have been made in describing the molecular biology of HBV, the host responses to HBV infection at various stages are

poorly defined. Previous studies have focused on the impact of HBV replication on the host gene and protein expression at the terminal HCC stage (Kim *et al.*, 2001; Okabe *et al.*, 2001; Li *et al.*, 2005; Sun *et al.*, 2007). Until recently, cDNA microarray, proteomic and metabonomic analysis of HBV transgenic mice livers identified genes in lipid biosynthesis, lipid metabolism and growth control pathways were affected by HBV in the early stage of infection (Hajjou *et al.*, 2005; Yang *et al.*, 2008). The unique proteomic profiles of the sera from patients with different stages of liver fibrosis and of the early fibrotic livers from HBV transgenic mice were also reported by Poon *et al.* (Poon *et al.*, 2005) and Spano *et al.* (Spano *et al.*, 2008) respectively. Collectively, the reported differentially expressed host genes induced by HBV replication were involved in many important biological functions, including metabolism, oxidoreduction, protein degradation and transport, signal transduction, transcription and replication, as well as cell defense..

In this part of study, we investigated the early changes of the proteomic profile of hepatocytes upon HBV replication using an inducible HBV-producing system. This system would ultimately eliminate the potential artificial observations caused by the difference of genetic backgrounds. By using 2-DE combined with MALDI-TOF/TOF MS and MS/MS analysis, 23 differentially expressed proteins were identified. Among them, 16 proteins were up-regulated and 7 were down-regulated by HBV replication. Concordant with previous findings (Hajjou *et al.*, 2005; Severi *et al.*, 2006; Tong *et al.*, 2008; Yang *et al.*, 2008; Liu *et al.*, 2009), the differentially expressed proteins identified

by the present study also participate in various functional aspects including oxidoreduction, metabolism, protein folding and transport, cell growth, transcription and signal transduction. This indicates that HBV infection is a multifactorial disease in which HBV replication perturbs the hepatic biochemical balance and signal transduction pathways.

Among the identified proteins, heterogeneous nuclear ribonucleoprotein K (HNRPK) was shown to be increased by 2-fold in the HBV-replicating HepAD38 cells. Such a finding was not surprising because HNRPK was shown to play crucial roles in the replication of HBV and other DNA/RNA viruses as a host supportive protein (Hsieh *et al.*, 1998; Ng *et al.*, 2005; Burnham *et al.*, 2007; Lin *et al.*, 2008; Wolf *et al.*, 2008; Zhang *et al.*, 2008). The up-regulation of HNRPK in HepAD38 cells when tetracycline was withdrawn would be a consequence of host response initiated by HBV to facilitate viral replication. In addition, several B-type HCC-associated proteins, such as superoxide dismutase 1, enolase 1, aldehyde dehydrogenase and proliferating cell nuclear antigen (Li *et al.*, 2005; Sun *et al.*, 2007), were also identified in our study. This suggests that these proteins might be carrying out crucial roles in HCC tumorigenesis. Taking together, all these findings add further support of HepAD38 as a reliable platform for screening novel biomarkers and therapeutic targets in HBV-related liver diseases.

In this study, GRP78 is one of the proteins that showed significant changes upon HBV

replication. It is best known as an ER chaperone and a central monitor of ER stress. It plays an essential role in a wide variety of cellular functions, including protein folding and assembly, degradation of misfolded proteins, Ca^{2+} binding, and the activation of unfolded protein response (UPR) to relieve ER stress and thus to protect cell from apoptosis.

Recently, the functional connection between the ER stress response and HBV infection has been reported. It was suggested that the response of GRP78 promoter and the changes in GRP78 levels upon HBV infection were viral genotypes/subgenotypes dependent (Chua *et al.*, 2005; Sugiyama *et al.*, 2006). Herein, GRP78 expression was demonstrated to be stimulated by HBV replication in HepAD38 cells and transient HBV-producing HepG2 cells. Contrary to HBV induction, GRP78 expression in HepAD38 cells was gradually attenuated in a time-dependent manner at the onset of HBV inhibition by introduction of tetracycline. The up-regulation of GRP78 upon HBV replication may be explained by the activation of UPR that enhanced the synthesis and translation of ER chaperones in ER stress (Ni and Lee, 2007) and the direct activation of GRP78 promoter by HBV proteins (Xu *et al.*, 1997).

Furthermore, the examination of paired pre- and post-lamivudine treatment patient liver biopsy specimens and the quantification of serum HBV DNA have revealed a statistically significant up-regulation in GRP78 expression in pre-treatment biopsies, which was concomitant with the high HBV loads in sera. These findings further

confirmed the inducible effects of HBV replication on GRP78 expression observed in the non-tetracycline-treated HepAD38 and pHBV-transfected HepG2 cells.

In conclusion, this is the first proteomic investigation performed on HepAD38 of the hepatocyte responses to HBV in the early stage of infection. Twenty-three cellular proteins were identified as differentially expressed, with GRP78 as one of the most significantly up-regulated proteins induced by HBV replication. And this induction was successfully validated in independent models, including HepAD38 cells, pHBV-transfected HepG2 cells and the pre-treatment liver biopsies of HBV-infected patients.

Table 2-1. Differentially expressed proteins identified by 2-DE and MS analysis between tetracycline-treated (HBV suppression) and non-tetracycline-treated (HBV induction) HepAD38 cells.[a]

Function	Spot no.[b]	Protein name	Abbrevation	NCBI accession no.	Theoretical molecular mass (Da)/pI	Peptide Count	Protein Score (CI)[c]	Unmatched masses no.	Sequence coverage (%)	-Fold change[d]
Antioxidant enzymes										
	19	Superoxide dismutase 1	SOD1	gi | 4507149	15925.9/5.70	3	115 (100%)	15	30	2.0
	31	Peroxiredoxin 2 isoform a	PRDX2	gi | 32189392	21878.2/5.66	9	235 (100%)	49	40	2.6
	37	Peroxiredoxin 3	PRDX3	gi | 14250063	27705.2/7.11	6	190 (100%)	35	24	3.9
Metabolism										
	10	Pyruvate dehydrogenase E1, beta subunit precursor	PDHB	gi | 387010	36464.4/5.38	12	393 (100%)	40	46	2.4
	12	Enolase 1	ENO1	gi | 4503571	47139.3/7.01	8	106 (100%)	20	25	-2.1
	20	Aldehyde dehydrogenase	ALDH	gi | 178390	56344.6/7.00	20	383 (100%)	37	45	2.4
	24	ATP synthase, delta subunit precursor	ATP5D	gi | 4502297	17479.2/5.38	2	84 (99.96%)	32	13	2.2
	25	ATP synthase, beta subunit precursor	ATP5B	gi | 32189394	56524.6/5.26	18	609 (100%)	40	49	4.6
	34	Cathepsin D preproprotein	CTSD	gi | 4503143	44523.6/6.10	11	294 (100%)	30	32	2.1
Cytoskeleton and transport proteins										
	4	Tubulin alpha 6	TUBA6	gi | 14389309	49863.5/4.96	5	85 (99.97%)	17	13	-2.1
	17	Lamin B1	LMNB1	gi | 5031877	66367.6/5.11	22	378 (100%)	19	37	-2.6
	30	Actin, beta	ACTB	gi | 14250401	40978.4/5.56	13	486 (100%)	50	49	3.0
	38	Fatty acid binding protein	FABP	gi | 182356	14169.4/6.60	4	151 (100%)	35	44	3.6
Gene transcription										
	1	Proliferating cell nuclear antigen	PCNA	gi | 4505641	28750.3/4.57	9	99 (100%)	36	37	2.0
	28	Heterogeneous nuclear	HNRPK	gi | 14165437	50996.4/5.19	14	307 (100%)	35	32	2.0

Table II. continued

	ribonucleoprotein K isoform a								
Heat shock proteins and chaperones									
6	Calreticulin precursor	CALR	gi | 4757900	48111.8/4.29	15	369 (100%)	35	47	-2.2
18	Chaperonin	CPN60	gi | 31542947	61016.4/5.70	19	428 (100%)	25	43	2.1
26	Glucose-regulated protein 78kDa	GRP78	gi | 16507237	72288.4/5.07	28	791 (100%)	32	50	5.0
33	Chaperonin containing TCP1, subunit 5 (epsilon)	CCT5	gi | 24307939	59632.8/5.45	11	125 (100%)	25	19	3.4
36	Protein disulfide isomerase-associated 3 precursor	PDIA3	gi | 21361657	56746.8/5.98	23	394 (100%)	36	51	6.6
39	Chaperonin containing TCP1, subunit 6A isoform a	CCT6A	gi | 4502643	57987.6/6.23	7	67 (98.30%)	23	14	-3.3
Cell proliferation, metastasis and signal transduction									
5	Laminin-binding protein	LAMBR	gi | 34234	31773.9/4.84	8	182 (100%)	15	36	-2.2
32	Prohibitin	PHB	gi | 4505773	29785.9/5.57	9	374 (100%)	22	35	-2.8

a. At a 2-fold difference cutoff in intensity, 40 spots were selected for further MALDI-TOF-MS/MS-MS analysis and 23 proteins were finally identified.

b. Spot numbers are shown in Fig. 2-1.

c. CI, confidence interval

d. The spot intensities were quantified using PDQuest™ software (Bio-rad, USA). The average –fold change of spot intensity for each protein was calculated from three independent experiments (non-tetracycline-treated HepAD38 *versus* tetracycline-treated HepAD38). $^{-}$, decrease.

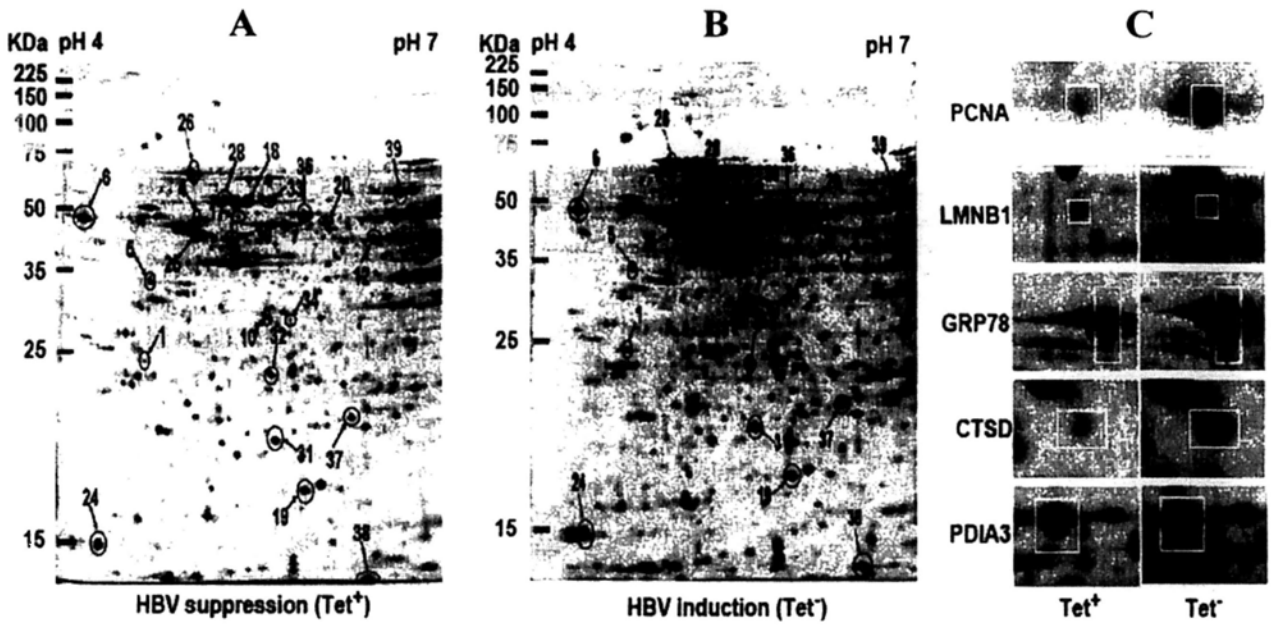

Fig. 2-1. Protein profile differences between tetracycline-treated and non-tetracycline-treated HepAD38 cells.

A and B, representative silver stained 2-DE maps of proteins from tetracycline-treated (HBV suppression, Tet^+; A) and non-tetracycline-treated (HBV induction, Tet^-; B) HepAD38 cells (n = 3). Twenty-three differentially expressed spots that were identified by MALDI-TOF-MS and MS/MS scanning were marked with numbers. C, enlarged sections of the 2-DE maps showing different expressions of spot 1 (PCNA), spot 17 (LMNB1), spot 26 (GRP78), spot 34 (CTSD) and spot 36 (PDIA3) between tetracycline-treated (Tet^+) and non-tetracycline-treated (Tet^-) HepAD38 cells.

A

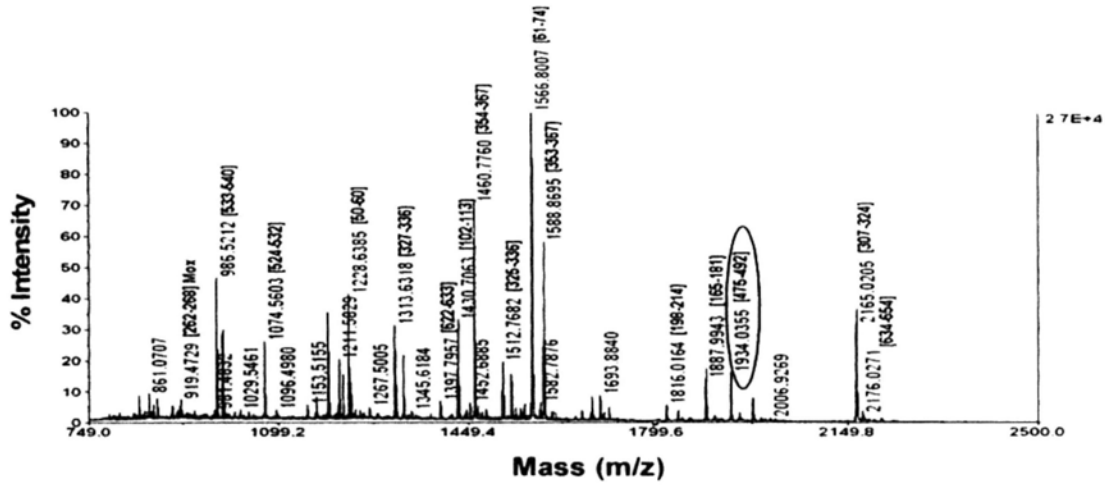

B

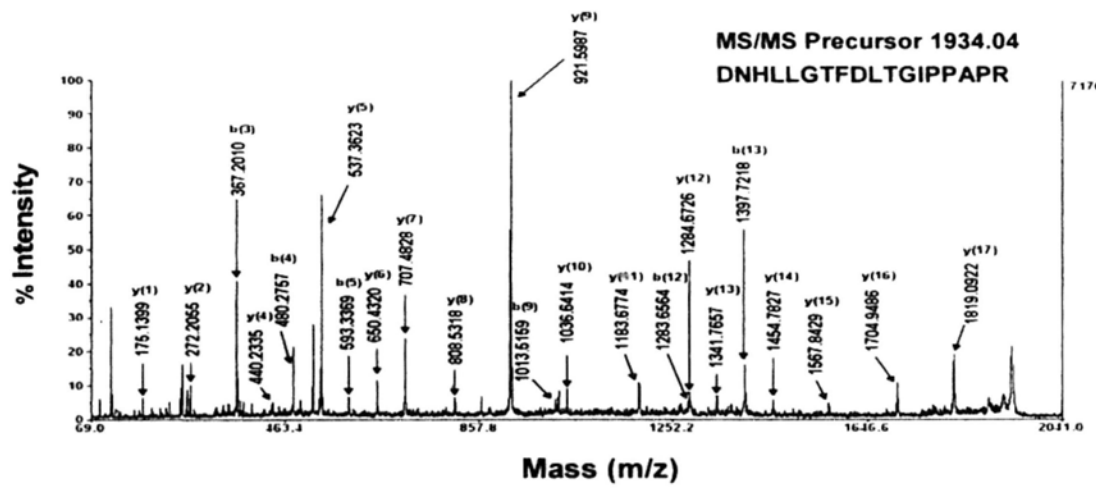

Fig. 2-2. Identification of GRP78 (spot 26) by MALDI-TOF MS and MS/MS analysis.

A, MALDI-TOF MS spectrum of GRP78 labeled with masses detected and peptide assignments. The precursor ion 1934.04 *m/z*, highlighted by open circle, was submitted for MS/MS scanning. Mox, oxidized methionine. B, MS/MS spectra of the precursor ion 1934.04 *m/z* for peptide DNHLLGTFDLTGIPPAPR of GRP78. b ions and y ions with corresponding peak values were marked.

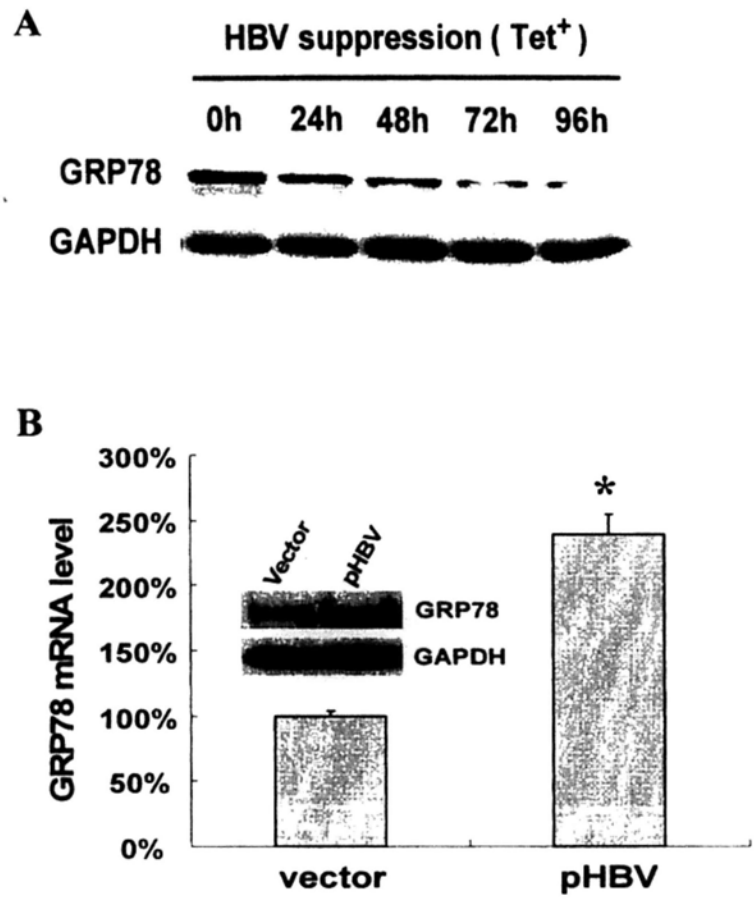

Fig. 2-3. Confirmation of GRP78 overexpression in HBV-replicating HepAD38 and pHBV-transfected HepG2 cells.

A, time-dependent decrease of GRP78 expression was revealed by Western blot in HepAD38 cells when HBV replication was suppressed by tetracycline. Tet^+, tetracycline treatment. B, elevated mRNA and protein (inset) expression of GRP78 were confirmed by quantitative PCR and Western blotting, respectively, in HepG2 cells 48 h post nucleofection. GAPDH was used as the internal control. Data are expressed as mean ± S.D.. Error bars represent S.D.. (n = 3; * $p < 0.01$).

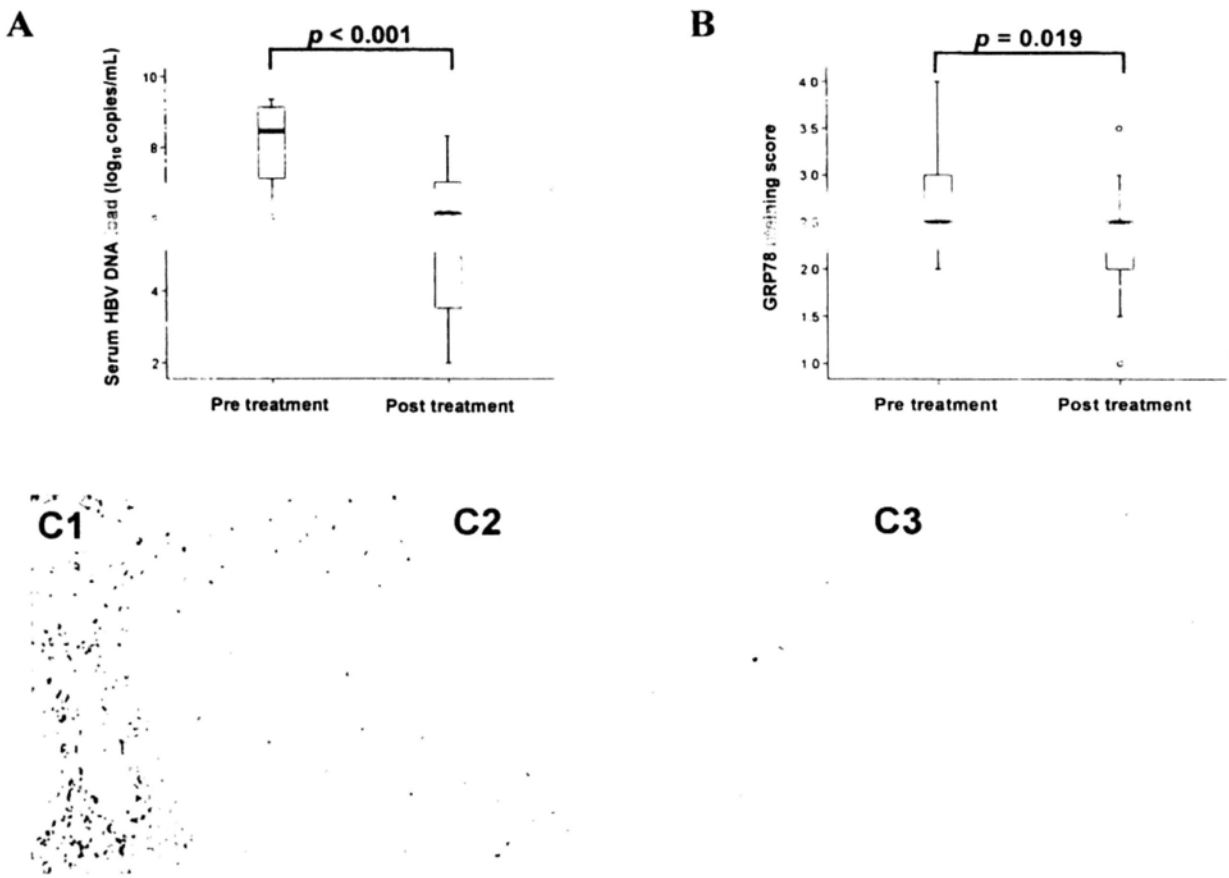

Fig. 2-4. GRP78 is down-regulated in post-lamivudine treatment liver biopsies.

A, serum HBV DNA levels of 19 CHB patients pre-treatment (median, 8.47 $\log_{10}$ copies/mL; range, 6-9.37 $\log_{10}$ copies/mL) and post-treatment (median, 6.18 $\log_{10}$ copies/mL; range, 2-8.33 $\log_{10}$ copies/mL; $p < 0.001$) with lamivudine. B, GRP78 staining scores of liver biopsies from 19 CHB patients pre-treatment (median, 2.5; range, 2-4) and post treatment (median, 2.5; range, 1-3.5; $p = 0.019$) with lamivudine. The box plots display the median (bold middle line), the 25th and 75th percentiles (box margins), and the minimum and maximum values (whiskers). Outlying values are expressed as circles and p values are indicated. C1-C3, representative microphotographs of GRP78 immunochemical staining in a pair of liver biopsies before (C1) and after (C2) lamivudine treatment. C3 is the negative control without primary antibody. (magnification, × 200).

Chapter 3

GRP78 Is an Intracellular Antiviral Factor against HBV

3.1 Introduction

In the previous chapter, we have demonstrated that GRP78 was one of the most strikingly elevated proteins induced by HBV replication in proteomic analysis, and its up-regulation was successfully confirmed at the transcription level by quantitative PCR and at the translation level by western blotting and immunohistochemical analysis respectively. Tremendous evidence have demonstrated GRP78 is a multifunctional protein and participates in various aspects of mammalian development (Luo *et al.*, 2006), neurodegenerative diseases (Rao and Bredesen, 2004), cancer progression (Fu and Lee, 2006) , diabetes (Scheuner *et al.*, 2005) and the pathogenesis of bacterial infections (Paton *et al.*, 2006). Several studies have reported that GRP78 interacts with HBV surface protein (Cho *et al.*, 2003; Awe *et al.*, 2008; Liu *et al.*, 2009). And recently, the functions of GRP78 in cellular rescue have been addressed (Lam *et al.*, 1997; He, 2006; Yoshimura and Luo, 2007; Singh *et al.*, 2008).

Considering that GRP78 plays important roles in protein folding and transport (Doms *et al.*, 1993; Cho *et al.*, 2003; Awe *et al.*, 2008), we hypothesized that GRP78 may be a host responsive factor that supports HBV replication, virion packaging and/or secretion. To test this hypothesis, we carried out both the loss- and gain-of-function studies to

fully characterize the role of GRP78 in HBV life cycle. In the loss-of-function study, siRNA targeting GRP78 was applied in pHBV-transfected HepG2 cells, and HBV DNA in both cytoplasm and culture medium was quantified. Reversely, GRP78 was artificially overexpressed in pHBV-transfected HepG2 cells in the gain-of-function study and HBV replication efficiency was then assessed. The kinetics of intracellular HBV virions in GRP78-silenced HepAD38 cells was also determined.

3.2 Materials and methods

3.2.1 Plasmid constructs

The pHBV (1.1-fold HBV genome, genotype C) was used to produce HBV virion as described (Chen *et al.*, 2003). The *Renilla* luciferase expression plasmid pSV40-RL (Promega, USA) was used as the internal control to normalize the transfection efficiency. The full-length complementary DNA encoding human GRP78 was obtained by reverse transcription-PCR amplification of HepG2 RNA using a set of specific primers (forward 5'-CGCGATATCGCCACCATGAAGCTCTCCCTGGTG-3'; reverse 5'-ATAAGAATGCGGCCGCCTACAACTCATCTTTTTCTGC-3', EcoR V and Not I sites, respectively, were underlined). The amplified PCR products were predigested with EcoR V and Not I restriction enzymes and then subcloned into the same sites of pAAV/EF1α vector to obtain a GRP78 expression plasmid, pAAV-GRP78. pAAV-EGFP was generated by replacing the expression cassette of GRP78 with the sequence encoding *EGFP* and used as the negative control. All constructs were verified by automated DNA sequencing.

3.2.2 siRNA synthesis

According to the "Dharmacon siDesign Center", two small interfering RNA (siRNA) oligonucleotide duplexes targeting human GRP78 mRNA (GenBank accession number NM_005347) were designed (siGRP78-1: sense, 5'-AAUUUCUGCCAUGGUUCUCACUAAAAU-3'; siGRP78-2: sense, 5'-AACUUCUACAGCUUCUGAUAAUGAGUC-3') and then synthesized by Sigma Proligo. The knockdown effects of both siRNAs were measured by real-time RT-PCR and Western blot assays. Finally, the siGRP78-1 which induced specific and potent GRP78 silencing in HepG2 cells, was chosen for the study. A non-specific siRNA targeting the replicase 1A region of the SARS-CoV genome (siSARS: sense, 5'GCACUUGUCUACCUUGAUGdTdT-3') (He *et al.*, 2003; He *et al.*, 2006), which had no homology to HBV or the human genome, was used as the negative control in this part of the study.

3.2.3 Cell culture and transfection

HepAD38 and HepG2 cells were maintained as described in Chapter 2 and kept in the logarithmic growth phase by routine passage every 2–3 days by using 0.025% trypsin-EDTA.

All transfections were carried out in 12-well plates using Lipofectamine^{TM} 2000 (Invitrogen, USA) according to the manufacturer's instructions. Transfections were

done in triplicates and repeated at least three times. For knockdown of GRP78, HepG2 cells were transfected with either siGRP78-1 or siSARS when cells reached about 70% confluence. A final concentration of 50 nmol/L was used for both siRNAs. Mock transfection was carried out concurrently with lipofectamine alone. For overexpression of GRP78, HepG2 cells were transfected with 1.6 μg of pAAV/EF1α (empty vector), pAAV-EGFP or pAAV-GRP78/well. Cells were lysed for Western blot analysis 48 h after transfection.

HepAD38 cells were transfected with 200 nmol/L siGRP78-1 or siSARS after tetracycline withdrawal. HepG2 cells were cotransfected with pHBV and pSV40-RL together with siGRP78-1/siSARS or pAAV-GRP78/ pAAV/EF1α. The final concentration of siRNAs was 50 nmol/L, and the ratio of transfected plasmids was pAAV-GRP78 or pAAV/EF1α : pHBV : pSV40-RL = 5 : 1 : 0.1. Two days after transfection, supernatants were collected for core-associated HBV DNA extraction and quantification as well as HBsAg and HBeAg detection. Cells were processed for HBV DNA quantification and luciferase activity measurement.

3.2.4 Luciferase assay

Luciferase activities in HepG2 cell lysates were determined by using a luciferase assay system (Promega, USA) according to the manufacturer's instructions. Each assay was repeated independently five times.

3.2.5 Quantitation of GRP78 mRNA expression level

Total RNA was isolated from HepAD38 cells using TRIzol reagent (Invitrogen, USA) according to the manufacturer's instructions. 1 μg of total RNA was subjected to reverse transcription using the ImProm-II™ Reverse Transcription System (Promega, USA). The quantitative real-time PCR was carried out in the ABI 7500 Real-Time PCR system with Power SYBR Green Master Mix (Applied Biosystems, USA), using the following program: 50 °C for 2 min, 95°C for 10 min followed by 40 cycles of 95°C for 15 s and 60°C for 1 min. Fluorescence signals were collected during the extension phase of each PCR cycle. Primers used for GRP78 and GAPDH are listed in Chapter 2. Serial ten-fold dilutions of GRP78 and GAPDH PCR fragments were used to calculate the standard curves respectively. All samples were run in triplicate and the experiment was repeated thrice. The mRNA level of GRP78 was normalized to the mRNA copies of GAPDH in the same sample and results were expressed as a percentage of the base-line level (at time point 0 h, set as 100%).

3.2.6 Western blotting

Cells were lysed on ice for 30 min in RIPA buffer and then centrifuged at 14,000 rpm for 10 min at 4°C. The supernatants were collected and stored at -80°C until use. Protein concentrations were determined by the Bradford method (Bio-Rad, USA). 20 μg protein /sample were resolved by 12% SDS-PAGE and transferred onto PVDF membranes. The membranes were blocked by 5% skim milk in TBST buffer for 1 h followed by an incubation with specific antibodies against GRP78 (1:500 dilution, Cell signaling

Technology, USA) or GAPDH (1:10,000 dilution, Santa Cruz Biotechnology, USA). After washing in TBST buffer three times, the membranes were hybridized with horseradish peroxidase-conjugated secondary antibodies (1:3,000 dilution, Santa Cruz Biotechnology, USA). Signals were developed using a chemiluminescence detection kit (Amersham, UK). Each immunoblot was done thrice to confirm the results.

3.2.7 Core-associated HBV DNA purification and quantitative analysis

Core-associated HBV DNA was extracted as described previously with minor modifications (Chen *et al.*, 2003). For extracellular virions, culture medium was collected 48 h post transfection and briefly centrifuged to remove cell debris. Viral core particles were precipitated with 10% polyethylene glycol 8000 in 0.5 M NaCl at 4°C overnight. After centrifugation at 16,000 x g for 30 min, viral cores were pelleted and subsequently treated with DNase I (100 μg/ml) in 50 mM Tris•HCL (pH 8.0) and 10 mM $MgCl_2$ at 37°C for 3 h. The mixture was further digested with 400 μg/ml of proteinase K in 15 mM EDTA, 100 mM NaCl and 0.5% SDS at 55°C for 2 h, followed by phenol/chloroform extraction. HBV DNA released from lysed cores was dissolved in TE buffer (10 mM Tris•HCL, pH 8.0, 1 mM EDTA). For intracellular virions, cells were lysed in 100 μl/well lysis buffer (1% Triton X-100 and 1 x Roche protease inhibitor mixture in PBS) 48 h post-transfection. 20 μl of the cell lysates was assayed for luciferase activity, and the remaining cell lysates were used for the purification of core-associated HBV DNA, which was processed as mentioned earlier.

The core-associated HBV DNA was quantitated by real-time PCR using Power SYBR Green Master Mix with forward primer 5'-AGTGTGGATTCGCACTCCT-3' and reverse primer 5'-GAGTTCTTCTTCTAGGGGACCTG-3'. Cycling parameters described above were performed with the ABI 7500 Real-Time PCR system. Serial dilutions of pHBV were used to generate the standard curve. All samples were analyzed in triplicate. The copy numbers of HBV DNA were normalized against the luciferase activities in the corresponding wells. Results were presented as a percentage of the negative control and confirmed by five independent experiments.

3.2.8 ELISA for determining the levels of HBsAg and HBeAg

The levels of HBsAg and HBeAg in the culture medium were measured by ELISA using the Murex HBsAg Version 3 Kit and Murex HBeAg/anti-HBe kit (Abbott Murex, UK) according to the manufacturer's instructions. Absorbance was measured at 450/690 nm using the Expert Plus microplate reader (ASYS Hitech, Austria) and the data were normalized to luciferase activity. All samples were examined in triplicate and results were expressed as -fold changes relative to the negative controls.

3.2.9 Statistical analysis

Data are expressed as mean ± S.D.. All statistical analyses were carried out with SPSS 14.0 software (SPSS Inc., USA). Two-tailed Student's *t* test was applied for two-group comparison. A p value less than 0.05 was considered as statistically significant.

3.3 Results

3.3.1 Suppression of GRP78 increases HBV replication and antigen expression

As shown in Fig. 3-1 A, the cytoplasmic and supernatant HBV titers (HBV DNA copy number/luciferase activity) caused by GRP78 silencing were nearly 4-fold and more than 6-fold higher than the corresponding untreated controls respectively. Concomitantly, the levels of both HBsAg and HBeAg in culture medium were significantly increased (Fig. 3-1 B). The silencing effect of siGRP78-1 was clearly demonstrated by Western blotting in Fig. 3-1 C.

3.3.2 Overexpression of GRP78 suppresses HBV replication and antigen expression

Herein the empty vector pAAV/EF1α was used instead of the EGFP expression plasmid as the negative control for the fluorescence emitted by EGFP perturbing the measurement of *Renilla* luciferase luminescence. Fig. 3-2 A shows a marked decrease of cytoplasmic and supernatant HBV titers upon GRP78 overexpression. The levels of both HBsAg and HBeAg in the culture medium were also significantly decreased (Fig. 3-2 B). Fig. 3-2 C illustrates the overexpression of GRP78 clearly after 48 h of transfection in the HepG2 cells.

3.3.3 Kinetics of intracellular HBV virions and GRP78 transcript levels

To further confirm the intracellular anti-HBV activity of GRP78, we investigated the intracellular HBV kinetics in HepAD38 cells with and without the silencing of GRP78 expression. As shown in Fig. 3-3 A, HBV replication was delayed for 24 hours after

tetracycline withdrawal. This may reflect the retention of tetracycline in the cytoplasm. Twenty-four hours after the withdrawal of tetracycline, the intracellular HBV continuously increased 15-fold from 24 to 96 h in GRP78-silenced HepAD38 cells. However, the intracellular HBV was significantly inhibited in HepAD38 cells treated with mock siRNAs against SARS-CoV ($p < 0.01$); particularly, the intracellular HBV levels were almost the same at time points 72 and 96 h. To show how GRP78 responded to HBV replication, we performed quantitative RT-PCR experiments to demonstrate the mRNA levels of GRP78. As shown in Fig. 3-3 B, the GRP78 transcripts rapidly increased 25% from 12 to 48 h and were maintained at almost the same high levels from 48 to 96 h in HepAD38 cells. In contrast, the GRP78 mRNA level was reduced by about 70% in those cells treated with specific siRNAs against GRP78 at 24 h and remained at the similar low levels until 96 h. Taking together, these results demonstrated that GRP78 responded to HBV replication and physiologically inhibited HBV replication.

3.4 Discussion

In this part of study, GRP78 was further selected for the functional assessment on HBV replication for the following reasons: (1) GRP78 is highly induced by HBV, as evidenced by a 5-fold increase in GRP78 expression upon HBV replication in our proteomic studies, and this induction was successfully confirmed in different cell models and clinical samples at both the transcription and translation levels; (2) GRP78 is a versatile molecule and plays important roles in cell proliferation, survival, differentiation and defense; (3) GRP78 has direct interactions with HBV proteins. (Awe

et al., 2008; Liu *et al.*, 2009).

Considering that GRP78 is an important HBV response factor and acts as a host master regulator in cell survival, we hypothesized that GRP78 might have a possible impact on HBV replication. To test this hypothesis, siRNA targeting GRP78 was used in pHBV-transfected HepG2 cells and HBV titers in both the cytoplasm and culture medium was quantified by real-time PCR. To our surprise, the down-regulation of GRP78 could eventually lead to the augmentation of both intracellular and extracellular HBV viral loads, which can be partially explained by the backup chaperones in ER that are also implicated in HBV virion formation and secretion (Werr and Prange, 1998; Prange *et al.*, 1999; Bai *et al.*, 2005). In order to further demonstrate the functional significance of GRP78 in HBV replication, we performed the reverse assay by overexpressing GRP78 in pHBV-transfected HepG2 cells. As expected, both intracellular and extracellular HBV virions were greatly reduced in the presence of high levels of GRP78, demonstrating that GRP78 functions as an endogenous anti-HBV factor.

To further confirm this conclusion, we studied the kinetics of intracellular HBV virions in GRP78-silenced HepAD38 cells. Our data showed that the intracellular HBV was significantly increased in GRP78-silenced HepAD38 cells from 24 h to 96 h post-tetracycline withdrawal, as compared with the counterparts treated with mock siRNAs. We also noticed that, in the mock siRNA-transfected HepAD38 cells, the

mRNA of GRP78 increased to a high level at 48 h; thereafter the intracellular HBV titers did not increase after 72 h. The delayed inhibition of HBV replication indicated that the accumulation of GRP78 protein was needed. Interestingly, as presented in Fig. 3-3, we found that the naturally elevated GRP78 by HBV reduced the ratio of HBV replication, but could not completely inhibit HBV replication. This could explain why HBV infection often causes chronic infection in children, whereas acute infection occurs in adults. Other mechanisms, *e.g.* the mature immune responses, serve as additional important antiviral forces that would synergize the antiviral effects in adults.

In conclusion, our findings provide the first direct demonstration that GRP78 can effectively modulate the replication efficiency of HBV and functions as an endogenous anti-HBV factor in hepatocytes, which offer deeper insights into the molecular mechanisms through which host cells survive viral infection.

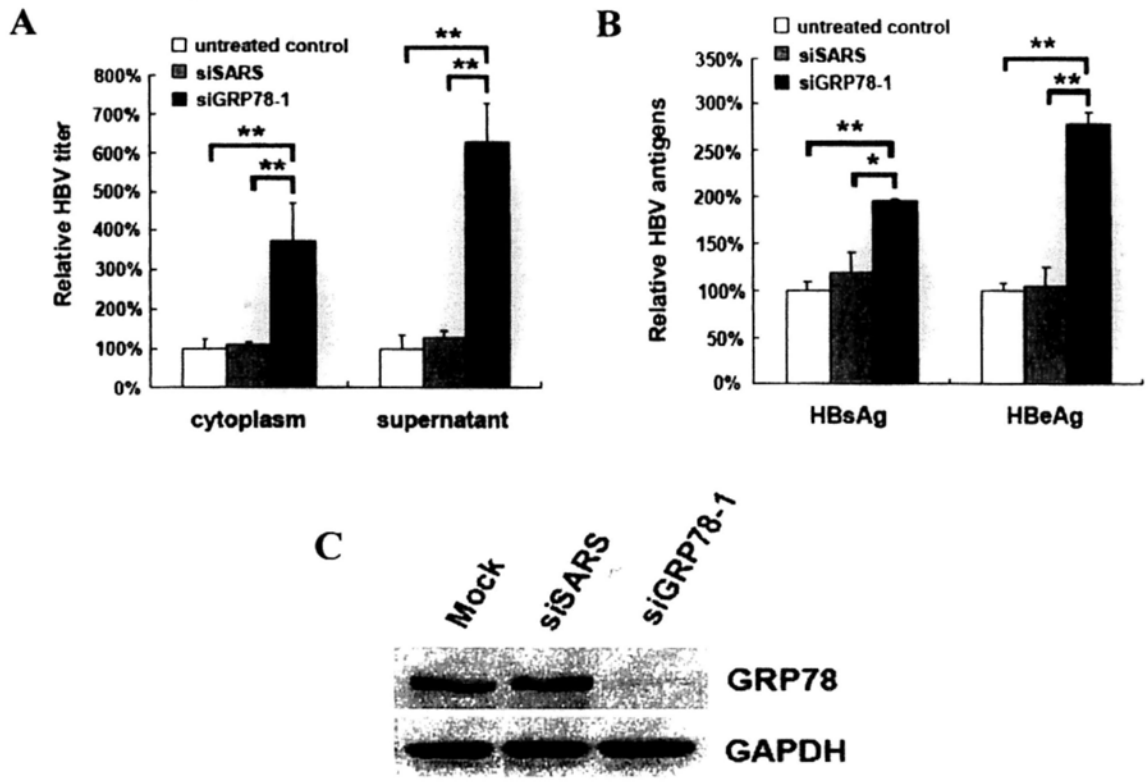

Fig. 3-1. Suppression of GRP78 increases HBV replication and antigen expression. The HBV titers (HBV/luciferase) of both cytoplasm and supernatant (A) and the levels (absorbance/luciferase) of both the secreted HBsAg and HBeAg (B) were significantly increased when GRP78 was knocked down. C, down-regulation of GRP78 by siGRP78-1 was confirmed by Western blotting in HepG2 cells 48 h post transfection (n = 3). Data are expressed as mean ± S.D.. (n = 5; * $p < 0.05$, ** $p < 0.01$).

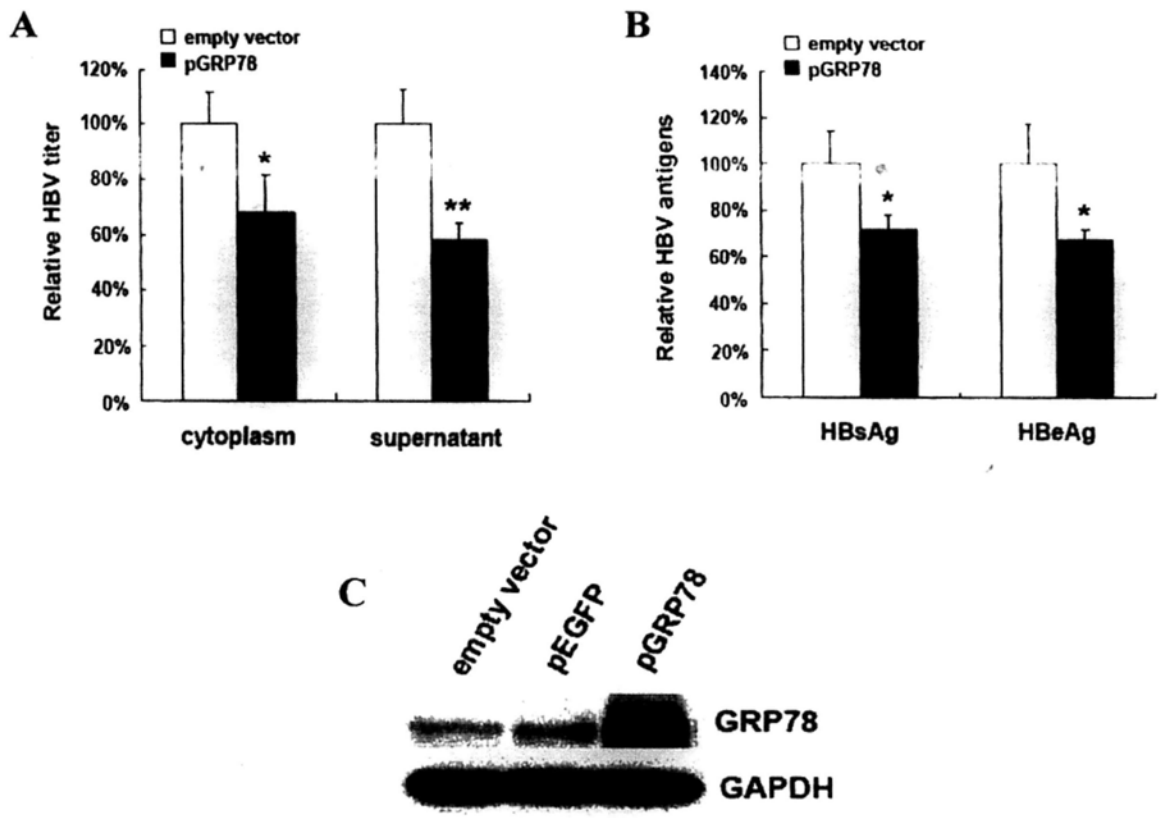

Fig. 3-2. Overexpression of GRP78 suppresses HBV replication and antigen expression. The HBV titers (HBV/luciferase) of both cytoplasm and supernatant (A) and the levels (absorbance/luciferase) of both the secreted HBsAg and HBeAg (B) were markedly decreased during the overexpression of GRP78. C, up-regulation of GRP78 was validated by Western blotting in pGRP78-transfected HepG2 cells 48 h post transfection (n = 3). Data are expressed as mean ± S.D.. (n = 5; * $p < 0.05$, ** $p < 0.01$).

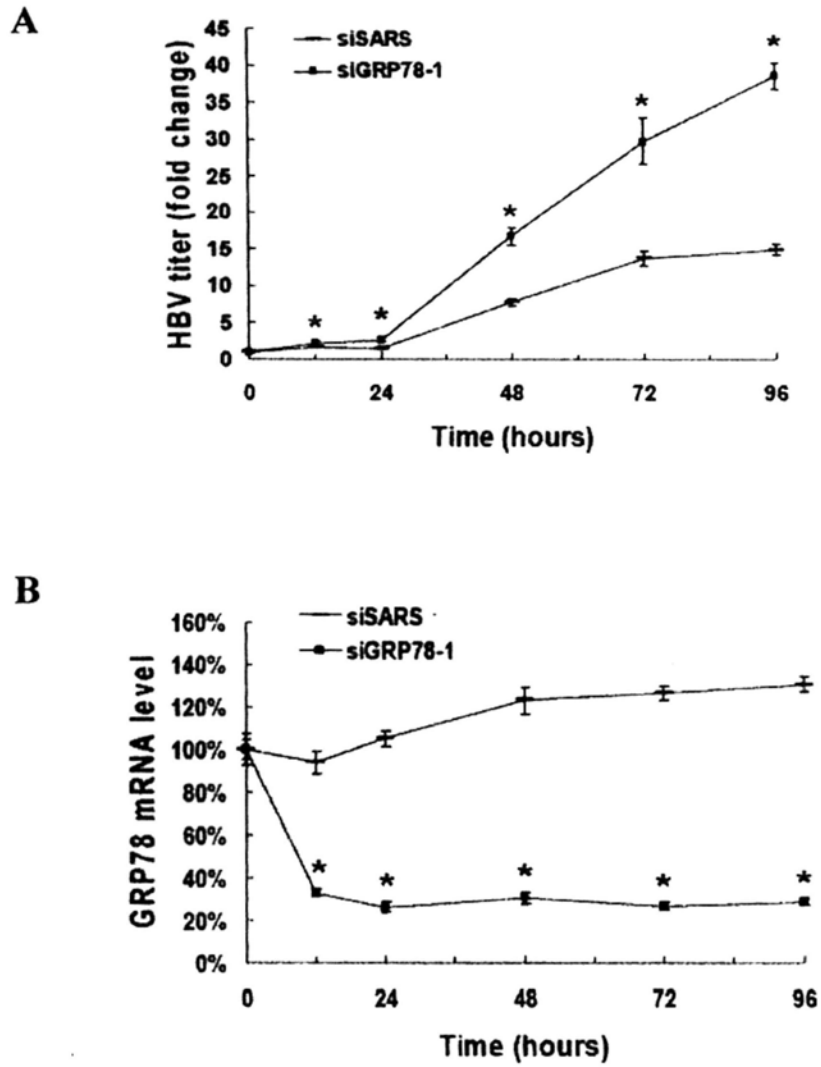

Fig. 3-3. Kinetics of HBV and GRP78 mRNA levels in HepAD38 cells. A, the intracellular HBV virions in siSARS- and siGRP78-1-treated HepAD38 cells; B, the mRNA levels of GRP78 in siSARS- and siGRP78-1-treated HepAD38 cells. The values were normalized with GAPDH mRNA levels (loading control) and expressed as -fold changes to the base-line level (at time point 0 h), which was set as 1. Data are expressed as mean ± S.D.. (n = 3; * $p < 0.01$, siGRP78-1 *versus.* siSARS at the same time point).

Chapter 4

GRP78 Inhibits HBV Replication through IFN-β 1-OAS-RNase L Pathway in HepG2 Cells

4.1 Introduction

As demonstrated in Chapter 3, the reduced HBV replication in the presence of high levels of GRP78 in HepG2 cells aroused our interest. To explore the mechanisms behind the phenomena, we first checked whether IFN response was activated in GRP78-overexpressing HepG2 cells.

It's well known that IFNs are a group of secreted cytokines and key components of the innate immunity response, which exhibit a broad range of biological and pharmacological activities, including antiviral, antiproliferative, antitumor and immunomodulatory effects (Stark G.R., 1998; Jonasch and Haluska, 2001). According to the type of receptor IFNs signal through, three major classes of IFNs have been identified, designated types I to III (Pestka *et al.*, 2004). Type I IFNs comprise a large group of molecules, including thirteen IFN-α subtypes in humans, IFN-β, -κ, -ε, -τ, -δ and -ω. They bind to the ubiquitously expressed cell surface receptor complex known as IFN-α receptor (IFNAR), which consists of IFNAR1 and IFNAR2, transduce distinct signals to nucleus and function as the first line of defense against viral infection. Type I IFNs are secreted by many cell types, including lymphocytes, macrophages,

fibroblasts, endothelial cells and others. Type II IFNs consists of only one member, IFN-γ, which is produced in activated T cells and natural killer cells. IFN-γ binds to the IFN-γ receptors (IFNGR) and elicits signals within target cells. The recently classified type III IFNs comprise three IFN- λ molecules, IFN- λ 1, - λ 2 and – λ 3, which are also referred to as IL-29, IL-28A and IL-28B respectively (Ank *et al.*, 2006; Uze and Monneron, 2007). Like type I IFNs, type III IFNs are also induced in many cells. These cytokines signal through the combined IFN- λ receptor 1 (IFNLR1) and interleukin-10 receptor 2 (IL-10R2) and share the same signal transduction pathway as type I IFNs.

The anti-viral mechanisms of IFNs have been extensively studied and a number of IFN-mediated signaling pathways have been revealed. The Janus tyrosine kinase (JAK)-signal transducer and activator of transcription (STAT) pathway is one of the best characterized IFN-signaling pathways (Stark, 1998). Following type I and type III IFNs binding to their corresponding receptors, signal transduction is initiated by two tyrosine kinases [*i.e.* tyrosine kinases 2 (TYK2) and JAK1], which recruit and phosphorylate the downstream STAT1 and STAT2 (Leung *et al.*, 1995; Darnell, 1998). The STAT1/STAT2 heterodimers associate with IFN-regulatory factor 9 (IRF9) to form IFN-stimulated gene factor 3 (ISGF3) complex, which then translocates to the nucleus and binds to the IFN-stimulated regulatory elements (ISREs) to induce the expression of IFN-stimulated genes (ISGs). As to type II IFNs responses, phosphorylated STAT1 are associated as homodimers to form IFN-γ activation factor (GAF) in the cytoplasm. These complexes thus migrate to the nucleus, bind to the γ-IFN-activated sequence (GAS) and drive the

IFN-γ-induced gene expression. The IFN-signaling is presented in Fig. 4-1.

Accumulating evidence has demonstrated that more than 300 ISGs are induced by IFNs (Der *et al.*, 1998). However, relatively few of the ISGs exhibit direct antiviral activities, such as inhibiting viral transcription, degrading viral RNA, translation suppression, modification of viral proteins and apoptosis induction. Several such proteins, which function as IFN antiviral effectors, have been well characterized, including IFN-stimulated protein of 15 kDa (ISG15), myxovirus resistance 1 (Mx1), Rnase L and protein kinase R (PKR). So far, the ISG15 ubiquitin-like pathway, the Mx pathway, the OAS-directed RNase L pathway and the PKR pathway have composed the main part of IFN-mediated antiviral response. These pathways are activated to a variable degree by IFNs to directly combat viruses and/or enhance the IFN response.

The endoplasmic reticulum is a sophisticated cellular machine for protein folding, assembly, modification and secretion. It employs efficient strategies to facilitate protein folding and prevent protein aggregation. However, a number of unfavorable exogenous and endogenous conditions can interfere with the functions of ER, leading to the accumulation of unfolded/misfolded protein in the ER lumen. To relieve the ER stress, the cell adopts adaptive responses by activating UPR, which is triggered by the activation of three ER transmembrane sensors, *i.e.* PERK, IRE1 ATF6. As protective mechanisms, UPR copes with ER stress by enhancing the expression of ER chaperones and folding enzymes, transiently inhibiting protein synthesis, degrading

unfolded/misfolded proteins and inducing apoptosis (Lee *et al.*, 1986; Brostrom *et al.*, 1996; Brodsky *et al.*, 1999; Kostova and Wolf, 2003).

To uncover the mechanisms involve in the anti-HBV function of GRP78, we first investigated whether IFN-mediated antiviral response was activated by GRP78 overexpression in HepG2 cells. Then, we assessed the ER stress and the activation of UPR signaling pathways induced by HBV replication in HepG2 cells, which also play important roles in cell defense and survival. Such information will provide us a more detailed picture of the combined virus-host network.

4.2 Materials and methods

4.2.1 Cell culture and transfection

HepG2 cells were maintained under routine conditions as described in Chapter 2.

For detecting the expression levels of IFNs and IFN-inducible genes triggered by GRP78 overexpression, HepG2 cells were nucleofected with pAAV-EGFP or pAAV-GRP78. After nucleofection, cells were transferred to 6-well plates and left for incubation for 48 h before real-time RT-PCR and Western blot analysis.

To assess the induction of unfolded protein response by HBV replication, HepG2 cells were transfected with pHBV or empty vector by nucleofection. Two days post-transfection, cells were submitted to RT-PCR and Western blot analysis.

4.2.2. Interferons treatment

To investigate the regulation of IFNs on GRP78 expression, HepG2 cells were treated with various concentrations of IFN-αA (1000 units/ml) or IFN-β-1a (0, 1, 10, 100 and 1000 units/ml, Sigma, USA) for the indicated intervals. After the indicated incubation periods, cells were harvested and lysed for real-time RT-PCR and Western blotting.

4.2.3 Quantitative PCR

Total RNA was isolated using TRIzol reagent (Invitrogen, USA) according to the manufacturer's instructions. 1 μg of total RNA was subjected to reverse transcription using the ImProm-II™ Reverse Transcription System (Promega, USA). The quantitative real-time PCR was carried out in the ABI 7500 Real-Time PCR system with Power SYBR Green Master Mix (Applied Biosystems, USA), using the following program: 50 °C for 2 min, 95°C for 10 min followed by 45 cycles of 95°C for 15 s and 60°C for 1 min. Fluorescence signals were collected during the extension phase of each PCR cycle. Primers used for *GRP78*, *IFN-α1*, *IFN-β1*, *ISG15*, *Mx1*, *OAS1*, *OAS2*, *OAS3*, OAS-like (*OASL*), *RNase L*, *PKR* and *GAPDH* are listed in Table 4-1. Standard curves for quantification were obtained by serial dilutions of the PCR products containing corresponding gene fragments. All samples were run in triplicate and the experiment was repeated thrice. The mRNA level of each target gene was normalized to the mRNA copies of GAPDH in the same sample and results were expressed as a percentage of the negative control (set as 100%).

4.2.4 XBP1 splicing assay

Total RNA was prepared from pHBV or empty vector-transfected HepG2 cells two days post-transfection using TRIzol reagent (Invitrogen, USA). The RNA was then reverse-transcribed into cDNA with oligo-dT primers using the ImProm-II™ Reverse Transcription System (Promega, USA) according to the manufacturer's instructions.

To analyze the splicing of the XBP-1 transcripts, we carried out RT-PCR experiments to amplify XBP-1 fragments with a pair of primers that span the splicing region of human XBP1 mRNA (forward, 5'-GAACCAGGAGTTAAGACAGCGC-3' and reverse, 5'-AGTCAATACCGCCAGAATCCAT-3'), using the following PCR program: 95°C for 5 min, 35 cycles of 95°C for 30s, 50°C for 30s, 72°C for 30s, and 72°C for 5 min. The PCR products were applied for electrophoreses on a 2% agarose gel and visualized by ethidium bromide staining.

4.2.5 Nuclear fraction preparation

pHBV or empty vector-transfected HepG2 cells were collected two days post-transfection. The cells were washed with ice-cold PBS and centrifuged at 2,000 rpm for 5 min at 4°C. The pellets were suspended in hypotonic buffer (10 mM Hepes, pH 7.9, 1.5 mM MgCl2, 10 mM KCl, 0.5 mM DTT, 0.1 mM EDTA, 0.1% Nonidet P-40 and 1 x Roche protease inhibitor cocktail) and lysed by 3 freeze-thaw cycles. Cytosolic fractions were obtained by centrifugation at 12,000 x g for 20 min at 4°C. The pellets

were resuspended in high-salt buffer (20 mM Hepes, pH 7.9, 25 % v/v glycerol, 420 mM NaCl, 1.5 mM $MgCl_2$, 0.5 mM DTT, 0.2 mM EDTA and 1 x Roche protease inhibitor cocktail) and incubated on ice for 40 min with occasional vortexing. The mixtures were then centrifuged at 14,000 x g for 20 min at 4°C and the supernatants were nuclear extract. Protein concentrations were measured by the Bradford method (Bio-Rad, USA).

4.2.6 Western blotting

For detection of GRP78, total PERK, phosphorylated PERK, total eIF-2 α , phosphorylated eIF-2 α and GAPDH, whole cell lysates were prepared as described in Chapter 2 and applied for Western blotting. For detection of p90 ATF6, cellular cytosolic fractions were used, whereas nuclear fractions were used for the detection of p50 ATF6. Immunoblots with antibodies against GRP78 (1:500 dilution, Cell signaling Technology, USA), P-Thr981-PERK(1:500 dilution, Santa Cruz Biotechnology, USA), PERK(1:1,000 dilution), P-Ser51-eIF2 α (1:1,000 dilution), eIF-2 α (1:1,000 dilution, Cell Signaling Technology, USA), ATF6 (1:200 dilution, Imgenex, USA) and GAPDH (1:500 dilution, Santa Cruz Biotechnology, USA) were performed using standard procedures as mentioned in Chapter 2. Each immunoblot was repeated thrice with similar results.

4.2.7 Statistical analysis

Data are expressed as mean ± S.D.. All statistical analyses were carried out with SPSS

14.0 software (SPSS Inc., USA). Two-tailed Student's *t* test was applied for two-group comparison. A *p* value less than 0.05 was considered as statistically significant.

4.3 Results

4.3.1 GRP78 inhibits HBV replication through IFN-β-dependent pathway in HepG2 cells

The mRNA levels of GRP78, IFN-β1, OAS1, OAS2 and RNaseL were all significantly up-regulated in the pGRP78-transfected HepG2 cells when compared with that in the control (*i.e.* cells transfected with pEGFP). However, no significant changes were observed for IFN-α1, ISG15, Mx1, OAS3, OASL and PKR (Fig. 4-2).

4.3.2 IFN-β-1a stimulates GRP78 overexpression in both dose- and time-dependent manners

To investigate whether there was a feedback regulation of GRP78 by IFNs, the expression level of GRP78 in both IFN-αA-treated and IFN-β-1a-treated HepG2 cells was examined. Our results showed that the mRNA expression of GRP78 increased positively with an increase of concentration of IFN-β-1a (Fig. 4-3A). In addition, IFN-β-1a treatment induced a time-dependent up-regulation of GRP78 transcripts in HepG2 cells with a peak level noted at 10 h post-treatment (Fig. 4-3B). Consistent with real-time PCR results, time-dependent stimulation of GRP78 protein expression by IFN-β-1a was also observed in HepG2 cells using Western blotting (Fig. 4-4A). In contrast, no obvious change of GRP78 protein level was observed after IFN-αA

treatment (Fig. 4-4B).

4.3.3 HBV replication induces unfolded protein response

To determine whether the IRE1-mediated pathway is activated upon HBV replication, we analyzed the splicing of XBP1 mRNA by RT-PCR using specific primers. In mock control (*i.e.* the empty vector-transfected HepG2 cells), only the unspliced XBP1 transcript was detected. On the contrary, in pHBV-transfected HepG2 cells, both the unspliced and spliced XBP1 transcripts, with the expected sizes of 199 bp and 173 bp respectively, were detected 48 h post-transfection (Fig. 4-5A).

To determine whether PERK is activated upon HBV replication, pHBV-transfected HepG2 cells were analyzed by immunoblot 48 h post-transfection using antibodies against PERK and phosphorylated PERK. As shown in Fig. 4-5B, significant elevation of total PERK and phosphorylated PERK levels was detected in pHBV-transfected HepG2 cells, as compared with the mock control. And the PERK downstream effector, eIF-2 α , was also activated upon HBV replication, as demonstrated by the enhanced phosphorylation of eIF-2 α in pHBV-transfected cells (Fig. 4-5B). Interestingly, by using antibodies against eIF-2 α , we showed that the expression level of total eIF-2 α also increased in pHBV-transfected HepG2 cells when comparing with the mock control (Fig. 4-5B).

In addition, the cleaved p50 fraction of ATF6 was clearly detected in the nuclear

fraction of the pHBV-transfected HepG2 cells 48 hours after transfection, which indicated HBV replication also activated the ATF6-mediated pathway in HepG2 cells (Fig. 4-5B).

4.4 Discussion

Interferons are a family of antiviral cytokines that can be triggered by innate immunity in response to viral infection. However, IFNs don't directly inhibit viral multiplication. Instead, the IFN-induced antiviral responses are mediated by ISGs, which are also referred to as antiviral effectors. They fight against virus by individually restricting all steps of viral life cycle and/or enhancing IFN responses.

ISG15 is one of the most prominently induced ISGs, sharing some common properties with ubiquitin (Loeb and Haas, 1992). With the help of several other ISGs encoding ubiquitin-associated enzymes, ISG15 is catalysed and conjugated to numerous protein substrates to regulate variable cellular responses and to inhibit viral multiplication, which is called ISGylation. Like ISG15, Mx proteins are also highly induced by type I IFNs. Mx proteins accumulate in the cytoplasm as oligomers, which recognize and trap viral nucleocapsids and then degrade them at the early stage of viral infection (Accola *et al.*, 2002). Some nuclear localized Mx proteins are found to block viral gene transcription by interfering viral polymerase (Krug, 1985; Pavlovic *et al.*, 1992). Unlike ISG15 and Mx proteins, the OAS and PKR are constitutively expressed at low levels and are rapidly increased upon type I IFNs stimulation. The IFN-induced OAS1

accumulates in the cytoplasm as an inactivate monomer. Following activation by viral double-stranded RNA, the OAS1 monomers are conjugated to form active tetramers that synthesize 2', 5'-oligoadenylates, which later activate RNase L. The binding of 2', 5'-oligoadenylates to RNase L triggers the degradation of viral and cellular single-stranded RNA (Floyd-Smith *et al.*, 1981; Wreschner *et al.*, 1981). Similar to OAS, the type I IFNs-induced PKR accumulates in the cytoplasm as an inactive monomer. Following activation by viral RNAs and other pathogen-associated molecules (Hsu *et al.*, 2004), PKR are phosphorylated and dimerized to form the active enzyme, which later phosphorylates eIF2 α to halt translation through undefined mechanisms.

In this part of study, we first checked whether IFN-triggered antiviral signaling pathways were activated by GRP78 overexpression in HepG2 cells. As shown in Fig. 4-2, elevated mRNA levels of IFN-β1, OAS1, OAS2 and RNase L were observed, suggesting an induction of IFN-β1 as well as the activation of the IFN-β1-regulated OAS/RNaseL signaling pathway during GRP78-induced HBV inhibition. However, three other effector pathways of the type I IFN-mediated antiviral response, *i.e.* the ISG15 ubiquitin-like pathway, the Mx GTPase pathway, and the PKR pathway, were less likely to be activated as demonstrated by minimal changes in the mRNA levels of related genes. Recent studies have shown that GRP78 is implicated in IFN-γ folding (Vandenbroeck *et al.*, 2006), induction (Brownlie *et al.*, 2006) and immune responses (Triantafilou *et al.*, 2001; Hegde *et al.*, 2006), yet the underlying mechanisms of how IFN-β induction was initiated in GRP78-overexpressing HepG2 cells have yet to be

elucidated. In addition, we also checked whether GRP78 and IFN-β1 could form an antiviral activation loop in response to HBV replication. Our data demonstrated that IFN-β-1a induced GRP78 overexpression in both dose- and time-dependent manners in HepG2 cells. As proposed in Fig. 4-6, GRP78 and IFN-β1 form a positive feedback loop where mutual activation of GRP78 and IFN-β1 occurs. Once autocrine or paracrine IFN-β binds to IFN receptors, the signaling cascades are initiated, and the IFN-stimulated genes (*e.g.* OAS1 and OAS2) are then induced. Thereafter, the downstream antiviral effector RNase L is specifically activated, and HBV suppression is resulted. Conversely, IFN-α was unlikely to be involved in GRP78-induced HBV suppression because no interactive effect was found between their changes in expression level. Taking together, our data suggest that the IFN-β1-regulated OAS/RNaseL pathway contributes to the anti-HBV effect of GRP78 in the HepG2 cells.

As mentioned in Chapter 2, the up-regulation of GRP78 upon HBV replication may be caused by the activation of UPR that enhanced the synthesis and translation of ER chaperones in ER stress (Ni and Lee, 2007). To test this hypothesis, we investigated whether the UPR signaling pathways, including the IRE1, the PERK and the ATF6 mediated-signal transduction, were activated by HBV replication. As shown in Fig. 4-5A, the IRE1 downstream effector XBP1 was slightly activated in pHBV-transfected HepG2 cells, as indicated by a faint spliced RT-PCR product. Concomitantly, the ATF6 was activated by HBV replication, as demonstrated by the presence of cleaved nuclear fraction. The activation of IRE1- and ATF6-meidated signal pathways in UPR response

strongly supports our hypothesis that the up-regulation of GRP78 upon HBV replication is attributed, at least in part, to the activation of UPR as host protective responses to relieve ER stress and maintain cell survival.

Meanwhile, we also noticed the levels of both phosphorylated PERK and phosphorylated eIF2 α were significantly increased upon HBV replication, which suggested the PERK-mediated translation attenuation was activated as a cellular protective strategy against ER stress and viral multiplication. This phenomena further urged us to investigate whether the level of total eIF-2 α was altered by HBV replication. Surprisingly, we found that HBV replication up-regulated the total eIF-2 α protein level, which suggested HBV might be able to overcome the UPR by inducing more eIF-2 α for translation.

In summary, the interaction between virus and host is highly complicated. On one hand, viruses make full use of the cellular machinery to facilitate their proliferation and adopt smart strategies to avoid host attacks; on the other hand, infected host cells exert antiviral response to cope with the viral persistent replication. Thus, once this finely tuned homeostasis is broken, the imbalance determines the outcomes of infection. The present study demonstrates for the first time that GRP78 exerts anti-HBV activities through IFN- β 1-regualted OAS/RNase L signaling pathway in hepatocytes. Further studies on the identification of viral targets targeted by GRP78 and the link between GRP78 and IFN- β induction are needed, which will undoubtedly increase our

understanding of the novel roles of GRP78 in cell rescue and defense.

Table 4-1. Primers used in the quantitative real-time PCR.

F, forward; R, reverse.

Gene	Genbank Accession No.	Sequences of primers
GRP78	NM_005347	F 5'-GACGGGCAAAGATGTCAGGAA-3'
		R 5'-TCATAGTAGACCGGAACAGATCCA-3'
IFN-α1	NM_024013	F 5'-GCCTCGCCCTTTGCTTTACT-3'
		R 5'-GGATCAGCTCATGGAGGACAGA-3'
IFN-β1	NM_002176	F 5'-GACCAACAAGTGTCTCCTCCAAA-3'
		R 5'-GAACTGCTGCAGCTGCTTAATC-3'
ISG15	NM_005101	F 5'- ATGGGCTGGGACCTGACG-3'
		R 5'-GCCAATCTTCTGGGTGATCTG-3'
Mx1	NM_002462	F 5'-GCTTGCTTTCACAGATGTTTCG-3'
		R 5'-AAGGGATGTGGCTGGAGATG-3'
OAS1	NM_016816	F 5'- TCCACCTGCTTCACAGAACTACA-3'
		R 5'- TGGGCTGTGTTGAAATGTGTTT-3'
OAS2	NM_016817	F 5'-TACCTGAAGCCCTACGAAGAATG-3'
		R 5'-TCAGCTTATCCCCAGTTTTATCG-3'
OAS3	NM_006187	F 5'-CCCTGGTCTGAGACTCACGTTT-3'
		R 5'-GACTTGTGGCTTGGGTTTGAC-3'
OASL	NM_003733	F 5'-CGTGAAACATCGGCCAACTAAG-3'
		R 5'-GTACCCATTTCCCAGGCATAGA-3'
RNase L	NM_021133	F 5'-TCATTCATCGTCTCTTCCATCCT-3'
		R 5'-ACATTCCGAAGCGTCCTATAGC-3'
PKR	NM_002759	F 5'-AATGATGGAAAGCGAACAAGGAGTA-3'
		R 5'-CTTCCACACAGTCAAGGTCCTTAGT-3'
GAPDH	NM_002046	F 5'-GATTCCACCCATGGCAAATTCCA-3'
		R 5'-TGGTGATGGGATTTCCATTGATGA-3'

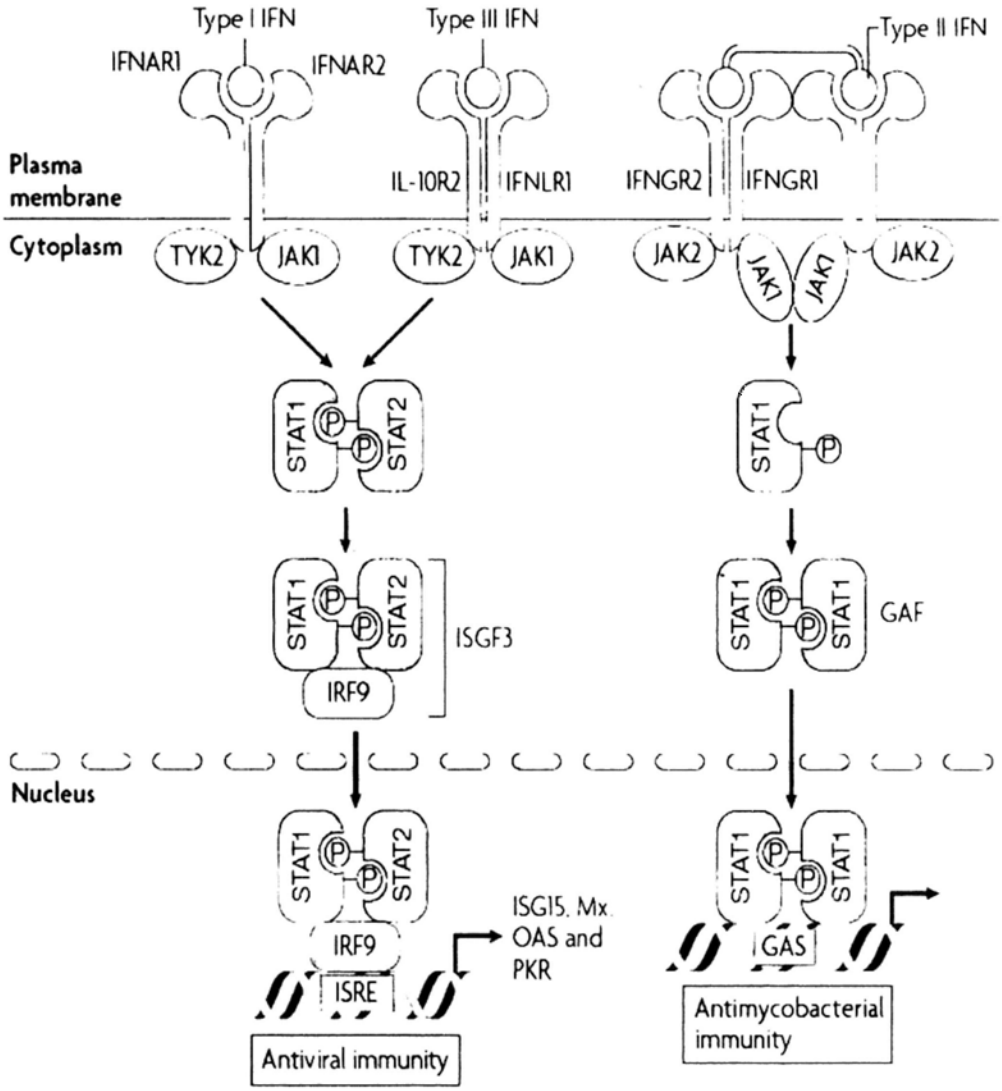

Fig. 4-1. IFN-induced signaling pathways.

The biological activities of IFNs are initiated by binding to their corresponding receptor complexes. Type I IFNs bind to a heterodimer of IFNα receptor 1 (IFNAR1) and IFNAR2, and type III IFNs bind to a combination of interleukin-10 receptor 2 (IL-10R2) and IFNλ receptor 1 (IFNLR1), while dimmers of the type II IFNs bind to a tetramer consisting of two IFNγ receptor 2 (IFNGR2) chains and two IFNGR1 chains. Following binding by IFNs, the receptor-associated tyrosine kinase 2 (TYK2) and Janus tyrosine kinase 1 (JAK1) are activated, which leads to the phosphorylation of the signal transducer and activator of transcription 1 (STAT1) and STAT2. For type I and type III IFNs responses, the phosphorylated STAT1/STAT2 heterodimer associates with IFN-regulatory factor 9 (IRF9) to form IFN-stimulated gene factor 3 (ISGF3), which is transported into the nucleus and binds to the IFN-stimulated response elements (ISREs) in target promoters to induce IFN-stimulated genes (ISGs) transcription. For type II IFNs responses, the phosphorylated STAT1 are associated with each other to form IFNγ activation factor (GAF), which migrates to the nucleus and binds to γ-IFN-activated sequence (GAS) to drive IFN-γ-induced genes expression. ISG15, IFN-stimulated protein of 15kDa; Mx, myxovirus resistance; OAS, 2', 5'-oligoadenylate synthetase; PKR, protein kinase R. (Sadler and Williams, 2008)

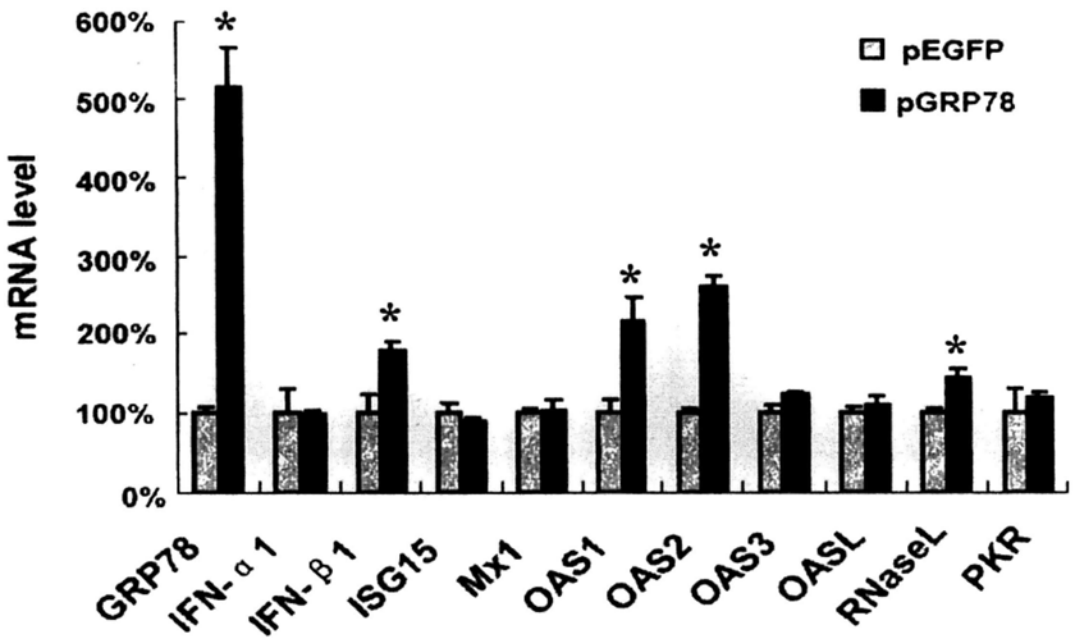

Fig. 4-2. Effects of GRP78 overexpression on IFNs and IFN-inducible genes' mRNA expression.

Total RNA was isolated from pGRP78- and pEGFP-transfected HepG2 cells 48h post-transfection. The mRNA expression levels of GRP78, IFNs (IFN-α1, IFN-β1) and IFN-inducible genes (ISG15, Mx1, OAS1, OAS2, OAS3, OASL, RNaseL and PKR) were measured by real-time RT-PCR. Data are expressed as mean ± S.D.. (n = 3; * $p <$ 0.01).

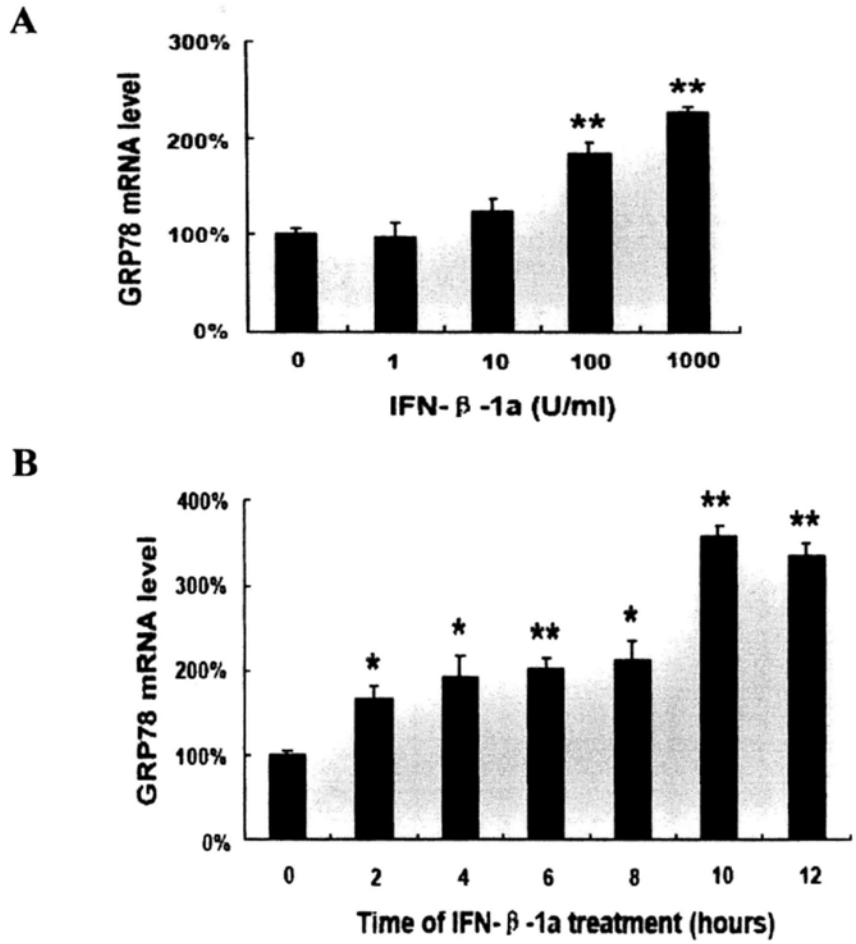

Fig. 4-3. IFN- β -1a stimulates GRP78 overexpression in both dose- and time-dependent manners. A, dose-dependent effect of IFN-β-1a on the GRP78 expression in HepG2 cells. Total RNA was isolated from HepG2 cells 8h after the treatment with varying concentrations of IFN-β-1a (0, 1, 10, 100 and 1000 units/ml) and real-time RT-PCR was performed to measure GRP78 expression. B, time-course change of the mRNA expression of GRP78 after IFN-β-1a treatment. Total RNA was extracted from HepG2 cells treated with 1000 units/ml IFN-β-1a at the indicated incubation time (0, 2, 4, 6, 8, 10 and 12 h) and used for real-time RT-PCR analysis. The expression levels of GRP78, IFNs and IFN-inducible genes were normalized to GAPDH mRNA level and are expressed as -fold changes to corresponding controls. Data are expressed as mean ± S.D.. (n = 3; * $p < 0.05$, ** $p < 0.01$).

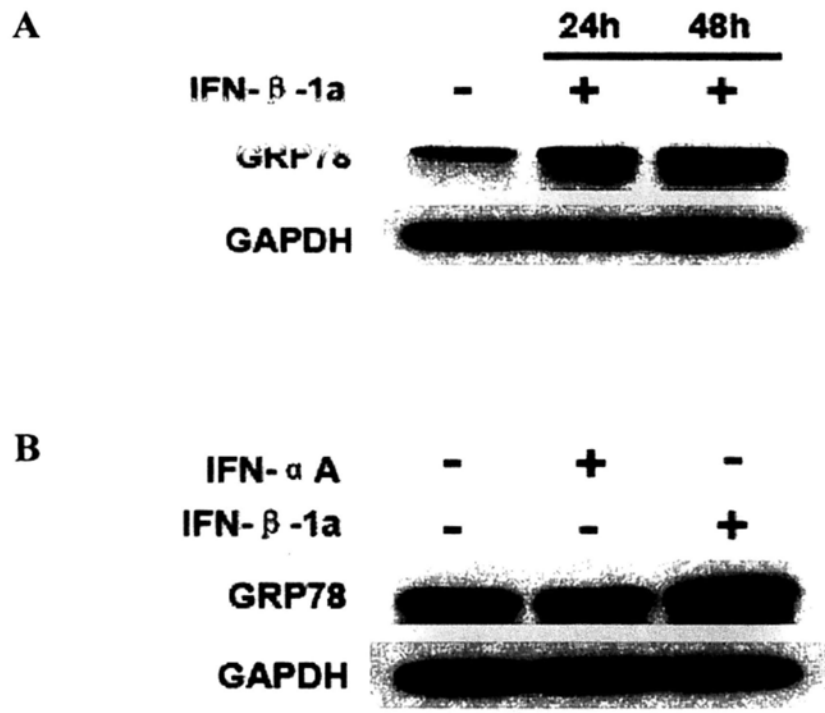

Fig. 4-4. GRP78 protein expression responses to IFN-β-1a stimulation time-dependently, but not IFN-αA.

A, time-dependent elevation of GRP78 protein expression induced by IFN-β-1a (1000 units/ml). B, GRP78 protein expression in response to IFN-αA (1000 units/ml) and IFN-β-1a (1000 units/ml) treatment, respectively, for 24 h. The results shown are representative of three independent experiments.

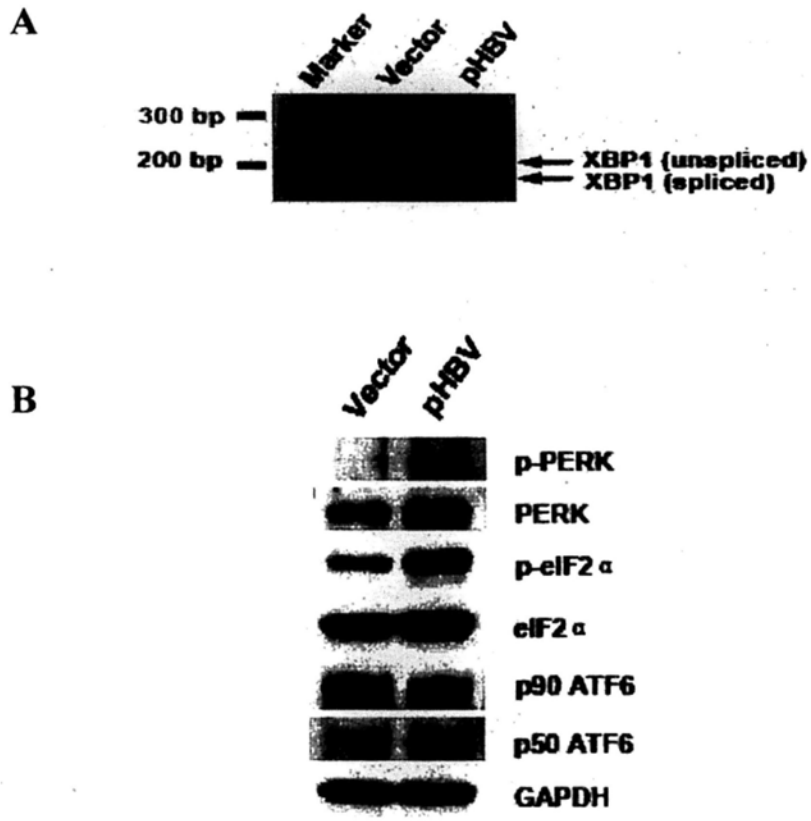

Fig. 4-5. HBV replication induces unfolded protein response in HepG2 cells.

A. RT-PCR analysis of XBP-1 mRNA splicing. The positions of the unspliced (199 bp) and spliced (173 bp) forms of XBP1 transcripts are indicated. B. Immunoblots illustrating the upregulation of p-PERK, PERK, p- eIF2 α , eIF2 α and the activation of ATF6 (uncleaved form, 90 kD; cleaved form, 50 kD) induced by HBV replication are shown. GAPDH was served as loading control. The results shown are representative of three independent experiments.

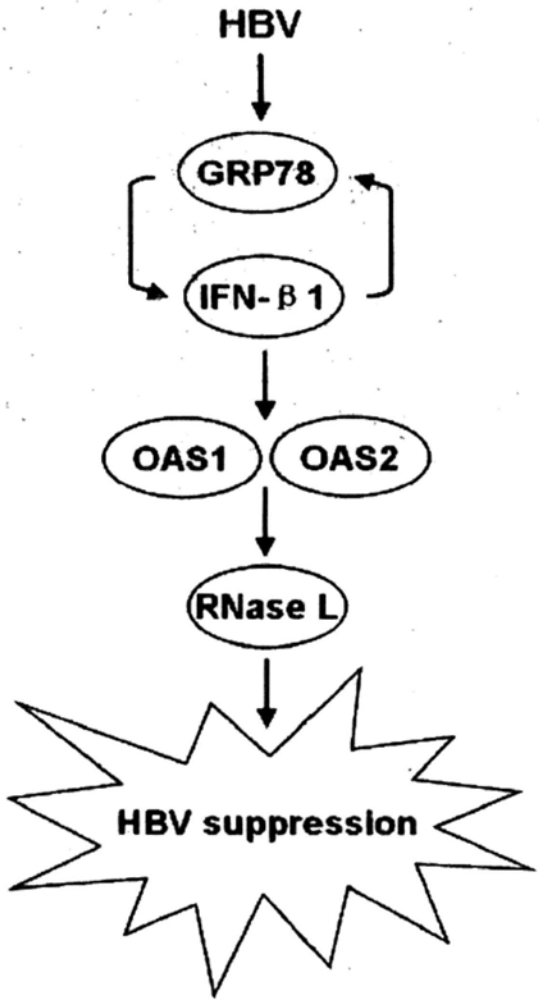

Fig. 4-6. Proposed mechanisms for the anti-HBV activity of GRP78 in HepG2 cells. The mutual activation of GRP78 and IFN-β1 may compose a positive feedback loop that amplifies signal by inducing OAS1 and OAS2 overexpression. The antiviral effector RNase L is then activated, thereby suppresses HBV replication.

Chapter 5

Summary and Perspectives

5.1 Summary

For the first time, our study presents the global changes in hepatocyte proteome upon HBV challenge using an inducible HBV-producing system and reveals the anti-HBV function of GRP78, which refines our knowledge of the complex HBV-host network and extends the protective roles of GRP78 to the cellular defense against HBV.

By using 2-DE combined with mass spectrometric analysis, 23 differentially expressed proteins were identified in our proteomic study. Among them, 16 proteins were up-regulated and 7 were down-regulated by HBV replication. Particularly, GRP78 was revealed as an intracellular anti-HBV factor using the gain- and loss-of-function strategies. More interestingly, IFN-β1-mediated OAS/RNase L signaling pathway was specifically activated by GRP78, and the positive regulatory circuit of GRP78 and IFN-β1, which greatly enhanced the IFN-β antiviral response, was built during the GRP78-induced HBV suppression. All these findings suggested a new defense against HBV in hepatocytes. To our knowledge, this is the first report on a natural intracellular anti-HBV mechanism in hepatocytes other than apolipoprotein B mRNA-editing enzyme catalytic-polypeptide (APOBEC) proteins. Our findings also suggest the potential beneficial effects of GRP78 in treating HBV infection in the future, as well as the development of novel anti-HBV drugs based on host response instead of virus itself

may be an alternative to overcome the resistance to the current nucleotide analogues caused by fast viral mutagenesis.

5.2 Perspectives

The present study demonstrates that GRP78 functions as an endogenous anti-HBV factor, which works *via* the IFN-β-mediated signaling pathway in hepatocytes. Some efforts towards the following aspects are currently underway and should be done in the future.

(1) The anti-HBV process of GRP78

To identify the HBV replicative intermediates targeted by GRP78, Southern and Northern blot analysis are necessary. Further studies towards the dynamic changes of HBV DNA, RNA and proteins regulated by GRP78 overexpression are also warranted, which help us to dissect the antiviral process of GRP78. In addition, to determine whether the activation of IFN- β 1-mediated OAS/RNase L signaling pathway is a necessary component of the GRP78-induced HBV suppression, further analysis of the HBV replication efficiency in IFN- β , OAS or RNase L deficient cell line is needed, which will provide additional support for our conclusion as the blockade of the IFN- β 1-mediated OAS/RNase L signal transduction may attenuate the antiviral effects of GRP78.

(2) The connection between GRP78 and IFN-β

It was reported that GRP78, as an immunotherapeutic agent, increased IFN-γ production and prevented the collagen-induced arthritis in HLA-DR1+/+ transgenic mice (Brownlie *et al.*, 2006). However, no other observations about the induction of IFN- β 1 by GRP78 have been reported so far. The connection between GRP78 and the specific activation of IFN- β 1 is unclear. Therefore, this is a very interesting topic for the future study, and potentially a new field.

(3) The link between ER stress and IFN response

Viral infection induces ER stress and IFN responses. In our study, we have demonstrated HBV replication triggers ER stress and UPR response in HepG2 cells, as demonstrated by the induction of GRP78 and the activation of PERK-, IRE1- and ATF6-mediated signal pathways. The components of the three UPR signal pathways either stimulate or inhibit viral replication in different physiological conditions, which thus determines the pathogenesis of viral infection and cell fate. Concomitantly, GRP78 overexpression activated the IFN-β-mediated antiviral response in our study. Therefore, we speculate that there may exist cross talk between UPR and IFN signal pathways in the process of GRP78-induced HBV suppression, which may contribute to the maintenance of cellular homeostasis. The investigation is now underway.

(4) Other mechanisms involved in the GRP78-mediated HBV suppression

In addition to IFN-β1, other cytokines, chemokines and/or endogenous anti-HBV factors may be involved in the regulation of HBV replication mediated by GRP78. This

should be evaluated in the future.

(5) The antiviral effects of GRP78 in different cell lines and on different HBV genotypes/subgenotypes/mutants

To determine whether GRP78 exerts anti-HBV activity in other hepatic cell lines, Huh7, L02 and MIHA cell lines, which also favor HBV replication *in vitro*, need to be tested.

Different HBV genotypes/subgenotypes/mutants respond to various antiviral treatments with varying degrees of susceptibility. We have demonstrated GRP78 inhibited HBV genotype C replication in the present study. In order to comprehensively validate the inhibitory effect of GRP78 on HBV replication, more HBV genotypes/subgenotypes/mutants need to be tested.

(6) *In vivo* study of the anti-HBV effects of GRP78

To investigate the full impact of GRP78 on HBV replication, *in vivo* study of the antiviral function of GRP78 in HBV-transgenic mice is required.

In conclusion, the above-mentioned research topics and directions are interesting, novel, and definitely worth substantial effort in the future, which will help us to decipher the anti-HBV function of GRP78 and to understand the complex interplay between HBV and host.

Appendix

Fig. A1. MS spectrum exclusion lists.

842.51;897.414;973.5318;1037.5267;1045.5642;1060.5639;1066.5169;1140.5649;1165.5853;1179.6010;1184.5911;1193.6166;1234.6796;1307.6782;1320.5834;1357.7188;1357.6963;1365.6399;1373.6549;1383.6909;1434.7705;1474.7494;1474.7858;1699.8251;1707.7727;1716.8517;1838.9149;1940.9352;1993.9772;2211.1046;2283.1807;2299.1756;2312.1482;2383.9524;2510.1323;2705.1617;2831.1947;3312.3087.

Fig. A2. Identification of superoxide dismutase 1 (SOD1) by MALDI-TOF MS analysis. A, MS spectrum of SOD1. B, Non-filtered MS peak lists of SOD1.

A

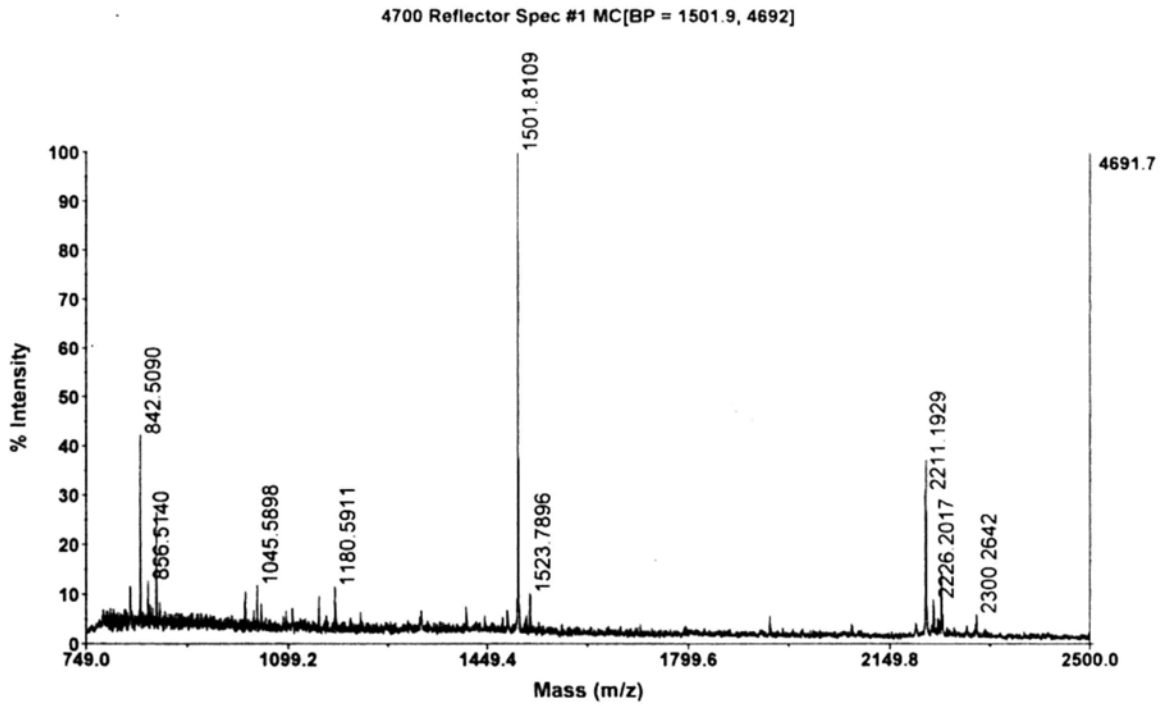

B 842.509033;856.513977;870.548462;1024.524780;1045.589844;1180.591064;1501.810913;1523.789551;2211.192871;2213.273682;2214.089600;2226.201660;2239.130615;2239.306152;2300.264160.

Fig. A3. Identification of peroxiredoxin 2 isoform a (PRDX2) by MALDI-TOF MS analysis. A, MS spectrum of PRDX2. B, Non-filtered MS peak lists of PRDX2.

A

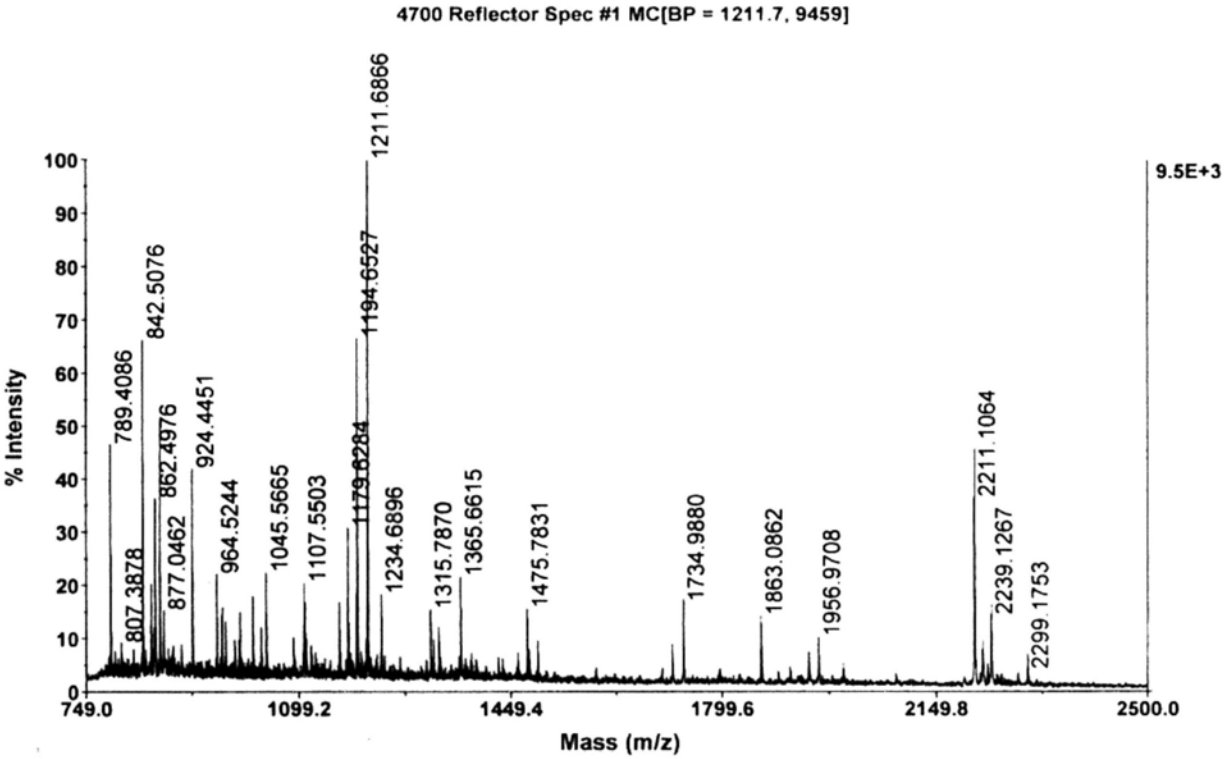

B

789.408569;807.387756;841.466187;842.507629;856.514343;861.072266;862.497559;864.495422;870.539551;877.046204;924.445068;964.524353;972.541809;973.538513;978.523865;993.504517;1000.520569;1002.536194;1023.535828;1037.534546;1045.566528;1090.539795;1106.544189;1107.550293;1108.551392;1109.509766;1111.632568;1118.519775;1165.593750;1179.628418;1193.632935;1194.652710;1209.657593;1210.657104;1211.686646;1233.643677;1234.689575;1315.786987;1320.608398;1329.662598;1365.661499;1383.691162;1460.782349;1475.783081;1479.760742;1493.752563;1716.897095;1734.988037;1863.086182;1940.933472;1956.970825;1996.980835;2211.106445;2225.103516;2233.104736;2239.126709;2299.175293.

Fig. A4. Identification of peroxiredoxin 3 (PRDX3) by MALDI-TOF MS analysis. A, MS spectrum of PRDX3. B, Non-filtered MS peak lists of PRDX3.

A

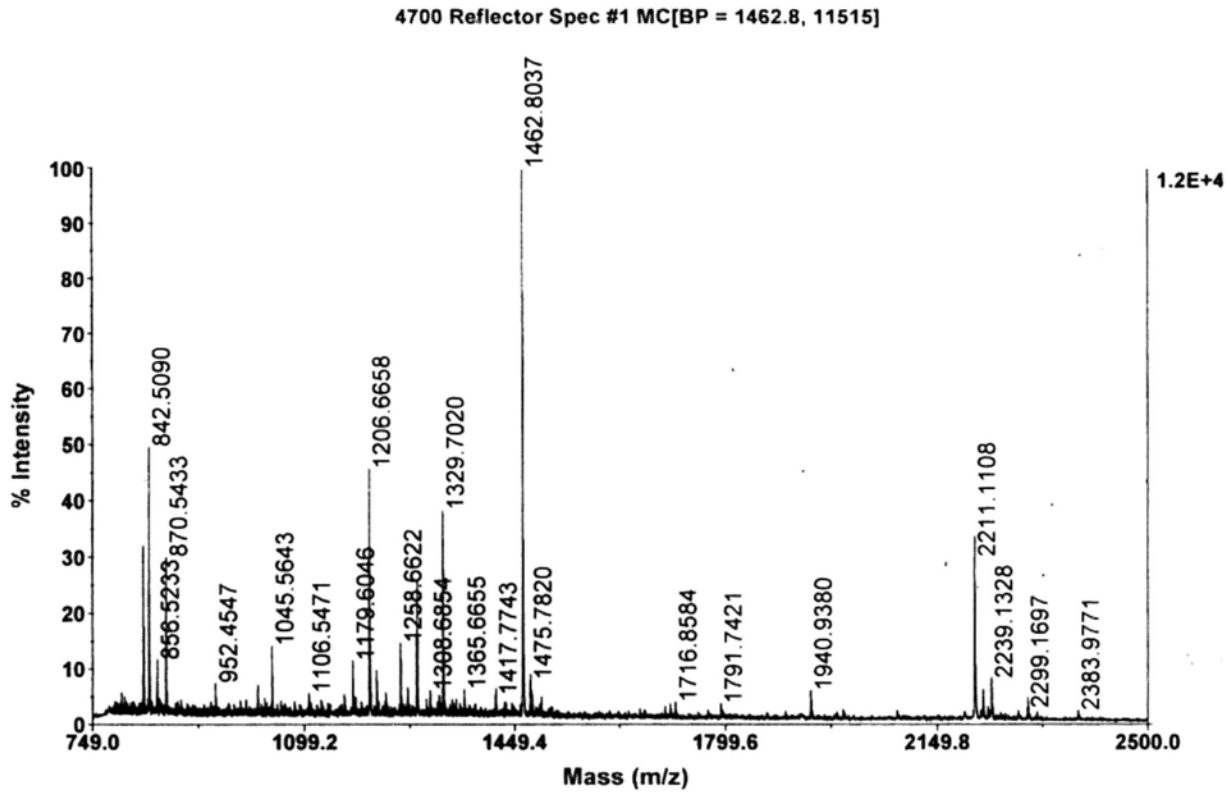

B

833.437927;842.509033;856.523254;870.543335;952.454712;1021.524841;1045.564331;1106.547119;1179.604614;1206.665771;1218.656250;1234.664307;1258.662231;1270.659058;1285.748779;1286.732666;1308.685425;1323.679199;1329.702026;1365.665527;1417.774292;1462.803711;1475.781982;1478.775757;1493.739868;1708.770874;1716.858398;1791.742065;1940.937988;2211.110840;2225.120117;2233.109375;2239.132813;2299.169678;2383.977051.

Fig. A5. Identification of pyruvate dehydrogenase E1 beta subunit precursor (PDHB) by MALDI-TOF MS analysis. A, MS spectrum of PDHB. B, Non-filtered MS peak lists of PDHB.

A

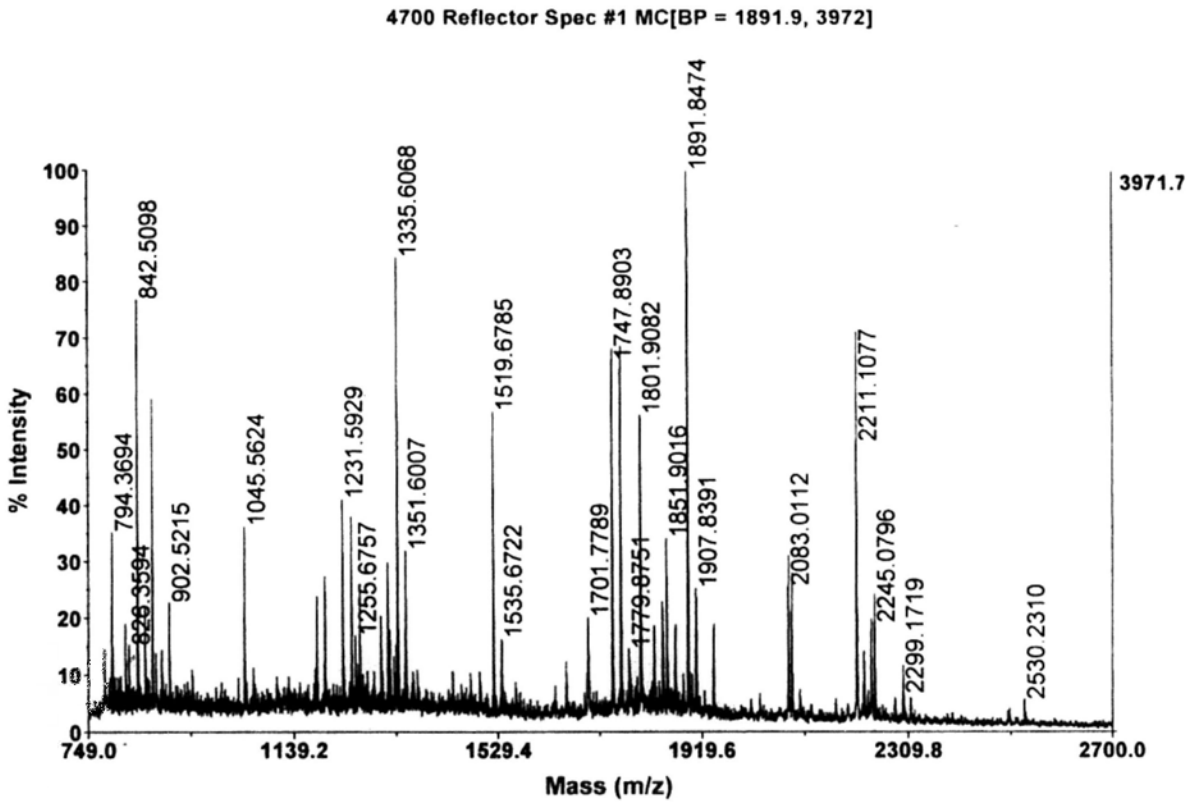

B 780.352539;793.376648;794.369446;819.488586;826.359375;841.464294;842.509827;856.521790;870.540466;888.490417;902.521484;1045.562378;1182.701660;1197.692749;1231.592896;1248.625244;1255.675659;1263.579224;1264.611084;1304.682007;1317.608032;1321.664551;1333.588379;1335.606812;1351.600708;1519.678467;1535.672241;1701.778931;1747.890259;1763.881104;1779.875122;1801.908203;1827.925781;1843.929810;1851.901611;1867.903687;1891.847412;1907.839111;1940.936035;2083.011230;2089.011719;2211.107666;2225.137207;2239.134033;2245.079590;2299.171875;2530.230957.

Fig. A6. Identification of enolase 1 (ENO1) by MALDI-TOF MS analysis. A, MS spectrum of ENO1. B, Non-filtered MS peak lists of ENO1.

A

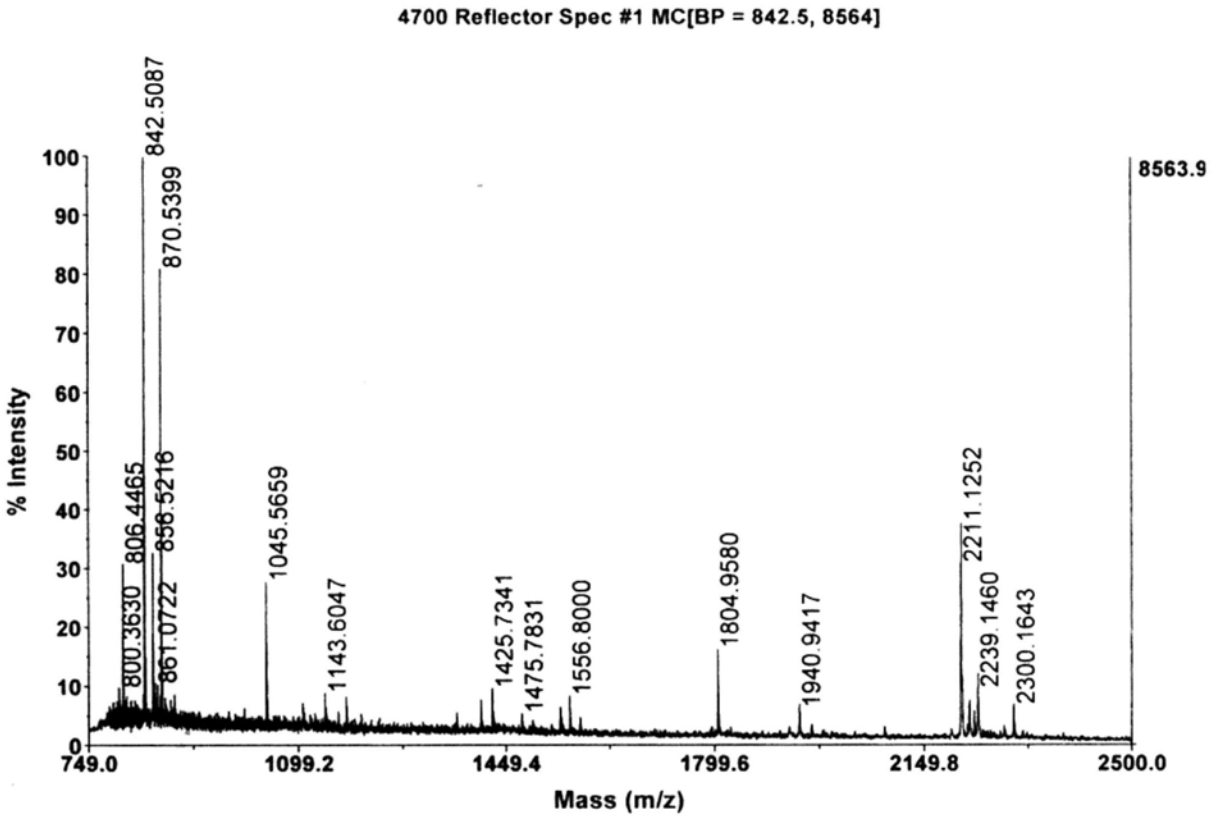

B 800.363037;806.446472;840.465881;842.508667;856.521606;861.072205;864.467163;870.539917;1045.565918;1143.604736;1179.590210;1406.714600;1425.734131;1475.783081;1540.779663;1556.800049;1804.958008;1940.941650;2211.125244;2225.111816;2233.123535;2239.145996;2299.179199;2300.164307

Fig. A7. Identification of aldehyde dehydrogenase (ALDH) by MALDI-TOF MS analysis. A, MS spectrum of ALDH. B, Non-filtered MS peak lists of ALDH.

A

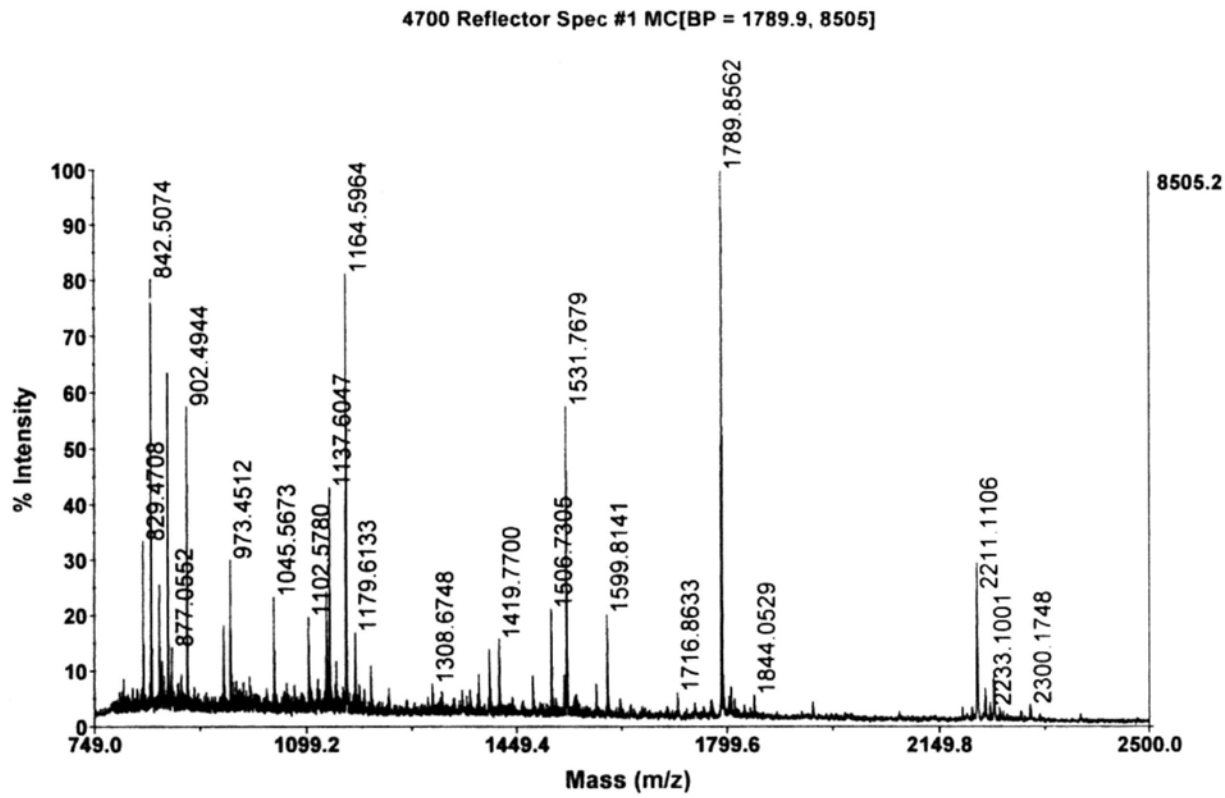

B

829.470764;841.479614;842.507385;856.515625;861.074524;864.463562;870.538269;877.055237;893.014221;902.494385;962.486572;973.451233;1005.445435;1045.567261;1102.578003;1118.565918;1132.597412;1134.592163;1136.591553;1137.604736;1146.573486;1148.589478;1163.581909;1164.596436;1178.601929;1179.613281;1205.661255;1308.674805;1385.769653;1403.775635;1419.770020;1475.781372;1506.730469;1527.788208;1528.773804;1531.767944;1581.797363;1599.814087;1716.863281;1789.856201;1803.830566;1844.052856;2211.110596;2225.115967;2233.100098;2239.129395;2300.174805.

Fig. A8. Identification of ATP synthase delta subunit precursor (ATP5D) by MALDI-TOF MS analysis. A, MS spectrum of ATP5D. B, Non-filtered MS peak lists of ATP5D.

A

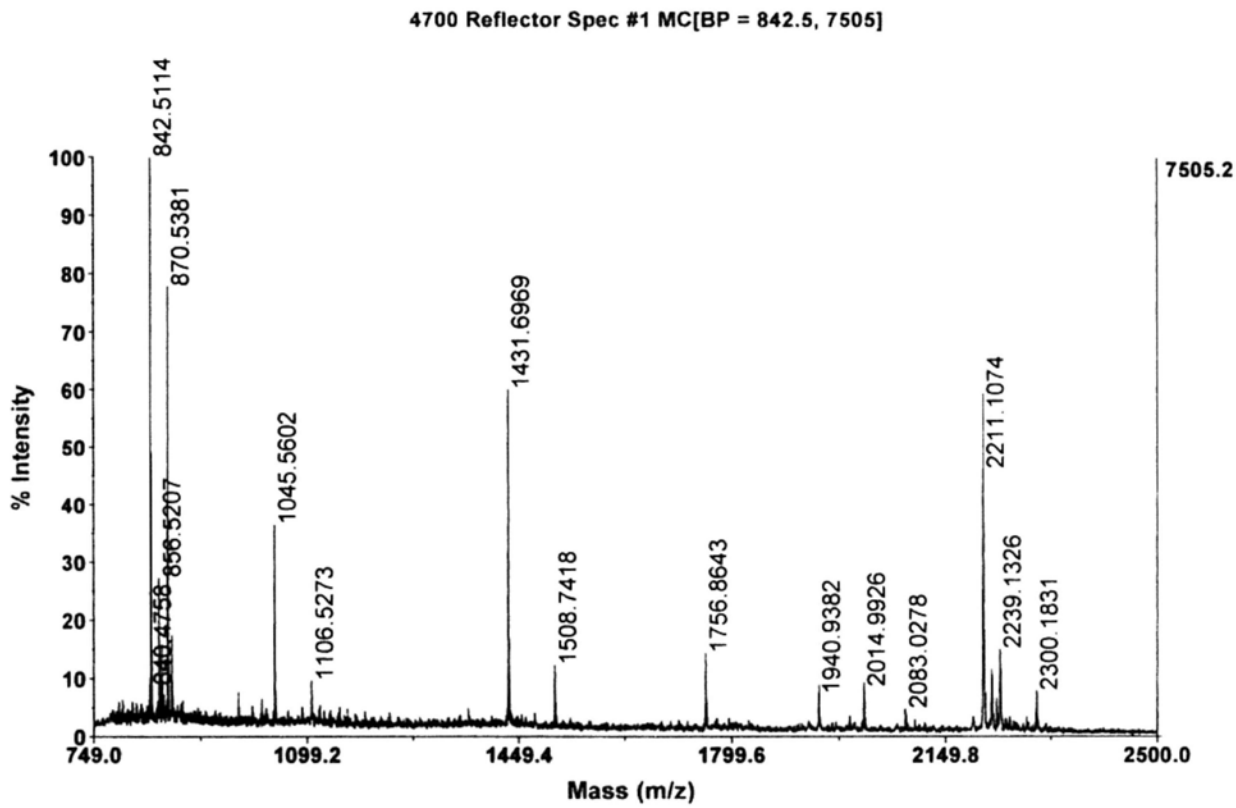

B 840.475769;842.511353;856.520691;861.070190;870.538147;877.032776;1045.560181;1106.527344;1430.678467;1431.696899;1507.746826;1508.741821;1755.856567;1756.864258;1940.938232;2014.992554;2083.027832;2210.090088;2211.107422;2225.123047;2233.102783;2238.121338;2239.132568;2299.168945;2300.183105.

Fig. A9. Identification of ATP synthase beta subunit precursor (ATP5B) by MALDI-TOF MS analysis. A, MS spectrum of ATP5B. B, Non-filtered MS peak lists of ATP5B.

A

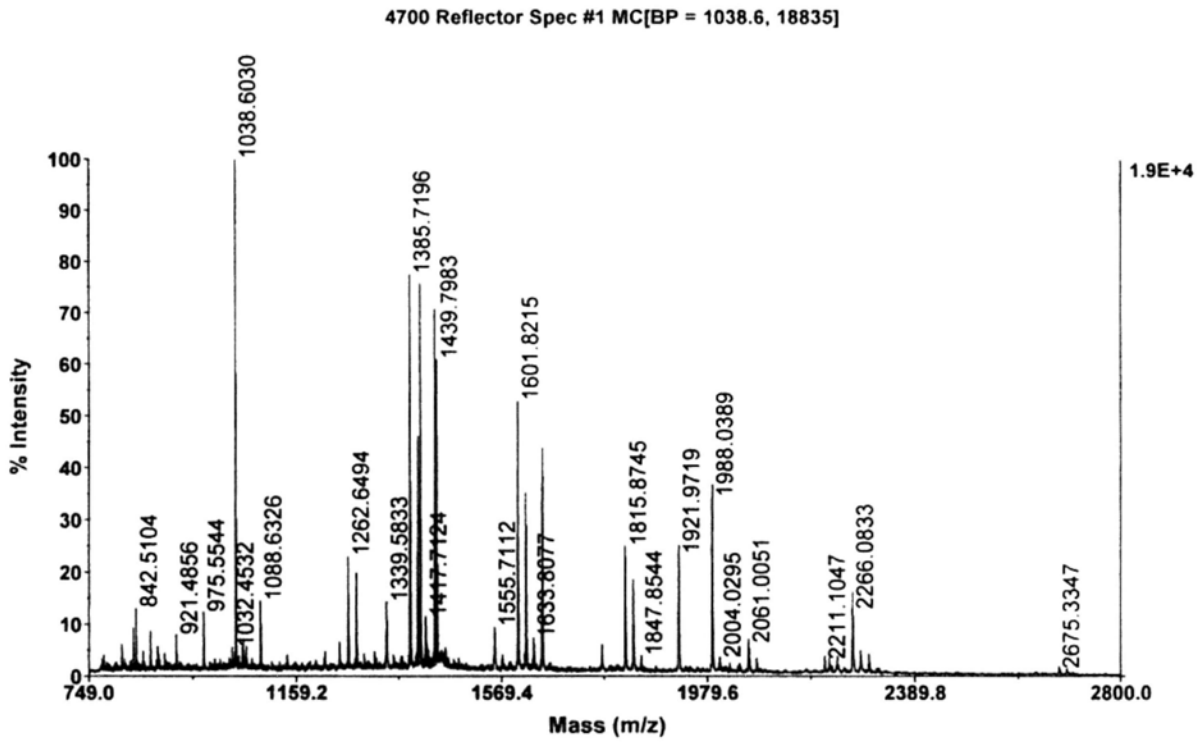

B

814.363708;837.386780;842.510376;856.502686;870.539551;885.445801;886.451965;899.507446;921.485596;975.554382;1032.453247;1036.568115;1038.603027;1052.575684;1054.582153;1059.514648;1088.632568;1245.628296;1262.649414;1278.639526;1315.737915;1339.583252;1385.719604;1401.709351;1405.693359;1406.693237;1417.712402;1420.685547;1433.717773;1435.765991;1439.798340;1455.779053;1457.780396;1555.711182;1601.821533;1615.815430;1617.813354;1633.807739;1649.868408;1650.926758;1769.777222;1815.874512;1831.872925;1847.854370;1921.971924;1988.038940;2004.029541;2061.005127;2077.001221;2211.104736;2220.016846;2236.052246;2266.083252;2282.063965;2298.076660;2675.334717;2691.355225.

Fig. A10. Identification of cathepsin D preproprotein (CTSD) by MALDI-TOF MS analysis. A, MS spectrum of CTSD. B, Non-filtered MS peak lists of CTSD.

A

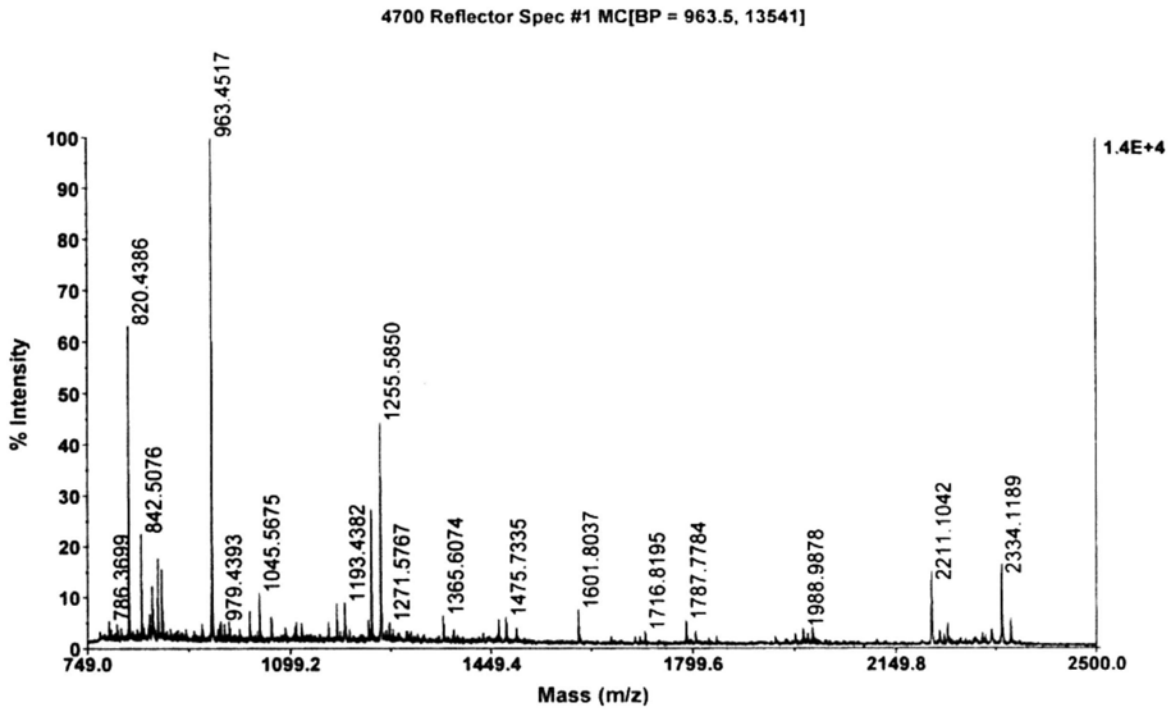

B 786.369873;820.438599;842.507568;856.513306;861.078796;862.429260;870.531311;877.053406;879.446472;961.424316;963.451721;977.431885;979.439331;1028.552979;1045.567505;1065.518921;1165.550171;1179.584229;1193.438232;1234.642822;1239.594849;1255.584961;1271.576660;1365.607422;1462.647217;1475.733521;1493.708252;1601.803711;1716.819458;1787.778442;1803.778320;1975.005005;1988.987793;1996.978271;2005.002808;2211.104248;2225.122314;2234.086670;2239.146729;2300.170654;2316.116211;2334.118896;2350.116943.

Fig. A11. Identification of tubulin alpha 6 (TUBA6) by MALDI-TOF MS analysis. A, MS spectrum of TUBA6. B, Non-filtered MS peak lists of TUBA6.

A

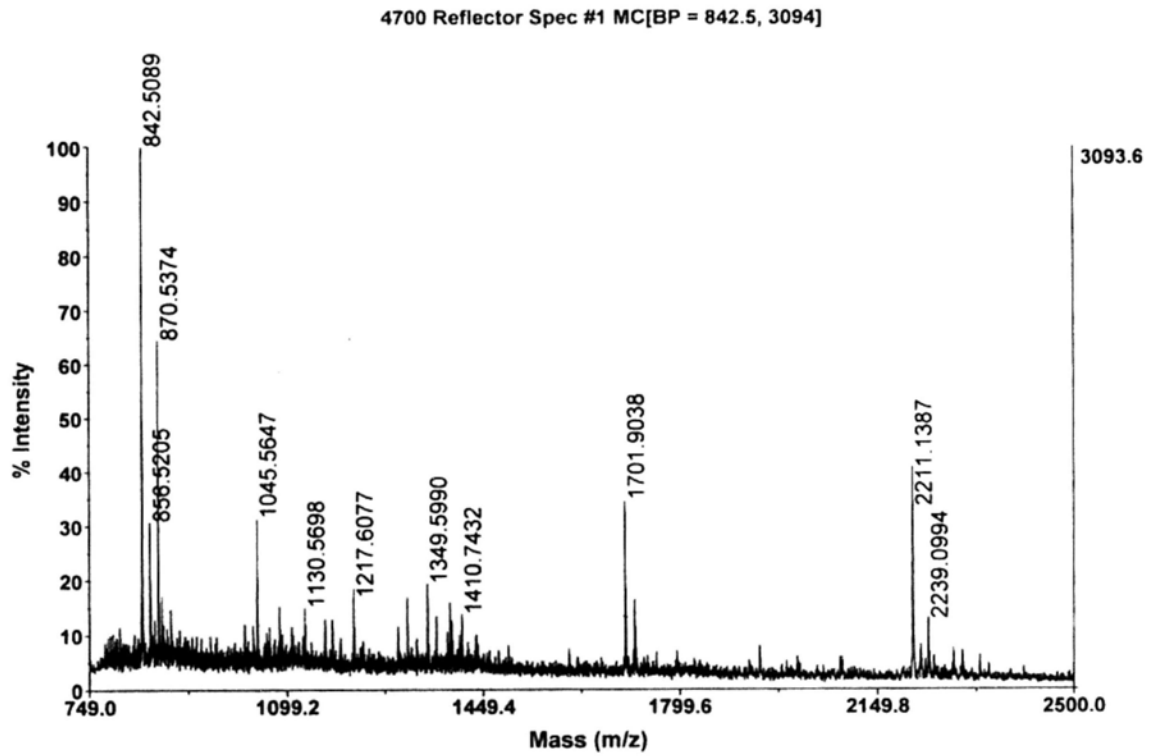

B 841.073547;842.508911;856.520508;870.537354;877.054077;1045.564697;1085.598145;113
0.569824;1217.607666;1313.649780;1349.598999;1389.672363;1410.743164;1701.903809;1
718.879517;2211.138672;2239.099365.

Fig. A12. Identification of lamin B1 (LMNB1) by MALDI-TOF MS analysis. A, MS spectrum of LMNB1. B, Non-filtered MS peak lists of LMNB1.

A

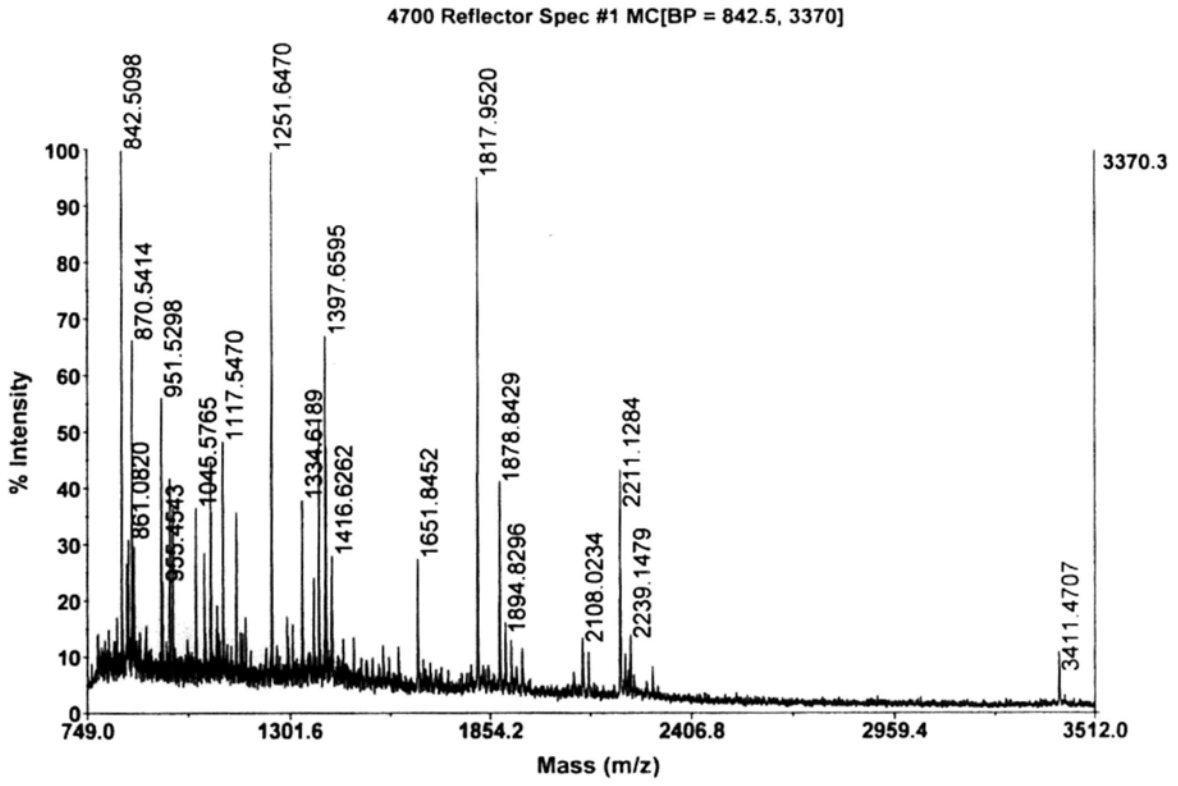

B 842.509827;856.508667;861.082031;870.541382;874.469788;877.050415;951.529846;955.454285;972.464966;974.479431;982.480408;1044.559204;1045.576538;1068.568481;1084.558105;1102.588745;1117.546997;1154.626465;1251.646973;1334.618896;1365.653198;1380.637329;1396.628052;1397.659546;1400.633545;1414.726074;1416.626221;1651.845215;1817.952026;1878.842896;1894.829590;1910.821533;2108.023438;2124.009277;2211.128418;2213.203613;2225.124268;2239.147949;3411.470703.

Fig. A13. Identification of actin beta subunit (ACTB) by MALDI-TOF MS analysis. A, MS spectrum of ACTB. B, Non-filtered MS peak lists of ACTB.

A

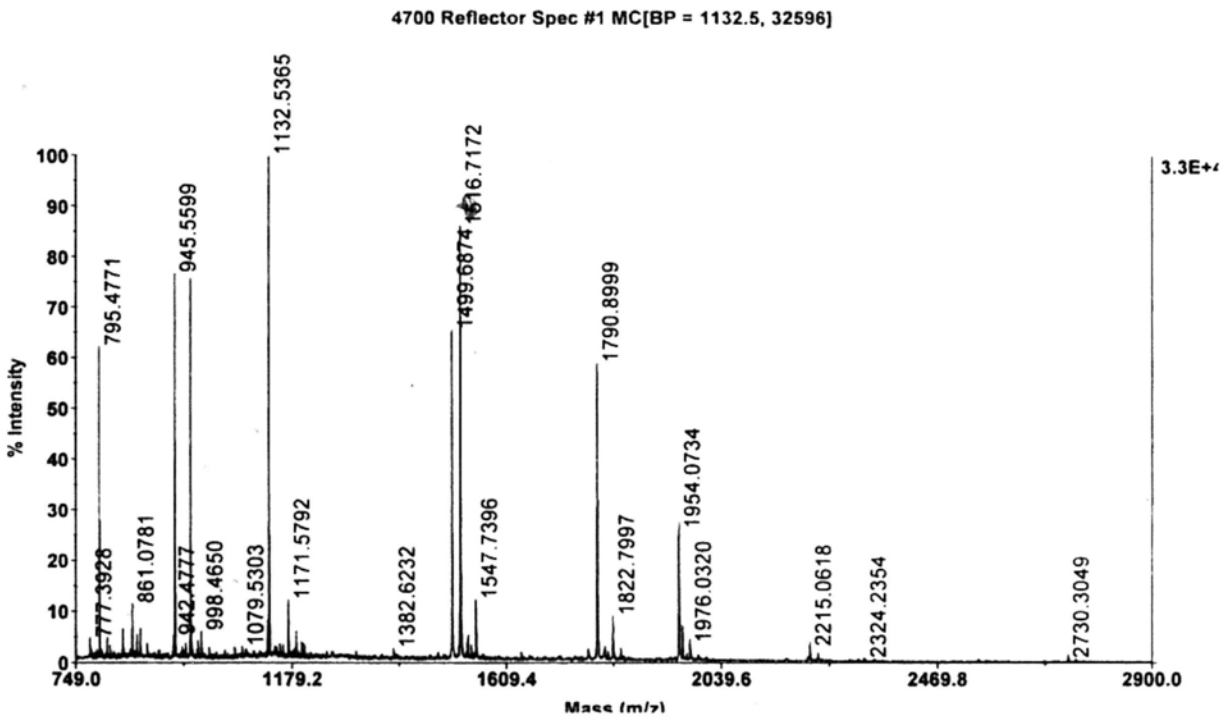

B 777.392822;795.477051;811.468445;817.450500;842.509216;861.078125;870.546692;877.050781;890.554443;942.477722;945.559937;967.521912;975.416260;976.455444;992.455322;998.465027;1064.642456;1079.530273;1130.521118;1132.536499;1154.519409;1161.609619;1171.579224;1187.569580;1198.528931;1203.566528;1382.623169;1498.696289;1499.687378;1513.682617;1515.731445;1516.717163;1520.724121;1521.702515;1529.722168;1530.707031;1531.712891;1532.713989;1538.695801;1546.702026;1547.739624;1772.881958;1788.869751;1790.899902;1804.869995;1806.877197;1812.882690;1821.812134;1822.799683;1837.803223;1838.796875;1954.073364;1960.916992;1970.056396;1976.031982;1992.953735;2212.092773;2215.061768;2231.074219;2324.235352;2730.304932.

Fig. A14. Identification of fatty acid binding protein (FABP) by MALDI-TOF MS analysis. A, MS spectrum of FABP. B, Non-filtered MS peak lists of FABP.

A

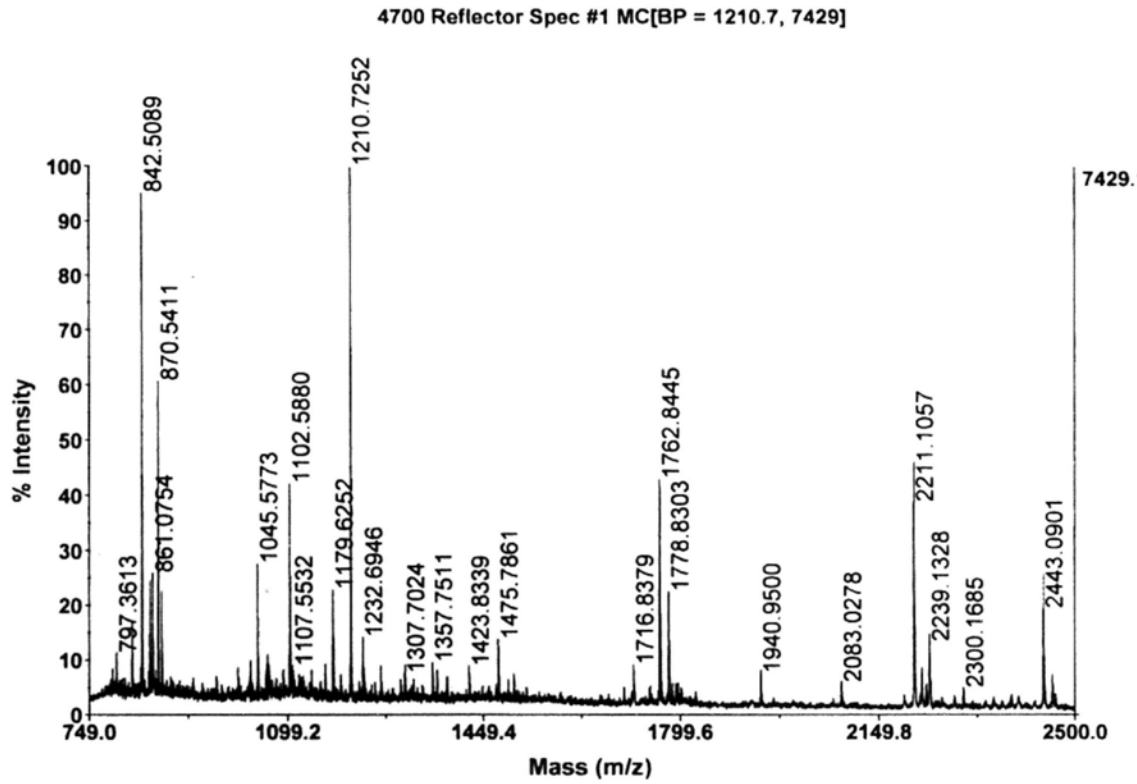

B

797.361267;824.439270;825.108215;841.464172;842.508911;856.513794;861.075378;
870.541077;877.035950;1033.521118;1045.577271;1061.574951;1063.526245;1065.52
8442;1102.588013;1107.553223;1165.581787;1179.625244;1210.725220;1232.694580;
1265.656982;1307.702393;1357.751099;1365.664063;1383.702759;1423.833862;1475.
786133;1503.742798;1716.837891;1762.844482;1778.830322;1784.828979;1791.7752
69;1794.832886;1940.949951;2083.027832;2211.105713;2225.111572;2233.073486;22
39.132813;2300.168457;2443.090088;2459.087158.

Fig. A15. Identification of proliferating cell nuclear antigen (PCNA) by MALDI-TOF MS analysis. A, MS spectrum of PCNA. B, Non-filtered MS peak lists of PCNA.

A

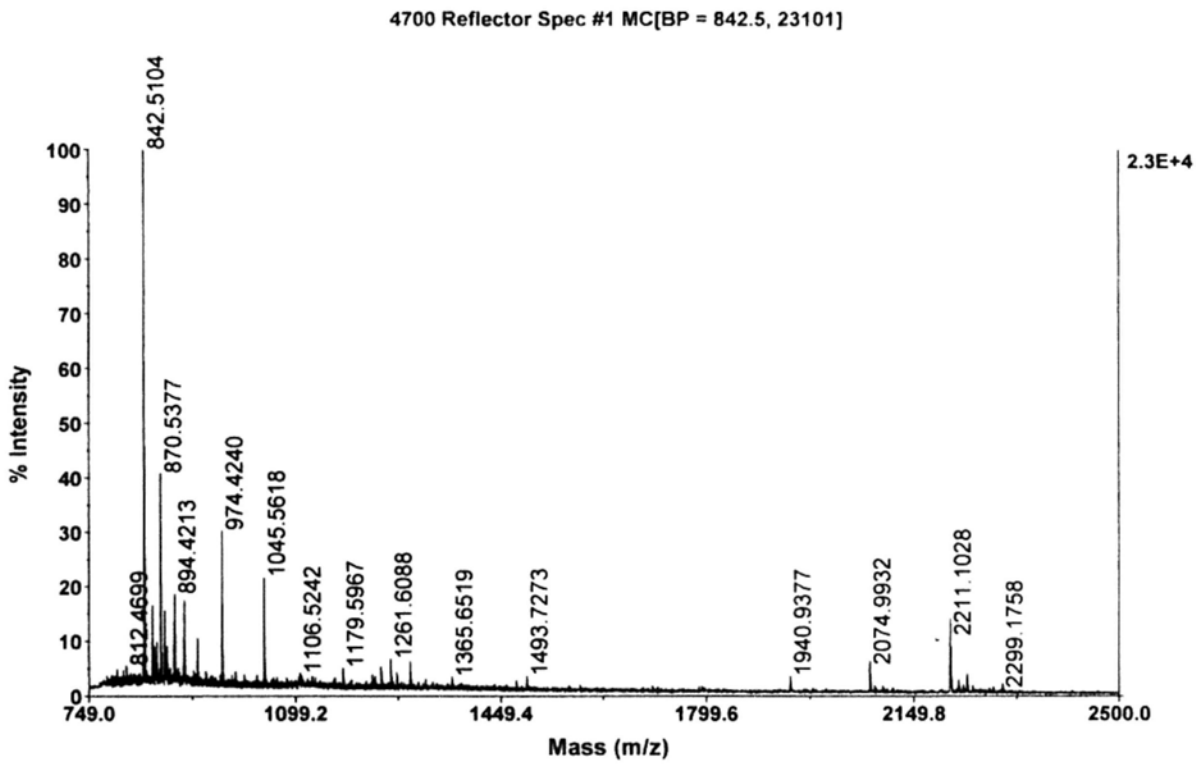

B

812.469910; 840.488281; 841.482666; 842.510376; 856.521912; 858.507324; 861.074890; 864.480286; 870.537659; 877.047668; 880.460693; 881.265259; 892.477051; 893.017517; 894.421326;908.465149;908.989685;910.409302;932.475281;974.423950;1045.561768;1106.524170;1179.596680;1229.593750;1244.590332;1260.583374;1261.608765;1271.594360;1293.630737;1294.624756;1365.651855;1475.745483;1493.727295;1940.937744;2074.993164;2084.007324;2096.961914;2211.102783;2225.118164;2233.084961;2239.131348;2249.079102;2299.175781.

Fig. A16. Identification of heterogeneous nuclear ribonucleoprotein K isoform a (HNRPK) by MALDI-TOF MS analysis. A, MS spectrum of HNRPK. B, Non-filtered MS peak lists of HNRPK.

A

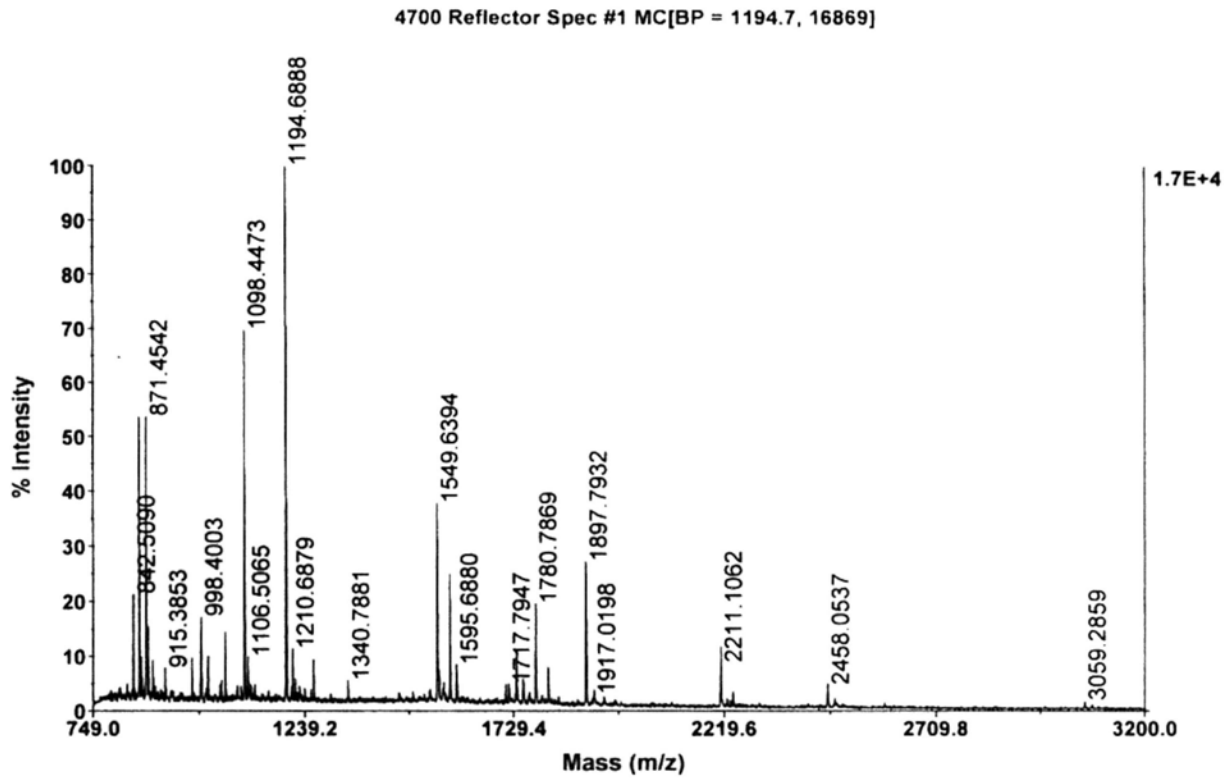

B

842.508972;855.460327;861.074707;870.523926;871.454163;877.045349;887.443787;915.385315;976.522339;997.438904;998.400330;1013.428345;1014.400696;1045.542114;1053.637207;1098.447266;1106.506470;1194.688843;1210.687866;1216.656494;1259.560669;1340.788086;1549.639404;1554.833740;1565.674683;1579.690796;1595.687988;1710.953613;1717.794678;1733.770508;1735.789673;1751.792236;1780.786865;1810.008789;1897.793213;1917.019775;2211.106201;2225.113037;2239.119141;2457.047852;2458.053711;2474.056641;3059.285889.

Fig. A17. Identification of calreticulin precursor (CALR) by MALDI-TOF MS analysis. A, MS spectrum of CALR. B, Non-filtered MS peak lists of CALR.

A

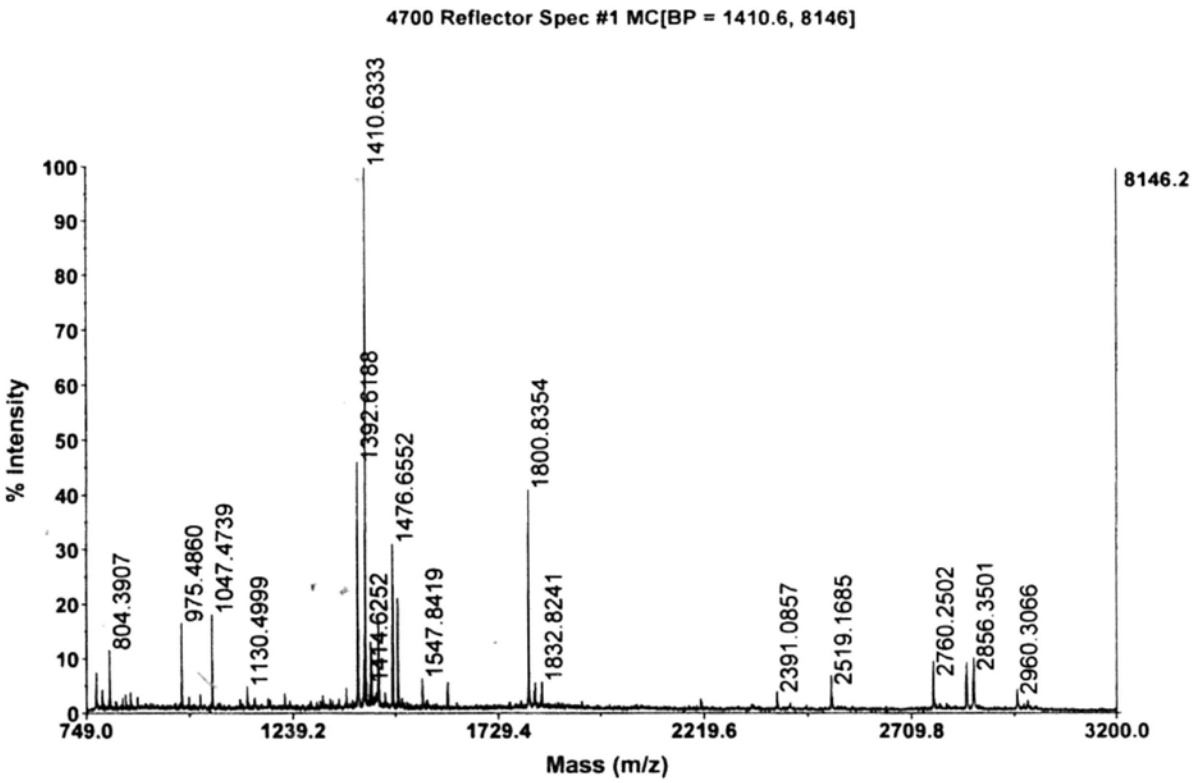

B 772.456787;788.402527;804.390747;842.509155;853.444580;975.485962;1019.568054;1047.473877;1130.499878;1366.615356;1392.618774;1408.608887;1410.633301;1414.625244;1422.618164;1424.603516;1426.619141;1440.610962;1442.611328;1476.655151;1488.657837;1547.841919;1607.764526;1800.835449;1815.845947;1816.823730;1832.824097;2391.085693;2519.168457;2760.250244;2839.312256;2856.350098;2960.306641;2986.256592.

Fig. A18. Identification of chaperonin (CPN60) by MALDI-TOF MS analysis. A, MS spectrum of CPN60. B, Non-filtered MS peak lists of CPN60.

A

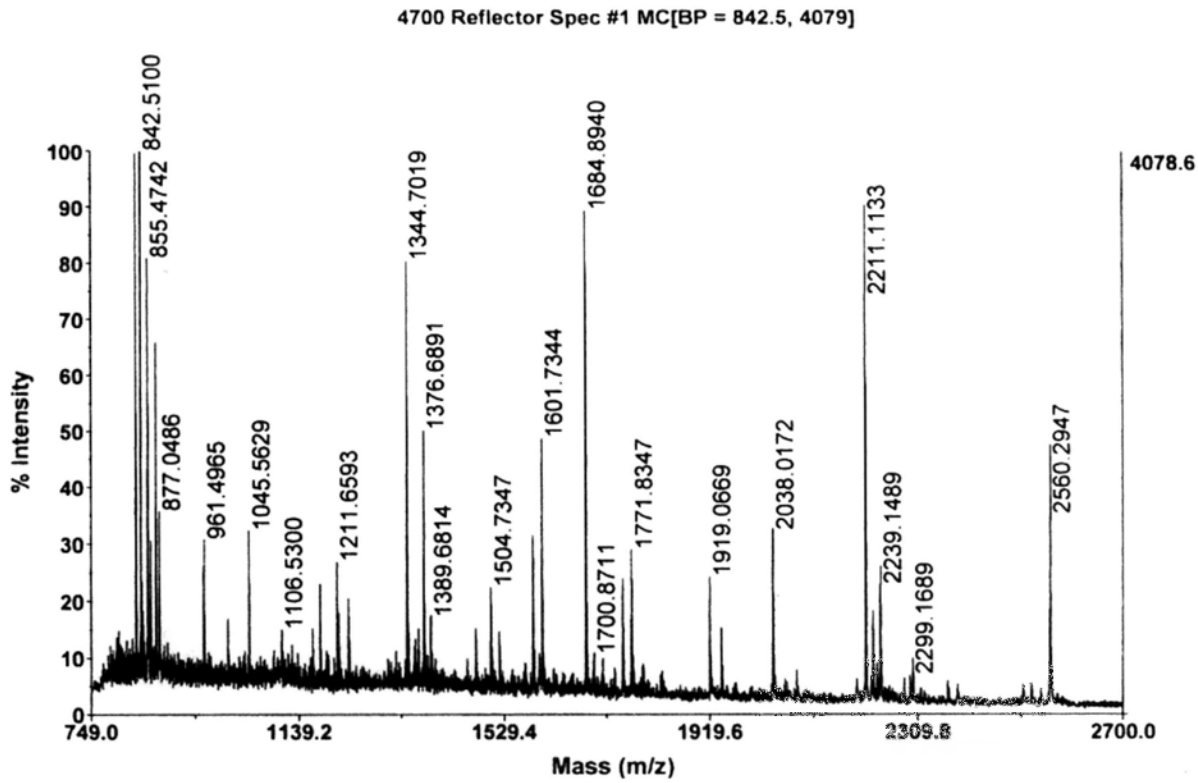

B

833.393433;842.510010;855.474243;861.073792;870.541626;877.048645;960.507446;961.496460;1006.487915;1045.562866;1106.530029;1179.590088;1211.659302;1215.646851;1233.590698;1344.701904;1358.672607;1366.645508;1376.689087;1389.681396;1475.736084;1504.734741;1520.737427;1584.712646;1601.734375;1684.894043;1700.871094;1716.852905;1754.814575;1771.834717;1919.066895;1940.935303;2038.017212;2211.113281;2225.121094;2233.092773;2239.148926;2299.168945;2560.294678.

Fig. A19. Non-filtered MS peak lists of glucose-regulated protein 78kDa (GRP78).

842.508423;852.400452;861.070679;870.537170;877.040955;903.467468;905.415466;914.48
3276;918.479431;919.472900;946.516846;981.483154;985.499390;986.521240;997.521240;1
029.546143;1074.560303;1096.498047;1153.515503;1168.568481;1191.647461;1210.585571
;1211.582886;1217.640625;1228.638550;1233.625488;1240.610107;1267.500488;1313.6318
36;1316.643555;1329.622803;1345.618408;1397.795654;1430.706299;1446.696899;1452.68
8477;1458.732544;1460.776001;1466.650391;1482.737549;1512.768188;1528.757813;1536.
786987;1544.764038;1550.788696;1552.805786;1564.780518;1566.800659;1580.777466;158
2.787598;1588.869507;1604.860596;1659.905518;1677.828613;1693.884033;1699.811157;1
709.875488;1816.016357;1836.952393;1887.994263;1904.992310;1934.035522;1950.025146
;1974.934448;2006.926880;2163.003906;2165.020508;2176.027100;2186.987549;2198.0141
60;2211.103516.

Fig. A20. Identification of chaperonin containing TCP1 subunit 5 (CCT5) by MALDI-TOF MS analysis. A, MS spectrum of CCT5. B, Non-filtered MS peak lists of CCT5.

A

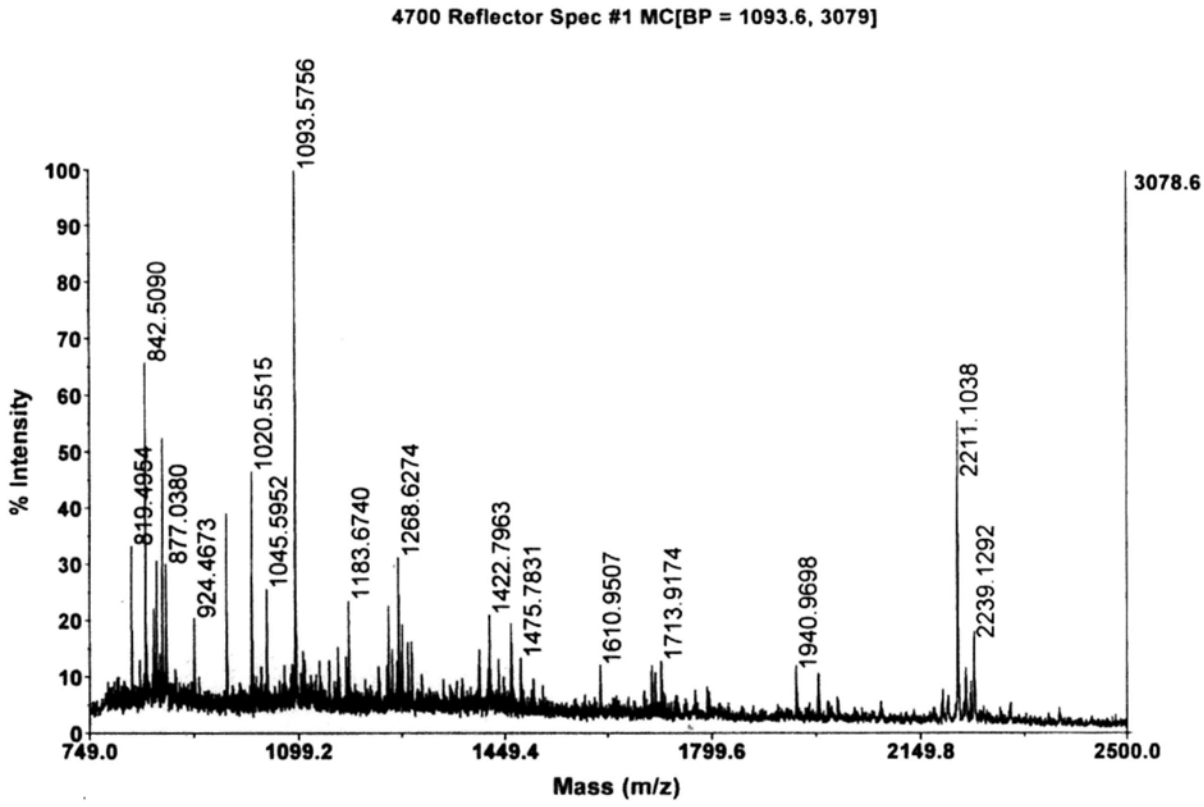

B 819.495422;842.508972;856.528076;861.071960;870.546936;877.038025;924.467285;978.538208;1020.551514;1045.595215;1093.575562;1183.673950;1251.609497;1257.717163;1268.627441;1273.723877;1284.626343;1290.726807;1404.783081;1422.796265;1459.723755;1475.783081;1610.950684;1697.928223;1703.849121;1713.917358;1940.969849;1977.977417;2211.103760;2225.119629;2234.086182;2239.129150.

Fig. A21. Identification of protein disulfide isomerase-associated 3 precursor (PDIA3) by MALDI-TOF MS analysis. A, MS spectrum of PDIA3. B, Non-filtered MS peak lists of PDIA3.

A

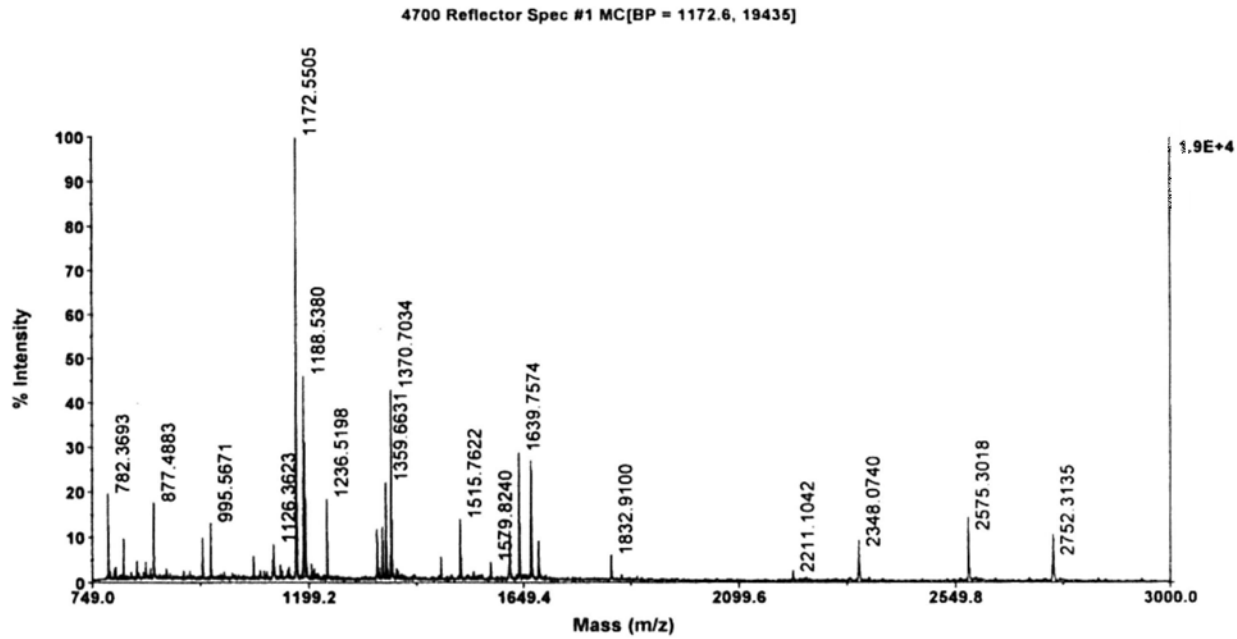

B

782.369324;794.342651;796.355713;798.352722;814.344604;842.509033;861.069153;870.534729;877.488281;903.490479;978.540039;995.567139;1084.566528;1124.552124;1126.362305;1140.540161;1155.521484;1171.522583;1172.550537;1186.532471;1188.537964;1191.601074;1194.600708;1204.542236;1210.524658;1236.519775;1341.681885;1347.693115;1352.692871;1359.663086;1363.661377;1368.677490;1370.703369;1381.649780;1474.719727;1514.716553;1515.762207;1543.746826;1579.823975;1618.692139;1619.777588;1639.757446;1663.734497;1664.770874;1680.762207;1832.910034;2211.104248;2348.073975;2575.301758;2751.310303;2752.313477.

Fig. A22. Identification of chaperonin containing TCP1 subunit 6A isoform a (CCT6A) by MALDI-TOF MS analysis. A, MS spectrum of CCT6A. B, Non-filtered MS peak lists of CCT6A.

A

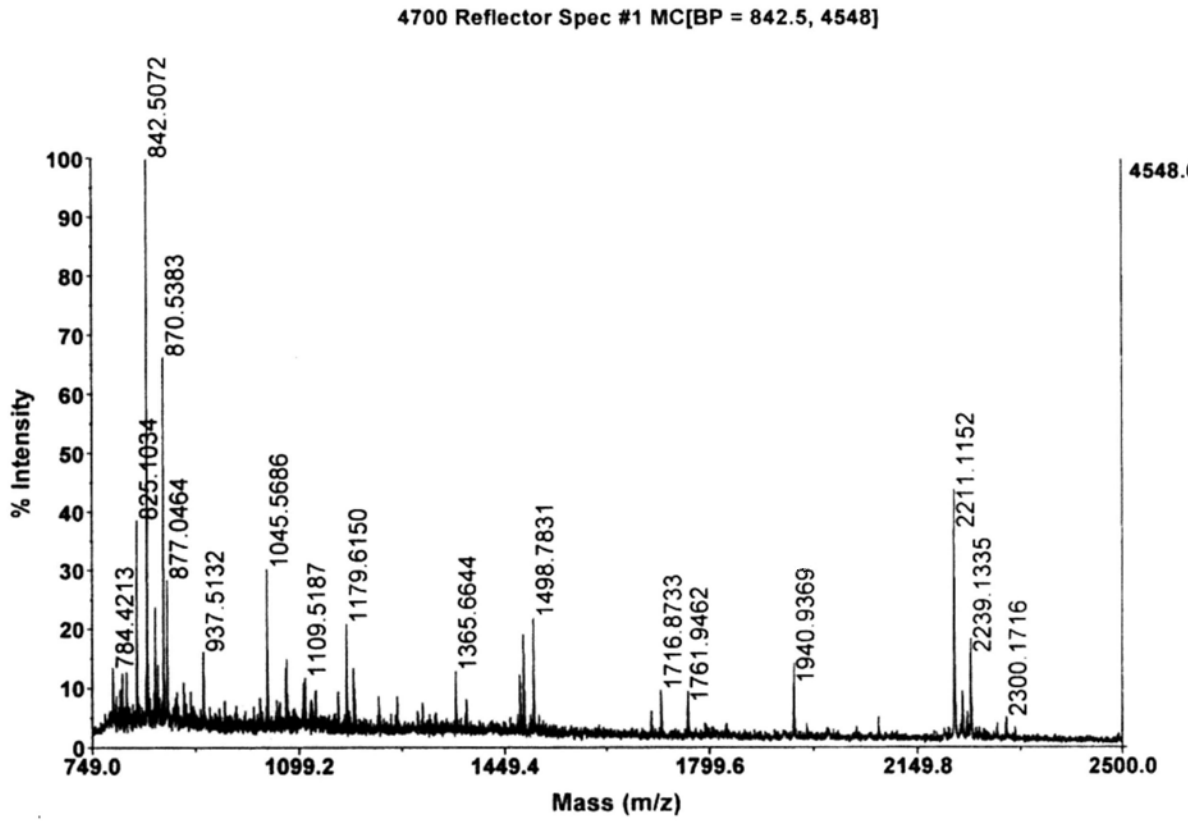

B

784.421265;800.444336;807.409851;825.103394;840.487549;841.068604;842.507202;856.523010;861.068604;870.538269;877.046387;937.513184;1045.568604;1076.595459;1078.578003;1106.547974;1109.518677;1179.614990;1191.586182;1365.664429;1475.781006;1481.756958;1498.783081;1716.873291;1761.946167;1940.936890;2211.115234;2225.111084;2233.066162;2239.133545;2300.171631.

Fig. A23. Identification of laminin-binding protein (LAMBR) by MALDI-TOF MS analysis. A, MS spectrum of LAMBR. B, Non-filtered MS peak lists of LAMBR.

A

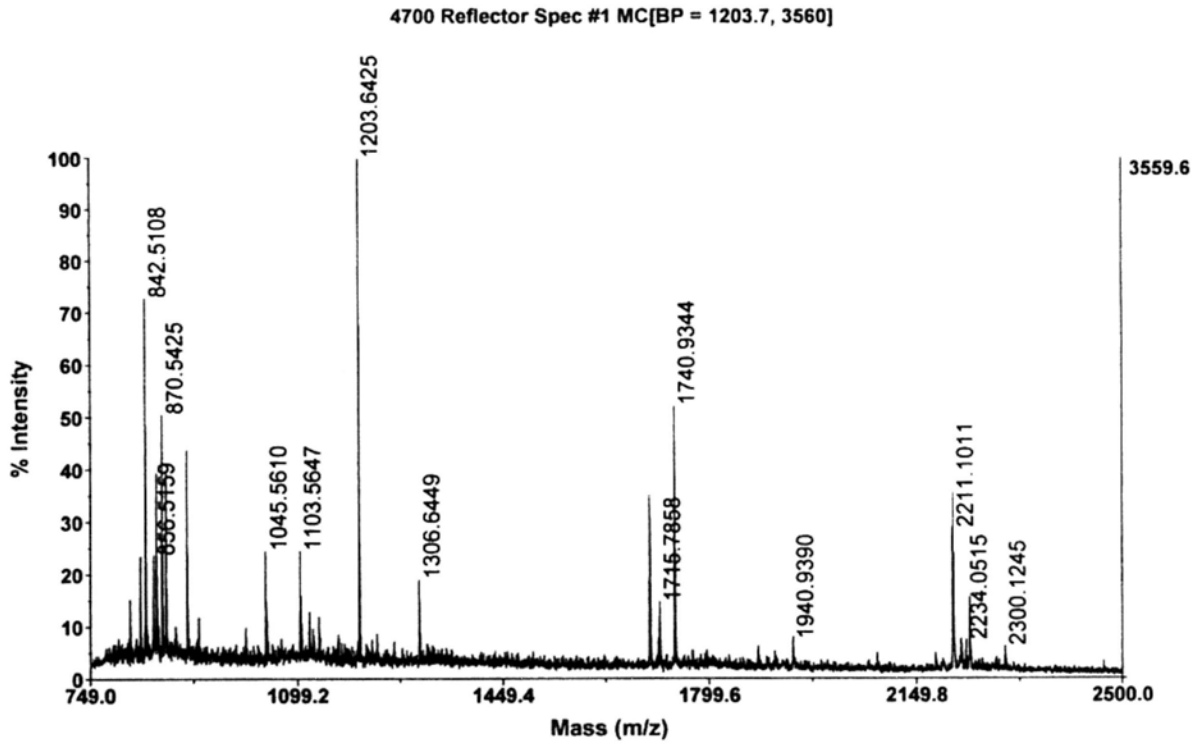

B

816.432861;833.454712;842.510803;856.515869;861.073181;870.542480;877.040894;912.549622;1045.561035;1103.564697;1203.642456;1306.644897;1698.845825;1713.789795;1715.785767;1740.934448;1940.938965;2211.101074;2225.083984;2234.051514;2239.125732;2300.124512.

Fig. A24. Identification of prohibitin (PHB) by MALDI-TOF MS analysis. A, MS spectrum of PHB. B, Non-filtered MS peak lists of PHB.

A

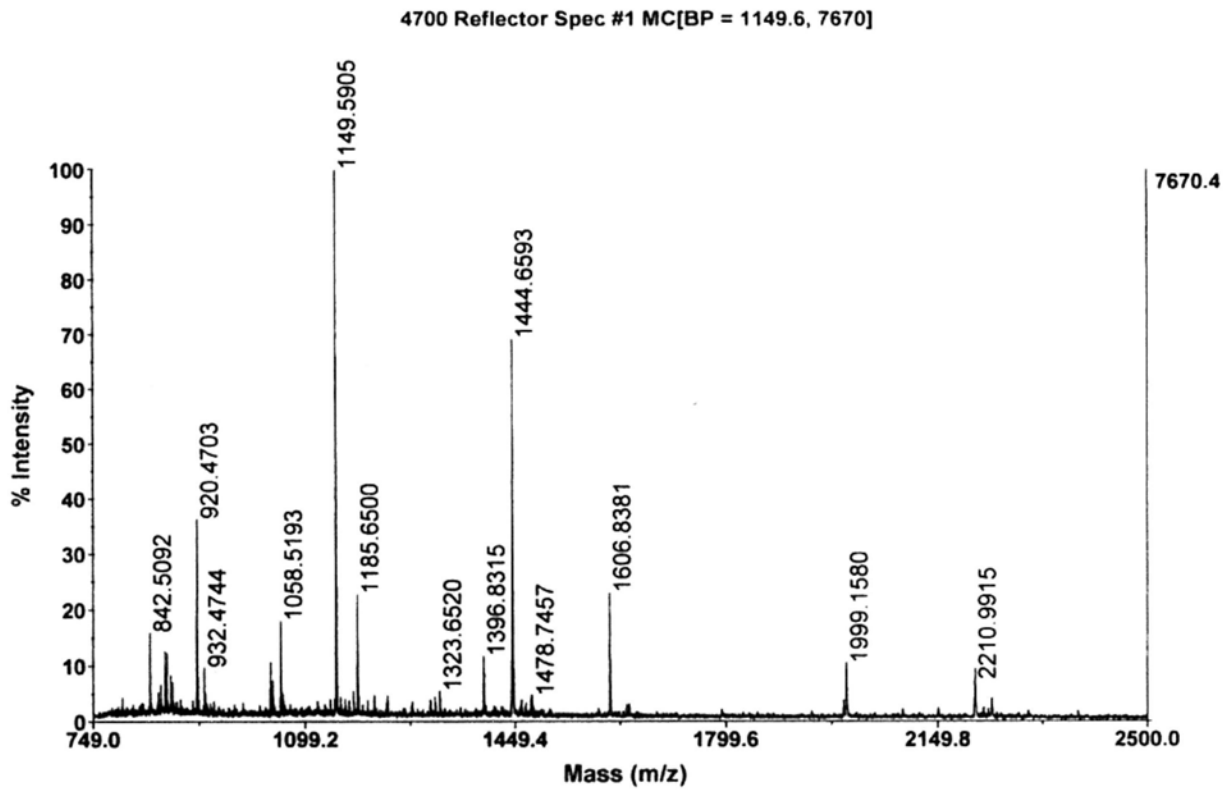

B

842.509155;856.512878;861.076477;867.495483;870.533691;877.052368;879.503296;920.470276;932.474365;1041.489624;1045.532227;1058.519287;1149.590454;1179.590942;1185.650024;1323.651978;1396.831543;1444.659302;1478.745728;1606.838135;1998.058472;1999.157959;2210.991455;2211.173096;2239.056641.

Bibliography

Abdelrahim, M., Liu, S., and Safe, S. (2005). Induction of endoplasmic reticulum-induced stress genes in Panc-1 pancreatic cancer cells is dependent on Sp proteins. J Biol Chem 280, 16508-16513.

Accola, M.A., Huang, B., Al Masri, A., and McNiven, M.A. (2002). The antiviral dynamin family member, MxA, tubulates lipids and localizes to the smooth endoplasmic reticulum. J Biol Chem 277, 21829-21835.

Ank, N., West, H., and Paludan, S.R. (2006). IFN-lambda: novel antiviral cytokines. J Interferon Cytokine Res 26, 373-379.

Arap, M.A., Lahdenranta, J., Mintz, P.J., Hajitou, A., Sarkis, A.S., Arap, W., and Pasqualini, R. (2004). Cell surface expression of the stress response chaperone GRP78 enables tumor targeting by circulating ligands. Cancer Cell 6, 275-284.

Arbuthnot, P., and Kew, M. (2001). Hepatitis B virus and hepatocellular carcinoma. Int J Exp Pathol 82, 77-100.

Awe, K., Lambert, C., and Prange, R. (2008). Mammalian BiP controls posttranslational ER translocation of the hepatitis B virus large envelope protein. FEBS Lett 582, 3179-3184.

Baas, T., Baskin, C.R., Diamond, D.L., Garcia-Sastre, A., Bielefeldt-Ohmann, H., Tumpey, T.M., Thomas, M.J., Carter, V.S., Teal, T.H., Van Hoeven, N., Proll, S., Jacobs, J.M., Caldwell, Z.R., Gritsenko, M.A., Hukkanen, R.R., Camp, D.G., 2nd, Smith, R.D., and Katze, M.G. (2006). Integrated molecular signature of disease: analysis of influenza virus-infected macaques through functional genomics and proteomics. J Virol 80, 10813-10828.

Bai, G.Q., Cheng, J., Zhang, S.L., Huang, Y.P., Wang, L., Liu, Y., and Lin, S.M. (2005). Screening of hepatocyte proteins binding to complete S protein of hepatitis B virus by yeast-two hybrid system. World J Gastroenterol 11, 3899-3904.

Bancroft, W.H., Mundon, F.K., and Russell, P.K. (1972). Detection of additional antigenic determinants of hepatitis B antigen. J Immunol 109, 842-848.

Baumeister, P., Luo, S., Skarnes, W.C., Sui, G., Seto, E., Shi, Y., and Lee, A.S. (2005). Endoplasmic reticulum stress induction of the Grp78/BiP promoter: activating mechanisms mediated by YY1 and its interactive chromatin modifiers. Mol Cell Biol 25, 4529-4540.

Beasley, R.P., Hwang, L.Y., Lin, C.C., and Chien, C.S. (1981). Hepatocellular carcinoma and hepatitis B virus. A prospective study of 22 707 men in Taiwan. Lancet 2, 1129-1133.

Bertolotti, A., Wang, X., Novoa, I., Jungreis, R., Schlessinger, K., Cho, J.H., West, A.B., and Ron, D. (2001). Increased sensitivity to dextran sodium sulfate colitis in IRE1beta-deficient mice. J Clin Invest 107, 585-593.

Bertolotti, A., Zhang, Y., Hendershot, L.M., Harding, H.P., and Ron, D. (2000). Dynamic interaction of BiP and ER stress transducers in the unfolded-protein response. Nat Cell Biol 2, 326-332.

Bole, D.G., Dowin, R., Doriaux, M., and Jamieson, J.D. (1989). Immunocytochemical localization of BiP to the rough endoplasmic reticulum: evidence for protein sorting by selective retention. J Histochem Cytochem 37, 1817-1823.

Brechot, C., Gozuacik, D., Murakami, Y., and Paterlini-Brechot, P. (2000). Molecular bases for the development of hepatitis B virus (HBV)-related hepatocellular carcinoma (HCC). Semin Cancer Biol 10, 211-231.

Brechot, C., Hadchouel, M., Scotto, J., Fonck, M., Potet, F., Vyas, G.N., and Tiollais, P. (1981a). State of hepatitis B virus DNA in hepatocytes of patients with hepatitis B surface antigen-positive and -negative liver diseases. Proc Natl Acad Sci U S A 78, 3906-3910.

Brechot, C., Pourcel, C., Louise, A., Rain, B., and Tiollais, P. (1981b). Detection of hepatitis B virus DNA sequences in human hepatocellular carcinoma in an integrated form. Prog Med Virol 27, 99-102.

Brewer, J.W., and Diehl, J.A. (2000). PERK mediates cell-cycle exit during the mammalian unfolded protein response. Proc Natl Acad Sci U S A 97, 12625-12630.

Brodsky, J.L., Werner, E.D., Dubas, M.E., Goeckeler, J.L., Kruse, K.B., and McCracken, A.A. (1999). The requirement for molecular chaperones during endoplasmic reticulum-associated protein degradation demonstrates that protein export and import are mechanistically distinct. J Biol Chem 274, 3453-3460.

Brostrom, C.O., Prostko, C.R., Kaufman, R.J., and Brostrom, M.A. (1996). Inhibition of translational initiation by activators of the glucose-regulated stress protein and heat shock protein stress response systems. Role of the interferon-inducible double-stranded RNA-activated eukaryotic initiation factor 2alpha kinase. J Biol Chem 271, 24995-25002.

Brownlie, R.J., Myers, L.K., Wooley, P.H., Corrigall, V.M., Bodman-Smith, M.D., Panayi, G.S., and Thompson, S.J. (2006). Treatment of murine collagen-induced arthritis by the stress protein BiP via interleukin-4-producing regulatory T cells: a novel function for an ancient protein. Arthritis Rheum 54, 854-863.

Bruni, R., D'Ugo, E., Villano, U., Fourel, G., Buendia, M.A., and Rapicetta, M. (2004). The win locus involved in activation of the distal N-myc2 gene upon WHV integration in woodchuck liver tumors harbors S/MAR elements. Virology 329, 1-10.

Burnham, A.J., Gong, L., and Hardy, R.W. (2007). Heterogeneous nuclear ribonuclear protein K interacts with Sindbis virus nonstructural proteins and viral subgenomic mRNA. Virology 367, 212-221.

Calfon, M., Zeng, H., Urano, F., Till, J.H., Hubbard, S.R., Harding, H.P., Clark, S.G., and Ron, D. (2002). IRE1 couples endoplasmic reticulum load to secretory capacity by processing the XBP-1 mRNA. Nature 415, 92-96.

Chan, H.L., Leung, N.W., Hui, A.Y., Wong, V.W., Liew, C.T., Chim, A.M., Chan, F.K., Hung, L.C., Lee, Y.T., Tam, J.S., Lam, C.W., and Sung, J.J. (2005). A randomized, controlled trial of combination therapy for chronic hepatitis B: comparing pegylated interferon-alpha2b and lamivudine with lamivudine alone. Ann Intern Med 142, 240-250.

Chen, Y., Du, D., Wu, J., Chan, C.P., Tan, Y., Kung, H.F., and He, M.L. (2003). Inhibition of hepatitis B virus replication by stably expressed shRNA. Biochem Biophys Res Commun 311, 398-404.

Chen, Y., Lin, M.C., Wang, H., Chan, C.Y., Jiang, L., Ngai, S.M., Yu, J., He, M.L., Shaw, P.C., Yew, D.T., Sung, J.J., and Kung, H.F. (2007). Proteomic analysis of EZH2 downstream target proteins in hepatocellular carcinoma. Proteomics 7, 3097-3104.

Cho, D.Y., Yang, G.H., Ryu, C.J., and Hong, H.J. (2003). Molecular chaperone GRP78/BiP interacts with the large surface protein of hepatitis B virus in vitro and in vivo. J Virol 77, 2784-2788.

Chua, P.K., Wang, R.Y., Lin, M.H., Masuda, T., Suk, F.M., and Shih, C. (2005). Reduced secretion of virions and hepatitis B virus (HBV) surface antigen of a naturally occurring HBV variant correlates with the accumulation of the small S envelope protein in the endoplasmic reticulum and Golgi apparatus. J Virol 79, 13483-13496.

Cox, J.S., Shamu, C.E., and Walter, P. (1993). Transcriptional induction of genes encoding endoplasmic reticulum resident proteins requires a transmembrane protein kinase. Cell 73, 1197-1206.

Custer, B., Sullivan, S.D., Hazlet, T.K., Iloeje, U., Veenstra, D.L., and Kowdley, K.V. (2004). Global epidemiology of hepatitis B virus. J Clin Gastroenterol 38, S158-168.
Darnell, J.E., Jr. (1998). Studies of IFN-induced transcriptional activation uncover the Jak-Stat pathway. J Interferon Cytokine Res 18, 549-554.

Davidson, D.J., Haskell, C., Majest, S., Kherzai, A., Egan, D.A., Walter, K.A., Schneider, A., Gubbins, E.F., Solomon, L., Chen, Z., Lesniewski, R., and Henkin, J. (2005). Kringle 5 of human plasminogen induces apoptosis of endothelial and tumor cells through surface-expressed glucose-regulated protein 78. Cancer Res 65, 4663-4672.

Dejean, A., Bougueleret, L., Grzeschik, K.H., and Tiollais, P. (1986). Hepatitis B virus DNA integration in a sequence homologous to v-erb-A and steroid receptor genes in a hepatocellular carcinoma. Nature 322, 70-72.

Der, S.D., Zhou, A., Williams, B.R., and Silverman, R.H. (1998). Identification of genes differentially regulated by interferon alpha, beta, or gamma using oligonucleotide arrays. Proc Natl Acad Sci U S A 95, 15623-15628.

Doitsh, G., and Shaul, Y. (2003). A long HBV transcript encoding pX is inefficiently exported from the nucleus. Virology 309, 339-349.

Doms, R.W., Lamb, R.A., Rose, J.K., and Helenius, A. (1993). Folding and assembly of viral membrane proteins. Virology 193, 545-562.

Dong, D., Ko, B., Baumeister, P., Swenson, S., Costa, F., Markland, F., Stiles, C., Patterson, J.B., Bates, S.E., and Lee, A.S. (2005). Vascular targeting and antiangiogenesis agents induce drug resistance effector GRP78 within the tumor microenvironment. Cancer Res 65, 5785-5791.

Duriez, M., Rossignol, J.M., and Sitterlin, D. (2008). The hepatitis B virus precore protein is retrotransported from endoplasmic reticulum (ER) to cytosol through the ER-associated degradation pathway. J Biol Chem 283, 32352-32360.

Elmore, L.W., Hancock, A.R., Chang, S.F., Wang, X.W., Chang, S., Callahan, C.P., Geller, D.A., Will, H., and Harris, C.C. (1997). Hepatitis B virus X protein and p53 tumor suppressor interactions in the modulation of apoptosis. Proc Natl Acad Sci U S A 94, 14707-14712.

Feitelson, M.A., Millman, I., Halbherr, T., Simmons, H., and Blumberg, B.S. (1986). A newly identified hepatitis B type virus in tree squirrels. Proc Natl Acad Sci U S A 83, 2233-2237.

Floyd-Smith, G., Slattery, E., and Lengyel, P. (1981). Interferon action: RNA cleavage

pattern of a (2'-5')oligoadenylate--dependent endonuclease. Science 212, 1030-1032.

Foti, D.M., Welihinda, A., Kaufman, R.J., and Lee, A.S. (1999). Conservation and divergence of the yeast and mammalian unfolded protein response. Activation of specific mammalian endoplasmic reticulum stress element of the grp78/BiP promoter by yeast Hac1. J Biol Chem 274, 30402-30409.

Fu, Y., and Lee, A.S. (2006). Glucose regulated proteins in cancer progression, drug resistance and immunotherapy. Cancer Biol Ther 5, 741-744.

Gottlob, K., Fulco, M., Levrero, M., and Graessmann, A. (1998). The hepatitis B virus HBx protein inhibits caspase 3 activity. J Biol Chem 273, 33347-33353.

Graef, E., Caselmann, W.H., Wells, J., and Koshy, R. (1994). Insertional activation of mevalonate kinase by hepatitis B virus DNA in a human hepatoma cell line. Oncogene 9, 81-87.

Guo, W.T., Wang, J., Tam, G., Yen, T.S., and Ou, J.S. (1991). Leaky transcription termination produces larger and smaller than genome size hepatitis B virus X gene transcripts. Virology 181, 630-636.

Hajjou, M., Norel, R., Carver, R., Marion, P., Cullen, J., Rogler, L.E., and Rogler, C.E. (2005). cDNA microarray analysis of HBV transgenic mouse liver identifies genes in lipid biosynthetic and growth control pathways affected by HBV. J Med Virol 77, 57-65.

Harding, H.P., Novoa, I., Zhang, Y., Zeng, H., Wek, R., Schapira, M., and Ron, D. (2000). Regulated translation initiation controls stress-induced gene expression in mammalian cells. Mol Cell 6, 1099-1108.

Harding, H.P., Zhang, Y., and Ron, D. (1999). Protein translation and folding are coupled by an endoplasmic-reticulum-resident kinase. Nature 397, 271-274.

Haze, K., Okada, T., Yoshida, H., Yanagi, H., Yura, T., Negishi, M., and Mori, K. (2001). Identification of the G13 (cAMP-response-element-binding protein-related protein) gene product related to activating transcription factor 6 as a transcriptional activator of the mammalian unfolded protein response. Biochem J 355, 19-28.

Haze, K., Yoshida, H., Yanagi, H., Yura, T., and Mori, K. (1999). Mammalian transcription factor ATF6 is synthesized as a transmembrane protein and activated by proteolysis in response to endoplasmic reticulum stress. Mol Biol Cell 10, 3787-3799.

He, B. (2006). Viruses, endoplasmic reticulum stress, and interferon responses. Cell Death Differ 13, 393-403.

He, M.L., Zheng, B., Peng, Y., Peiris, J.S., Poon, L.L., Yuen, K.Y., Lin, M.C., Kung, H.F., and Guan, Y. (2003). Inhibition of SARS-associated coronavirus infection and replication by RNA interference. Jama 290, 2665-2666.

He, M.L., Zheng, B.J., Chen, Y., Wong, K.L., Huang, J.D., Lin, M.C., Peng, Y., Yuen, K.Y., Sung, J.J., and Kung, H.F. (2006). Kinetics and synergistic effects of siRNAs targeting structural and replicase genes of SARS-associated coronavirus. FEBS Lett 580, 2414-2420.

Hegde, N.R., Chevalier, M.S., Wisner, T.W., Denton, M.C., Shire, K., Frappier, L., and Johnson, D.C. (2006). The role of BiP in endoplasmic reticulum-associated degradation of major histocompatibility complex class I heavy chain induced by cytomegalovirus proteins. J Biol Chem 281, 20910-20919.

Hong, M., Lin, M.Y., Huang, J.M., Baumeister, P., Hakre, S., Roy, A.L., and Lee, A.S. (2005). Transcriptional regulation of the Grp78 promoter by endoplasmic reticulum stress: role of TFII-I and its tyrosine phosphorylation. J Biol Chem 280, 16821-16828.

Horikawa, I., and Barrett, J.C. (2001). cis-Activation of the human telomerase gene (hTERT) by the hepatitis B virus genome. J Natl Cancer Inst 93, 1171-1173.

Hoshino, T., Nakaya, T., Araki, W., Suzuki, K., Suzuki, T., and Mizushima, T. (2007). Endoplasmic reticulum chaperones inhibit the production of amyloid-beta peptides. Biochem J 402, 581-589.

Hou, J., Liu, Z., and Gu, F. (2005). Epidemiology and Prevention of Hepatitis B Virus Infection. Int J Med Sci 2, 50-57.

Hsieh, T.Y., Matsumoto, M., Chou, H.C., Schneider, R., Hwang, S.B., Lee, A.S., and Lai, M.M. (1998). Hepatitis C virus core protein interacts with heterogeneous nuclear ribonucleoprotein K. J Biol Chem 273, 17651-17659.

Hsu, L.C., Park, J.M., Zhang, K., Luo, J.L., Maeda, S., Kaufman, R.J., Eckmann, L., Guiney, D.G., and Karin, M. (2004). The protein kinase PKR is required for macrophage apoptosis after activation of Toll-like receptor 4. Nature 428, 341-345.

Hu, J., and Seeger, C. (1996). Hsp90 is required for the activity of a hepatitis B virus reverse transcriptase. Proc Natl Acad Sci U S A 93, 1060-1064.

Huan, B., and Siddiqui, A. (1993). Regulation of hepatitis B virus gene expression. J Hepatol 17 Suppl 3, S20-23.

Hytiroglou, P., and Theise, N.D. (2006). Telomerase activation in human hepatocarcinogenesis. Am J Gastroenterol 101, 839-841.

Iwawaki, T., Hosoda, A., Okuda, T., Kamigori, Y., Nomura-Furuwatari, C., Kimata, Y., Tsuru, A., and Kohno, K. (2001). Translational control by the ER transmembrane kinase/ribonuclease IRE1 under ER stress. Nat Cell Biol 3, 158-164.

Jacob, J.R., Sterczer, A., Toshkov, I.A., Yeager, A.E., Korba, B.E., Cote, P.J., Buendia, M.A., Gerin, J.L., and Tennant, B.C. (2004). Integration of woodchuck hepatitis and N-myc rearrangement determine size and histologic grade of hepatic tumors. Hepatology 39, 1008-1016.

Jiang, H.Y., Wek, S.A., McGrath, B.C., Scheuner, D., Kaufman, R.J., Cavener, D.R., and Wek, R.C. (2003). Phosphorylation of the alpha subunit of eukaryotic initiation factor 2 is required for activation of NF-kappaB in response to diverse cellular stresses. Mol Cell Biol 23, 5651-5663.

Jiang, X.S., Tang, L.Y., Dai, J., Zhou, H., Li, S.J., Xia, Q.C., Wu, J.R., and Zeng, R. (2005). Quantitative analysis of severe acute respiratory syndrome (SARS)-associated coronavirus-infected cells using proteomic approaches: implications for cellular responses to virus infection. Mol Cell Proteomics 4, 902-913.

Jindadamrongwech, S., Thepparit, C., and Smith, D.R. (2004). Identification of GRP 78 (BiP) as a liver cell expressed receptor element for dengue virus serotype 2. Arch Virol 149, 915-927.

Jonasch, E., and Haluska, F.G. (2001). Interferon in oncological practice: review of interferon biology, clinical applications, and toxicities. Oncologist 6, 34-55.

Kaufman, R.J. (1999). Stress signaling from the lumen of the endoplasmic reticulum: coordination of gene transcriptional and translational controls. Genes Dev 13, 1211-1233.

Kaufman, R.J. (2002). Orchestrating the unfolded protein response in health and disease. J Clin Invest 110, 1389-1398.

Kidd-Ljunggren, K., Miyakawa, Y., and Kidd, A.H. (2002). Genetic variability in hepatitis B viruses. J Gen Virol 83, 1267-1280.

Kim, C.M., Koike, K., Saito, I., Miyamura, T., and Jay, G. (1991). HBx gene of hepatitis B virus induces liver cancer in transgenic mice. Nature 351, 317-320.

Kim, M.Y., Park, E., Park, J.H., Park, D.H., Moon, W.S., Cho, B.H., Shin, H.S., and Kim, D.G. (2001). Expression profile of nine novel genes differentially expressed in hepatitis B virus-associated hepatocellular carcinomas. Oncogene 20, 4568-4575.

Kim, S.H., Hong, S.P., Kim, S.K., Lee, W.S., and Rho, H.M. (1992). Replication of a mutant hepatitis B virus with a fused X-C reading frame in hepatoma cells. J Gen Virol 73 (Pt 9), 2421-2424.

Kokame, K., Kato, H., and Miyata, T. (2001). Identification of ERSE-II, a new cis-acting element responsible for the ATF6-dependent mammalian unfolded protein response. J Biol Chem 276, 9199-9205.

Kostova, Z., and Wolf, D.H. (2003). For whom the bell tolls: protein quality control of the endoplasmic reticulum and the ubiquitin-proteasome connection. Embo J 22, 2309-2317.

Kozutsumi, Y., Segal, M., Normington, K., Gething, M.J., and Sambrook, J. (1988). The presence of malfolded proteins in the endoplasmic reticulum signals the induction of glucose-regulated proteins. Nature 332, 462-464.

Kramvis, A., and Kew, M.C. (2005). Relationship of genotypes of hepatitis B virus to mutations, disease progression and response to antiviral therapy. J Viral Hepat 12, 456-464.

Krug, R.M., Shaw, M., Broni, B., Shapiro, G. , Haller, O. (1985). Inhibition of influenza viral messenger RNA synthesis in cells expressing the interferon-induced Mx gene product. . J. Virol 56, 201-206.

Kuang, S.Y., Lekawanvijit, S., Maneekarn, N., Thongsawat, S., Brodovicz, K., Nelson, K., and Groopman, J.D. (2005). Hepatitis B 1762T/1764A mutations, hepatitis C infection, and codon 249 p53 mutations in hepatocellular carcinomas from Thailand. Cancer Epidemiol Biomarkers Prev 14, 380-384.

Kumar, R., Krause, G.S., Yoshida, H., Mori, K., and DeGracia, D.J. (2003). Dysfunction of the unfolded protein response during global brain ischemia and reperfusion. J Cereb Blood Flow Metab 23, 462-471.

Ladner, S.K., Otto, M.J., Barker, C.S., Zaifert, K., Wang, G.H., Guo, J.T., Seeger, C., and King, R.W. (1997). Inducible expression of human hepatitis B virus (HBV) in stably transfected hepatoblastoma cells: a novel system for screening potential inhibitors of HBV replication. Antimicrob Agents Chemother 41, 1715-1720.

Lai, C.L., Ratziu, V., Yuen, M.F., and Poynard, T. (2003). Viral hepatitis B. Lancet 362, 2089-2094.

Lam, M., Stallcup, M., and Distelhorst, C.W. (1997). Expression of a defective mouse mammary tumor virus envelope glycoprotein precursor which binds stably to GRP78 within the lumen of the endoplasmic reticulum is associated with decreased

glucocorticoid-induced apoptosis in mouse lymphoma cells. Cell Death Differ 4, 283-288.

Lavanchy, D. (2004). Hepatitis B virus epidemiology, disease burden, treatment, and current and emerging prevention and control measures. J Viral Hepat 11, 97-107.

Le Bouvier, G.L. (1971). The heterogeneity of Australia antigen. J Infect Dis 123, 671-675.

Lee, A.H., Iwakoshi, N.N., and Glimcher, L.H. (2003). XBP-1 regulates a subset of endoplasmic reticulum resident chaperone genes in the unfolded protein response. Mol Cell Biol 23, 7448-7459.

Lee, A.S. (2001). The glucose-regulated proteins: stress induction and clinical applications. Trends Biochem Sci 26, 504-510.

Lee, A.S. (2007). GRP78 induction in cancer: therapeutic and prognostic implications. Cancer Res 67, 3496-3499.

Lee, A.S., Wells, S., Kim, K.S., and Scheffler, I.E. (1986). Enhanced synthesis of the glucose/calcium-regulated proteins in a hamster cell mutant deficient in transfer of oligosaccharide core to polypeptides. J Cell Physiol 129, 277-282.

Lee, K., Tirasophon, W., Shen, X., Michalak, M., Prywes, R., Okada, T., Yoshida, H., Mori, K., and Kaufman, R.J. (2002). IRE1-mediated unconventional mRNA splicing and S2P-mediated ATF6 cleavage merge to regulate XBP1 in signaling the unfolded protein response. Genes Dev 16, 452-466.

Leung, S., Qureshi, S.A., Kerr, I.M., Darnell, J.E., Jr., and Stark, G.R. (1995). Role of STAT2 in the alpha interferon signaling pathway. Mol Cell Biol 15, 1312-1317.

Li, C., Tan, Y.X., Zhou, H., Ding, S.J., Li, S.J., Ma, D.J., Man, X.B., Hong, Y., Zhang, L., Li, L., Xia, Q.C., Wu, J.R., Wang, H.Y., and Zeng, R. (2005). Proteomic analysis of hepatitis B virus-associated hepatocellular carcinoma: Identification of potential tumor markers. Proteomics 5, 1125-1139.

Li, J., and Lee, A.S. (2006). Stress induction of GRP78/BiP and its role in cancer. Curr Mol Med 6, 45-54.

Li, M., Baumeister, P., Roy, B., Phan, T., Foti, D., Luo, S., and Lee, A.S. (2000). ATF6 as a transcription activator of the endoplasmic reticulum stress element: thapsigargin stress-induced changes and synergistic interactions with NF-Y and YY1. Mol Cell Biol 20, 5096-5106.

Liang, X., Qu, Z., Zhang, Z., Du, J., Liu, Y., Cui, M., Liu, H., Gao, L., Han, L., Liu, S., Cao, L., Zhao, P., and Sun, W. (2008). Blockade of preS2 down-regulates the apoptosis of HepG2.2.15 cells induced by TRAIL. Biochem Biophys Res Commun 369, 456-463.

Lin, J.Y., Li, M.L., Huang, P.N., Chien, K.Y., Horng, J.T., and Shih, S.R. (2008). Heterogeneous nuclear ribonuclear protein K interacts with the enterovirus 71 5' untranslated region and participates in virus replication. J Gen Virol 89, 2540-2549.

Liu, K., Qian, L., Wang, J., Li, W., Deng, X., Chen, X., Sun, W., Wei, H., Qian, X., Jiang, Y., and He, F. (2009). Two-dimensional blue native/SDS-PAGE analysis reveals heat shock protein chaperone machinery involved in hepatitis B virus production in HepG2.2.15 cells. Mol Cell Proteomics 8, 495-505.

Loeb, K.R., and Haas, A.L. (1992). The interferon-inducible 15-kDa ubiquitin homolog conjugates to intracellular proteins. J Biol Chem 267, 7806-7813.

Lok, A.S. (2002). Chronic hepatitis B. N Engl J Med 346, 1682-1683.

Luo, S., Mao, C., Lee, B., and Lee, A.S. (2006). GRP78/BiP is required for cell proliferation and protecting the inner cell mass from apoptosis during early mouse embryonic development. Mol Cell Biol 26, 5688-5697.

Ma, Y., and Hendershot, L.M. (2003). Delineation of a negative feedback regulatory loop that controls protein translation during endoplasmic reticulum stress. J Biol Chem 278, 34864-34873.

Magnius, L.O., and Norder, H. (1995). Subtypes, genotypes and molecular epidemiology of the hepatitis B virus as reflected by sequence variability of the S-gene. Intervirology 38, 24-34.

Mannova, P., Fang, R., Wang, H., Deng, B., McIntosh, M.W., Hanash, S.M., and Beretta, L. (2006). Modification of host lipid raft proteome upon hepatitis C virus replication. Mol Cell Proteomics 5, 2319-2325.

Mao, C., Dong, D., Little, E., Luo, S., and Lee, A.S. (2004). Transgenic mouse model for monitoring endoplasmic reticulum stress in vivo. Nat Med 10, 1013-1014; author reply 1014.

Mao, C., Tai, W.C., Bai, Y., Poizat, C., and Lee, A.S. (2006). In vivo regulation of Grp78/BiP transcription in the embryonic heart: role of the endoplasmic reticulum stress response element and GATA-4. J Biol Chem 281, 8877-8887.

Marion, P.L., Oshiro, L.S., Regnery, D.C., Scullard, G.H., and Robinson, W.S. (1980). A virus in Beechey ground squirrels that is related to hepatitis B virus of humans. Proc

Natl Acad Sci U S A 77, 2941-2945.

Mason, W.S., Seal, G., and Summers, J. (1980). Virus of Pekin ducks with structural and biological relatedness to human hepatitis B virus. J Virol 36, 829-836.

McCullough, K.D., Martindale, J.L., Klotz, L.O., Aw, T.Y., and Holbrook, N.J. (2001). Gadd153 sensitizes cells to endoplasmic reticulum stress by down-regulating Bcl2 and perturbing the cellular redox state. Mol Cell Biol 21, 1249-1259.

Mesaeli, N., Nakamura, K., Opas, M., and Michalak, M. (2001). Endoplasmic reticulum in the heart, a forgotten organelle? Mol Cell Biochem 225, 1-6.

Miller, D.G., Adam, M.A., and Miller, A.D. (1990). Gene transfer by retrovirus vectors occurs only in cells that are actively replicating at the time of infection. Mol Cell Biol 10, 4239-4242.

Misra, U.K., Deedwania, R., and Pizzo, S.V. (2005). Binding of activated alpha2-macroglobulin to its cell surface receptor GRP78 in 1-LN prostate cancer cells regulates PAK-2-dependent activation of LIMK. J Biol Chem 280, 26278-26286.

Misra, U.K., Deedwania, R., and Pizzo, S.V. (2006). Activation and cross-talk between Akt, NF-kappaB, and unfolded protein response signaling in 1-LN prostate cancer cells consequent to ligation of cell surface-associated GRP78. J Biol Chem 281, 13694-13707.

Miyakawa, Y., and Mizokami, M. (2003). Classifying hepatitis B virus genotypes. Intervirology 46, 329-338.

Mori, K., Ma, W., Gething, M.J., and Sambrook, J. (1993). A transmembrane protein with a cdc2+/CDC28-related kinase activity is required for signaling from the ER to the nucleus. Cell 74, 743-756.

Nagaraju, K., Casciola-Rosen, L., Lundberg, I., Rawat, R., Cutting, S., Thapliyal, R., Chang, J., Dwivedi, S., Mitsak, M., Chen, Y.W., Plotz, P., Rosen, A., Hoffman, E., and Raben, N. (2005). Activation of the endoplasmic reticulum stress response in autoimmune myositis: potential role in muscle fiber damage and dysfunction. Arthritis Rheum 52, 1824-1835.

Nakagawa, T., Zhu, H., Morishima, N., Li, E., Xu, J., Yankner, B.A., and Yuan, J. (2000). Caspase-12 mediates endoplasmic-reticulum-specific apoptosis and cytotoxicity by amyloid-beta. Nature 403, 98-103.

Nassal, M. (1999). Hepatitis B virus replication: novel roles for virus-host interactions. Intervirology 42, 100-116.

Ng, L.F., Chan, M., Chan, S.H., Cheng, P.C., Leung, E.H., Chen, W.N., and Ren, E.C. (2005). Host heterogeneous ribonucleoprotein K (hnRNP K) as a potential target to suppress hepatitis B virus replication. PLoS Med 2, e163.

Ni, M., and Lee, A.S. (2007). ER chaperones in mammalian development and human diseases. FEBS Lett 581, 3641-3651.

Niwa, M., Sidrauski, C., Kaufman, R.J., and Walter, P. (1999). A role for presenilin-1 in nuclear accumulation of Ire1 fragments and induction of the mammalian unfolded protein response. Cell 99, 691-702.

Norder, H., Courouce, A.M., Coursaget, P., Echevarria, J.M., Lee, S.D., Mushahwar, I.K., Robertson, B.H., Locarnini, S., and Magnius, L.O. (2004). Genetic diversity of hepatitis B virus strains derived worldwide: genotypes, subgenotypes, and HBsAg subtypes. Intervirology 47, 289-309.

Norder, H., Courouce, A.M., and Magnius, L.O. (1992). Molecular basis of hepatitis B virus serotype variations within the four major subtypes. J Gen Virol 73 (Pt 12), 3141-3145.

Novoa, I., Zeng, H., Harding, H.P., and Ron, D. (2001). Feedback inhibition of the unfolded protein response by GADD34-mediated dephosphorylation of eIF2alpha. J Cell Biol 153, 1011-1022.

Okabe, H., Satoh, S., Kato, T., Kitahara, O., Yanagawa, R., Yamaoka, Y., Tsunoda, T., Furukawa, Y., and Nakamura, Y. (2001). Genome-wide analysis of gene expression in human hepatocellular carcinomas using cDNA microarray: identification of genes involved in viral carcinogenesis and tumor progression. Cancer Res 61, 2129-2137.

Okamoto, H., Imai, M., Shimozaki, M., Hoshi, Y., Iizuka, H., Gotanda, T., Tsuda, F., Miyakawa, Y., and Mayumi, M. (1986). Nucleotide sequence of a cloned hepatitis B virus genome, subtype ayr: comparison with genomes of the other three subtypes. J Gen Virol 67 (Pt 11), 2305-2314.

Okamoto, H., Tsuda, F., Sakugawa, H., Sastrosoewignjo, R.I., Imai, M., Miyakawa, Y., and Mayumi, M. (1988). Typing hepatitis B virus by homology in nucleotide sequence: comparison of surface antigen subtypes. J Gen Virol 69 (Pt 10), 2575-2583.

Ono, M., Morisawa, K., Nie, J., Ota, K., Taniguchi, T., Saibara, T., and Onishi, S. (1998). Transactivation of transforming growth factor alpha gene by hepatitis B virus preS1. Cancer Res 58, 1813-1816.

Orito, E., Mizokami, M., Ina, Y., Moriyama, E.N., Kameshima, N., Yamamoto, M., and

Gojobori, T. (1989). Host-independent evolution and a genetic classification of the hepadnavirus family based on nucleotide sequences. Proc Natl Acad Sci U S A 86, 7059-7062.

Panayi, G.S., and Corrigall, V.M. (2006). BiP regulates autoimmune inflammation and tissue damage. Autoimmun Rev 5, 140-142.

Parker, R., Phan, T., Baumeister, P., Roy, B., Cheriyath, V., Roy, A.L., and Lee, A.S. (2001). Identification of TFII-I as the endoplasmic reticulum stress response element binding factor ERSF: its autoregulation by stress and interaction with ATF6. Mol Cell Biol 21, 3220-3233.

Parkin, D.M. (2001). Global cancer statistics in the year 2000. Lancet Oncol 2, 533-543.
Parkin, D.M., Bray, F., Ferlay, J., and Pisani, P. (2001). Estimating the world cancer burden: Globocan 2000. Int J Cancer 94, 153-156.

Paschen, W., and Mengesdorf, T. (2005). Cellular abnormalities linked to endoplasmic reticulum dysfunction in cerebrovascular disease--therapeutic potential. Pharmacol Ther 108, 362-375.

Paton, A.W., Beddoe, T., Thorpe, C.M., Whisstock, J.C., Wilce, M.C., Rossjohn, J., Talbot, U.M., and Paton, J.C. (2006). AB5 subtilase cytotoxin inactivates the endoplasmic reticulum chaperone BiP. Nature 443, 548-552.

Pavlovic, J., Haller, O., and Staeheli, P. (1992). Human and mouse Mx proteins inhibit different steps of the influenza virus multiplication cycle. J Virol 66, 2564-2569.

Pestka, S., Krause, C.D., and Walter, M.R. (2004). Interferons, interferon-like cytokines, and their receptors. Immunol Rev 202, 8-32.

Pisani, P., Parkin, D.M., Bray, F., and Ferlay, J. (1999). Estimates of the worldwide mortality from 25 cancers in 1990. Int J Cancer 83, 18-29.

Poon, T.C., Hui, A.Y., Chan, H.L., Ang, I.L., Chow, S.M., Wong, N., and Sung, J.J. (2005). Prediction of liver fibrosis and cirrhosis in chronic hepatitis B infection by serum proteomic fingerprinting: a pilot study. Clin Chem 51, 328-335.

Prange, R., Werr, M., and Loffler-Mary, H. (1999). Chaperones involved in hepatitis B virus morphogenesis. Biol Chem 380, 305-314.

Rao, R.V., and Bredesen, D.E. (2004). Misfolded proteins, endoplasmic reticulum stress and neurodegeneration. Curr Opin Cell Biol 16, 653-662.

Ringrose, J.H., Jeeninga, R.E., Berkhout, B., and Speijer, D. (2008). Proteomic studies

reveal coordinated changes in T-cell expression patterns upon infection with human immunodeficiency virus type 1. J Virol 82, 4320-4330.

Roe, T., Reynolds, T.C., Yu, G., and Brown, P.O. (1993). Integration of murine leukemia virus DNA depends on mitosis. Embo J 12, 2099-2108.

Rutkowski, D.T., and Kaufman, R.J. (2004). A trip to the ER: coping with stress. Trends Cell Biol 14, 20-28.

Sadler, A.J. and Williams, B.R.G.. (2008). Interferon-inducible antiviral effectors. Nat Rev Immunol 8, 559-568.

Schaefer, S. (2007). Hepatitis B virus taxonomy and hepatitis B virus genotypes. World J Gastroenterol 13, 14-21.

Scheuner, D., Song, B., McEwen, E., Liu, C., Laybutt, R., Gillespie, P., Saunders, T., Bonner-Weir, S., and Kaufman, R.J. (2001). Translational control is required for the unfolded protein response and in vivo glucose homeostasis. Mol Cell 7, 1165-1176.

Scheuner, D., Vander Mierde, D., Song, B., Flamez, D., Creemers, J.W., Tsukamoto, K., Ribick, M., Schuit, F.C., and Kaufman, R.J. (2005). Control of mRNA translation preserves endoplasmic reticulum function in beta cells and maintains glucose homeostasis. Nat Med 11, 757-764.

Seeger, C., and Mason, W.S. (2000). Hepatitis B virus biology. Microbiol Mol Biol Rev 64, 51-68.

Sells, M.A., Chen, M.L., and Acs, G. (1987). Production of hepatitis B virus particles in Hep G2 cells transfected with cloned hepatitis B virus DNA. Proc Natl Acad Sci U S A 84, 1005-1009.

Severi, T., Ying, C., Vermeesch, J.R., Cassiman, D., Cnops, L., Verslype, C., Fevery, J., Arckens, L., Neyts, J., and van Pelt, J.F. (2006). Hepatitis B virus replication causes oxidative stress in HepAD38 liver cells. Mol Cell Biochem 290, 79-85.

Shafritz, D.A., Shouval, D., Sherman, H.I., Hadziyannis, S.J., and Kew, M.C. (1981). Integration of hepatitis B virus DNA into the genome of liver cells in chronic liver disease and hepatocellular carcinoma. Studies in percutaneous liver biopsies and post-mortem tissue specimens. N Engl J Med 305, 1067-1073.

Shen, J., Chen, X., Hendershot, L., and Prywes, R. (2002). ER stress regulation of ATF6 localization by dissociation of BiP/GRP78 binding and unmasking of Golgi localization signals. Dev Cell 3, 99-111.

Shi, Y., Vattem, K.M., Sood, R., An, J., Liang, J., Stramm, L., and Wek, R.C. (1998). Identification and characterization of pancreatic eukaryotic initiation factor 2 alpha-subunit kinase, PEK, involved in translational control. Mol Cell Biol 18, 7499-7509.

Singh, O.V., Pollard, H.B., and Zeitlin, P.L. (2008). Chemical rescue of deltaF508-CFTR mimics genetic repair in cystic fibrosis bronchial epithelial cells. Mol Cell Proteomics 7, 1099-1110.

Spano, D., Cimmino, F., Capasso, M., D'Angelo, F., Zambrano, N., Terracciano, L., and Iolascon, A. (2008). Changes of the hepatic proteome in hepatitis B-infected mouse model at early stages of fibrosis. J Proteome Res 7, 2642-2653.

Sprengel, R., Kaleta, E.F., and Will, H. (1988). Isolation and characterization of a hepatitis B virus endemic in herons. J Virol 62, 3832-3839.

Sriburi, R., Jackowski, S., Mori, K., and Brewer, J.W. (2004). XBP1: a link between the unfolded protein response, lipid biosynthesis, and biogenesis of the endoplasmic reticulum. J Cell Biol 167, 35-41.

Stark, G.R., Kerr, I.M., Williams, B.R., Silverman, R.H., Schreiber, R.D.. (1998). How cells respond to Interferons. Annu Rev Biochem 67, 227-264.

Sugauchi, F., Ohno, T., Orito, E., Sakugawa, H., Ichida, T., Komatsu, M., Kuramitsu, T., Ueda, R., Miyakawa, Y., and Mizokami, M. (2003). Influence of hepatitis B virus genotypes on the development of preS deletions and advanced liver disease. J Med Virol 70, 537-544.

Sugiyama, M., Tanaka, Y., Kato, T., Orito, E., Ito, K., Acharya, S.K., Gish, R.G., Kramvis, A., Shimada, T., Izumi, N., Kaito, M., Miyakawa, Y., and Mizokami, M. (2006). Influence of hepatitis B virus genotypes on the intra- and extracellular expression of viral DNA and antigens. Hepatology 44, 915-924.

Summers, J., Smolec, J.M., and Snyder, R. (1978). A virus similar to human hepatitis B virus associated with hepatitis and hepatoma in woodchucks. Proc Natl Acad Sci U S A 75, 4533-4537.

Sun, F.C., Wei, S., Li, C.W., Chang, Y.S., Chao, C.C., and Lai, Y.K. (2006). Localization of GRP78 to mitochondria under the unfolded protein response. Biochem J 396, 31-39.

Sun, W., Xing, B., Sun, Y., Du, X., Lu, M., Hao, C., Lu, Z., Mi, W., Wu, S., Wei, H., Gao, X., Zhu, Y., Jiang, Y., Qian, X., and He, F. (2007). Proteome analysis of hepatocellular carcinoma by two-dimensional difference gel electrophoresis: novel protein markers in hepatocellular carcinoma tissues. Mol Cell Proteomics 6, 1798-1808.

Sung, V.M., and Lai, M.M. (2002). Murine retroviral pseudotype virus containing hepatitis B virus large and small surface antigens confers specific tropism for primary human hepatocytes: a potential liver-specific targeting system. J Virol 76, 912-917.

Takada, S., Gotoh, Y., Hayashi, S., Yoshida, M., and Koike, K. (1990). Structural rearrangement of integrated hepatitis B virus DNA as well as cellular flanking DNA is present in chronically infected hepatic tissues. J Virol 64, 822-828.

Thomas, X., Campos, L., Le, Q.H., and Guyotat, D. (2005). Heat shock proteins and acute leukemias. Hematology 10, 225-235.

Tirasophon, W., Lee, K., Callaghan, B., Welihinda, A., and Kaufman, R.J. (2000). The endoribonuclease activity of mammalian IRE1 autoregulates its mRNA and is required for the unfolded protein response. Genes Dev 14, 2725-2736.

Tirasophon, W., Welihinda, A.A., and Kaufman, R.J. (1998). A stress response pathway from the endoplasmic reticulum to the nucleus requires a novel bifunctional protein kinase/endoribonuclease (Ire1p) in mammalian cells. Genes Dev 12, 1812-1824.

Tong, A., Wu, L., Lin, Q., Lau, Q.C., Zhao, X., Li, J., Chen, P., Chen, L., Tang, H., Huang, C., and Wei, Y.Q. (2008). Proteomic analysis of cellular protein alterations using a hepatitis B virus-producing cellular model. Proteomics 8, 2012-2023.

Triantafilou, K., Fradelizi, D., Wilson, K., and Triantafilou, M. (2002). GRP78, a coreceptor for coxsackievirus A9, interacts with major histocompatibility complex class I molecules which mediate virus internalization. J Virol 76, 633-643.

Triantafilou, M., Fradelizi, D., and Triantafilou, K. (2001). Major histocompatibility class one molecule associates with glucose regulated protein (GRP) 78 on the cell surface. Hum Immunol 62, 764-770.

Uze, G., and Monneron, D. (2007). IL-28 and IL-29: newcomers to the interferon family. Biochimie 89, 729-734.

Vandenbroeck, K., Martens, E., and Alloza, I. (2006). Multi-chaperone complexes regulate the folding of interferon-gamma in the endoplasmic reticulum. Cytokine 33, 264-273.

Wands, J.R. (2004). Prevention of hepatocellular carcinoma. N Engl J Med 351, 1567-1570.

Wang, H.C., Huang, W., Lai, M.D., and Su, I.J. (2006). Hepatitis B virus pre-S mutants, endoplasmic reticulum stress and hepatocarcinogenesis. Cancer Sci 97, 683-688.

Wang, J., Chenivesse, X., Henglein, B., and Brechot, C. (1990). Hepatitis B virus integration in a cyclin A gene in a hepatocellular carcinoma. Nature 343, 555-557.

Wang, X.Z., Harding, H.P., Zhang, Y., Jolicoeur, E.M., Kuroda, M., and Ron, D. (1998). Cloning of mammalian Ire1 reveals diversity in the ER stress responses. Embo J 17, 5708-5717.

Wang, Y., Shen, J., Arenzana, N., Tirasophon, W., Kaufman, R.J., and Prywes, R. (2000). Activation of ATF6 and an ATF6 DNA binding site by the endoplasmic reticulum stress response. J Biol Chem 275, 27013-27020.

Wang, Z., Huang, Y., Wen, S., Zhou, B., and Hou, J. (2007). Hepatitis B virus genotypes and subgenotypes in China. Hepatol Res 37, S36-41.

Watson, L.M., Chan, A.K., Berry, L.R., Li, J., Sood, S.K., Dickhout, J.G., Xu, L., Werstuck, G.H., Bajzar, L., Klamut, H.J., and Austin, R.C. (2003). Overexpression of the 78-kDa glucose-regulated protein/immunoglobulin-binding protein (GRP78/BiP) inhibits tissue factor procoagulant activity. J Biol Chem 278, 17438-17447.

Werr, M., and Prange, R. (1998). Role for calnexin and N-linked glycosylation in the assembly and secretion of hepatitis B virus middle envelope protein particles. J Virol 72, 778-782.

Werstuck, G.H., Lentz, S.R., Dayal, S., Hossain, G.S., Sood, S.K., Shi, Y.Y., Zhou, J., Maeda, N., Krisans, S.K., Malinow, M.R., and Austin, R.C. (2001). Homocysteine-induced endoplasmic reticulum stress causes dysregulation of the cholesterol and triglyceride biosynthetic pathways. J Clin Invest 107, 1263-1273.

Wolf, D., Witte, V., Clark, P., Blume, K., Lichtenheld, M.G., and Baur, A.S. (2008). HIV Nef enhances Tat-mediated viral transcription through a hnRNP-K-nucleated signaling complex. Cell Host Microbe 4, 398-408.

Wreschner, D.H., McCauley, J.W., Skehel, J.J., and Kerr, I.M. (1981). Interferon action--sequence specificity of the ppp(A2'p)nA-dependent ribonuclease. Nature 289, 414-417.

Xu, Z., Jensen, G., and Yen, T.S. (1997). Activation of hepatitis B virus S promoter by the viral large surface protein via induction of stress in the endoplasmic reticulum. J Virol 71, 7387-7392.

Yaginuma, K., Kobayashi, H., Kobayashi, M., Morishima, T., Matsuyama, K., and Koike, K. (1987). Multiple integration site of hepatitis B virus DNA in hepatocellular carcinoma and chronic active hepatitis tissues from children. J Virol 61, 1808-1813.

Yan, W., Frank, C.L., Korth, M.J., Sopher, B.L., Novoa, I., Ron, D., and Katze, M.G. (2002). Control of PERK eIF2alpha kinase activity by the endoplasmic reticulum stress-induced molecular chaperone P58IPK. Proc Natl Acad Sci U S A 99, 15920-15925.

Yang, F., Yan, S., He, Y., Wang, F., Song, S., Guo, Y., Zhou, Q., Wang, Y., Lin, Z., Yang, Y., Zhang, W., and Sun, S. (2008). Expression of hepatitis B virus proteins in transgenic mice alters lipid metabolism and induces oxidative stress in the liver. J Hepatol 48, 12-19.

Yang, H.I., Lu, S.N., Liaw, Y.F., You, S.L., Sun, C.A., Wang, L.Y., Hsiao, C.K., Chen, P.J., Chen, D.S., and Chen, C.J. (2002). Hepatitis B e antigen and the risk of hepatocellular carcinoma. N Engl J Med 347, 168-174.

Ye, J., Rawson, R.B., Komuro, R., Chen, X., Dave, U.P., Prywes, R., Brown, M.S., and Goldstein, J.L. (2000). ER stress induces cleavage of membrane-bound ATF6 by the same proteases that process SREBPs. Mol Cell 6, 1355-1364.

Yen, T.S. (1996). Hepadnaviral X Protein:Review of Recent Progress. J Biomed Sci 3, 20-30.

Yim, E.K., Meoyng, J., Namakoong, S.E., Um, S.J., and Park, J.S. (2004). Genomic and proteomic expression patterns in HPV-16 E6 gene transfected stable human carcinoma cell lines. DNA Cell Biol 23, 826-835.

Yoshida, H., Haze, K., Yanagi, H., Yura, T., and Mori, K. (1998). Identification of the cis-acting endoplasmic reticulum stress response element responsible for transcriptional induction of mammalian glucose-regulated proteins. Involvement of basic leucine zipper transcription factors. J Biol Chem 273, 33741-33749.

Yoshida, H., Matsui, T., Hosokawa, N., Kaufman, R.J., Nagata, K., and Mori, K. (2003). A time-dependent phase shift in the mammalian unfolded protein response. Dev Cell 4, 265-271.

Yoshida, H., Matsui, T., Yamamoto, A., Okada, T., and Mori, K. (2001a). XBP1 mRNA is induced by ATF6 and spliced by IRE1 in response to ER stress to produce a highly active transcription factor. Cell 107, 881-891.

Yoshida, H., Okada, T., Haze, K., Yanagi, H., Yura, T., Negishi, M., and Mori, K. (2000). ATF6 activated by proteolysis binds in the presence of NF-Y (CBF) directly to the cis-acting element responsible for the mammalian unfolded protein response. Mol Cell Biol 20, 6755-6767.

Yoshida, H., Okada, T., Haze, K., Yanagi, H., Yura, T., Negishi, M., and Mori, K. (2001b). Endoplasmic reticulum stress-induced formation of transcription factor complex ERSF including NF-Y (CBF) and activating transcription factors 6alpha and 6beta that activates the mammalian unfolded protein response. Mol Cell Biol 21, 1239-1248.

Yoshimura, F.K., and Luo, X. (2007). Induction of endoplasmic reticulum stress in thymic lymphocytes by the envelope precursor polyprotein of a murine leukemia virus during the preleukemic period. J Virol 81, 4374-4377.

Zhang, W., Zhang, X., Tian, C., Wang, T., Sarkis, P.T., Fang, Y., Zheng, S., Yu, X.F., and Xu, R. (2008). Cytidine deaminase APOBEC3B interacts with heterogeneous nuclear ribonucleoprotein K and suppresses hepatitis B virus expression. Cell Microbiol 10, 112-121.

Zhang, X., Zhang, H., and Ye, L. (2006). Effects of hepatitis B virus X protein on the development of liver cancer. J Lab Clin Med 147, 58-66.

Zinszner, H., Kuroda, M., Wang, X., Batchvarova, N., Lightfoot, R.T., Remotti, H., Stevens, J.L., and Ron, D. (1998). CHOP is implicated in programmed cell death in response to impaired function of the endoplasmic reticulum. Genes Dev 12, 982-995.